

PATHOLOGICAL AND PATHOPHYSIOLOGICAL ALTERATIONS IN TEMPORAL
LOBE STRUCTURES AFTER MILD TRAUMATIC BRAIN INJURY

by

Camila Almeida

Thesis submitted to the Faculty of the
Neuroscience Graduate Program
Uniformed Services University of the Health Sciences
In partial fulfillment of the requirements for the degree of
Doctor of Philosophy 2014



UNIFORMED SERVICES UNIVERSITY, SCHOOL OF MEDICINE GRADUATE PROGRAMS
Graduate Education Office (A 1045), 4301 Jones Bridge Road, Bethesda, MD 20814




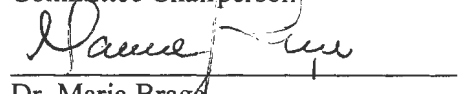
DISSERTATION APPROVAL FOR THE DOCTORAL DISSERTATION IN THE NEUROSCIENCE
GRADUATE PROGRAM

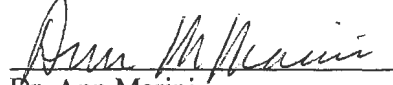
Title of Dissertation: "Pathological and Pathophysiological Alterations in Temporal Lobe Structure After Mild Traumatic Brain Injury"

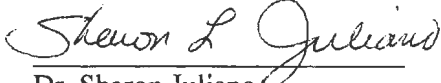
Name of Candidate: Camila Almeida
Doctor of Philosophy Degree
January 31, 2014


DISSERTATION AND ABSTRACT APPROVED:

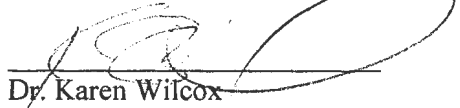
 DATE: 02/18/2014
Dr. Gregory Mueller
DEPARTMENT OF ANATOMY, PHYSIOLOGY, AND GENETICS
Committee Chairperson

 01/31/14
Dr. Maria Bragg
DEPARTMENT OF ANATOMY, PHYSIOLOGY, AND GENETICS
Dissertation Advisor

 1/31/14
Dr. Ann Marini
DEPARTMENT OF NEUROLOGY
Committee Member

 1/31/14
Dr. Sharon Juliano
DEPARTMENT OF ANATOMY, PHYSIOLOGY, AND GENETICS
Committee Member

 1/31/14
Dr. Thomas Flagg
DEPARTMENT OF ANATOMY, PHYSIOLOGY, AND GENETICS
Committee Member

 1/31/14
Dr. Karen Wilcox
DEPARTMENT OF PHARMACOLOGY AND TOXICOLOGY
University of Utah
Committee Member

ACKNOWLEDGMENTS

I have a lot of people to be thankful for.

Dr. Maria Braga, for giving me the opportunity to acquire my Ph.D. under her supervision. Very few professors would accept the challenge of supervising and sponsoring a student who did not even speak English when first came to United States, but I am glad she did. I want to thank her for mentoring my research, teaching me through her experiences and giving me the opportunity to grow and learn while working in her lab.

The staff of Dr. Maria Braga Lab for creating the friendliest work environment. I owe a lot to all of them, including those who are no longer working in the lab. I want to thank Dr. Felicia Qashu for teaching me how to do animal surgery. The skills learned through that experience were crucial in the development of my present work. I want to thank Adriana de Sousa, Daniel Stevens and Katia Rossetti for being wonderfully skilled lab technicians whose work not only sped up my own but also made the achievement of this Ph.D. easier. I would like to recognize Eric Prager for contributing to some of my experiments, patiently discussing data, helping me with statistics, revising my writings and for keeping me motivated. I would also like to thank Dr. Taiza Figueiredo and Dr. Volodymyr Pidoplichko for contributing to some of the experiments herein presented. I would like to thank Dr. Vassiliki Anderjaska, Dr. Franco Rossetti, Robert Long II and Steven Mueller for providing ideas, discussions and feedbacks.

Dr. Gregory Mueller for being the chair of my thesis committee. He was always available for discussions and provided immeasurable help and thoughtful advice. I would also like to thank all the other committee members: Dr. Sharon Juliano, Dr. Ann Marini, Dr. Thomas Flagg and Dr. Karen Wilcox. I appreciate all the discussions we had and all the helpful comments and feedback each one gave me. All significantly contributed to my present work and to my scientific learning.

Dr. Rachel Ribeiro for being the initial link between Dr. Maria Braga and I and for offering all the support I needed during the application process. For becoming such an amazing friend throughout these last six years, always offering the scientific and emotional support that I needed.

My loving husband, Davi Suhett, for literally giving up his career and plans to come to United States to pursue my dreams with me. There are no words sufficient enough to express how much I appreciate everything he has done and all the support he has given me. He is essential in my life because without him, I would not have completed this Ph.D.

Julia Suhett, my sweet baby girl who has been in my life for only eight months but has already added endless joy to it.

Family and friends, for making life easier and happier by giving me emotional support, adding countless moments of laughter to my life during the good and bad times. My

parents, Idenir and José Carlos de Almeida, for being my greatest cheerleaders. My sister, Cassia Almeida, for being such a good friend, offering help with daily tasks and making more time available in order for my Ph.D. to be completed.

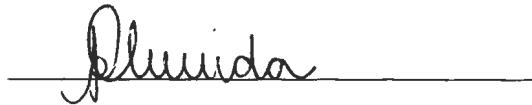
Last, but not least, I want to thank God for giving me life and the opportunity to attain this Ph.D. I know that everything I am and everything I have comes from Him. I would have never gotten this far if it was not for His care and provision for my life. I thank Him for giving me the wisdom, perseverance and strength that I needed to complete this chapter in my life.

DEDICATION

I dedicate this work to my father, José Carlos de Almeida, because nobody has had a greater impact on my education. As I prepare to acquire a higher academic degree, I realize that I owe much of this achievement to him. My father put every effort into providing me the best education possible. He always challenged me to give my best, and he proved to me that anything is possible if I persevere through difficult times. He taught me to constantly try again, never giving up, until I got to where I wanted to be. Moreover, he taught me that knowledge is the most valuable thing one can attain. Inspiring me to pursue an education, my father's life was a great example in showing me that being educated could change one's life. His influence on my life got me to where I am today, and I can say that I will be forever honored to be his daughter.

COPYRIGHT STATEMENT

The author hereby certifies that the use of any copyrighted material in the dissertation manuscript entitled: “Pathological and pathophysiological alterations in temporal lobe structures after mild traumatic brain injury” is appropriately acknowledged and, beyond brief excerpts, is with the permission of the copyright owner.

A handwritten signature in black ink, appearing to read 'Almeida', is written over a horizontal line.

Camila P. De Almeida

Program in Neuroscience
Uniformed Services University
February 12th 2014

ABSTRACT

Pathological and Pathophysiological Alterations in Temporal Lobe Structures After Mild Traumatic Brain Injury:

Author: **Camila P. de Almeida**, Doctor of Philosophy, 2013

Thesis directed by: **Maria Braga, D.D.S., Ph.D.**

Department of Anatomy, Genetics and Physiology

Mild traumatic brain injury (mTBI) accounts for 80% of all head trauma cases annually. Patients that suffer from mTBI present with an array of physical, cognitive and emotional symptoms (e.g., headache, disorientation, confusion, irritability) known as postconcussive syndrome (PCS), which resolves fairly quickly after injury. Nonetheless, victims of a mTBI are at risk of developing long-lasting cognitive and neuropsychiatric disorders, including memory deficits and anxiety. The absence of clear damage to the brain that can explain both the symptoms observed in PCS and the development of anxiety and cognitive disorders represents a challenge in the field of mTBI. The objective of this dissertation was to investigate the molecular, functional, and morphological alterations that contribute to the development of cognitive impairments and anxiety disorders following mTBI. We used the controlled cortical impact (CCI) model of traumatic brain injury (TBI) to induce mTBI in rats and investigated the pathophysiological alterations to the hippocampus and amygdala, as these two brain regions play a major role in the development of cognitive impairment and anxiety

disorders, respectively. Microarray analysis showed that transcripts encoding the chemokines Ccl2 and Ccl7, inflammatory mediators Lcn2 and Timp1, immunocyte activators Ccr5 and Fcgr2b, the MHC II immune response-related genes Cd74 and RT1-Da, the complement component C3, and the transcription factor Klf4 were upregulated in the hippocampus 1 (Ccl2, Ccl7, Lcn2, Timp1), 7 (Ccr5, Fcgr2b, Cd74, RT1-Da, C3) and 30 (Klf4) days after CCI, suggesting that inflammation may play an important role in the pathophysiology of mTBI. Additionally, rats experiencing mTBI developed cognitive impairments and anxiety like-behaviors following injury, but these abnormalities were not associated with significant reductions in the total number of neurons in the CA1 field of hippocampus or basolateral amygdala (BLA). Moreover, there was a significant loss of GAD67+ cells in both brain regions 7 days after mTBI. In addition, the surface expression of $\alpha 1$, $\beta 2$ and $\gamma 2$ subunits of the GABA_A receptor was significantly reduced 7 days after injury in the hippocampus and amygdala. Consistently, GABAergic inhibitory synaptic transmission was impaired both in the CA1 and BLA. Seven days after mTBI the frequency and amplitude of spontaneous and miniature GABA_A-receptor mediated inhibitory postsynaptic currents (IPSCs) were decreased in both regions. In the BLA, but not the CA1, we also found that the function and expression of $\alpha 7$ -nAChRs, a receptor previously shown to play key roles in cognition and anxiety, were increased 7 days after injury.

Our results suggest that a model of mTBI leads to molecular, functional and morphological alterations in the absence of clear damage to the brain. We found that the GABAergic synaptic transmission is specifically affected by mTBI causing a significant reduction in the inhibitory tonus in the basolateral nucleus of the amygdala and CA1

subfield of the hippocampus. This may result in increased excitability in both brain areas and contribute to a functional imbalance that may be the underlying cause of cognitive impairment and anxiety disorders.

TABLE OF CONTENTS

ABSTRACT.....	viii
LIST OF TABLES	xiv
LIST OF FIGURES	xv
CHAPTER 1: Introduction	1
Traumatic Brain Injury	1
Mild Traumatic Brain Injury.....	2
Long-term Disabilities	3
Memory Deficits.....	4
Anxiety Disorders.....	5
Hippocampus	6
Amygdala.....	11
Neurochemical and Cellular Mechanisms of Neuropathology of mTBI.....	14
Animal Models of TBI.....	20
Fluid Percussion Injury.....	22
Weight-drop	22
Blast-induced TBI.....	23
Controlled Cortical Impact	23
Thesis Proposal	25
CHAPTER 2: Temporal course of changes in gene expression suggests a cytokine- related mechanism for long- term hippocampal alteration after controlled cortical impact	28
Abstract.....	28
Introduction.....	30
Materials and Methods.....	31
Animals	31
Controlled Cortical Impact (CCI) surgery	32
Fixation and Tissue Processing.....	32
Stereological Quantification.	33
RNA Extraction, Microarray Procedure and Analysis	34
Bioinformatic Analysis.....	36
qRT-PCR.....	37
Statistical analysis.....	37
Results.....	39
Analysis of TBI severity	39
Transcriptome Response to CCI	40
Analysis of mRNA levels in hippocampus following TBI	52
Discussion	56

Acknowledgements.....	59
CHAPTER 3: Reduced GABAergic Inhibitory Transmission in the BLA and the Development of Anxiety-like Behaviors After mTBI	60
Abstract	60
Introduction.....	61
Experimental Procedures	63
Animals	63
Controlled Cortical Impact Injury.....	63
Behavioral Analysis	64
Open Field Test.....	64
Immunohistochemistry	65
Fixation and Tissue Processing.....	65
GAD-67 Immunohistochemistry.	65
Stereological Quantification.	66
Amygdala Slice Electrophysiology.....	67
Biotinylation and Western Blot	70
Statistical Analysis.....	71
Results.....	72
Anxiety-like behaviors increase 7 days after CCI	72
Neuropathology of Principal Neurons and Interneurons in the BLA after CCI	73
Alterations in GABA _A -mediated spontaneous and miniature IPSCs	77
Reduced membrane expression of GABA _A receptor subunits	81
Alterations in α_7 -nAChR-mediated currents after mTBI.....	82
Increased membrane expression of α_7 -nAChRs after CCI	85
Discussion	86
CHAPTER 4: Specific loss of interneurons and reduced GABAergic inhibitory synaptic transmission in the CA1 field of hippocampus – implications for cognitive impairment after mild traumatic brain injury	91
Abstract	91
Introduction.....	93
Experiemntal Procedures	95
Animals	95
Controlled Cortical Impact Injury.....	96
Passive Avoidance	96
Immunohistochemistry	97
Fixation and Tissue Processing.....	97
GAD-67 Immunohistochemistry.	98
Stereological Quantification.	98
Electrophysiological Experiments	100
Biotinylation and Western Blot	102
Statistical Analysis.....	103
Results.....	104
Memory impairments after mTBI.....	104
Loss of GABAergic interneurons	105

Reduced Inhibitory tone in the CA1	107
Reduced surface expression of GABA _A receptor subunits in the hippocampus	111
Unaltered function and surface expression of α_7 -nAChRs	112
Discussion	116
CHAPTER 5: Discussion and Future Directions	120
APPENDIX A: Additional Publications	130
Expression of miRNAs and their cooperative regulation of the pathophysiology in traumatic brain injury.....	130
Presynaptic facilitation of glutamate release in the basolateral amygdala: a mechanism for the anxiogenic and seizurogenic function of GluK1 receptors.	131
Acetylcholinesterase inhibition in the basolateral amygdala plays a key role in the induction of status epilepticus after soman exposure.	133
The recovery of acetylcholinesterase activity and the progression of neuropathological and pathophysiological alterations in the rat basolateral amygdala after soman-induced status epilepticus: Relation to anxiety-like behavior.	135
ASIC1a Activation Enhances Inhibition in the Basolateral Amygdala and Reduces Anxiety.....	137
REFERENCES	139

LIST OF TABLES

Table 1. Symptoms and signs associated with mTBI. (321).....	3
Table 2. Commonly used animal models of TBI.	21
Table 3. List of Primers for qRT-PCR.....	38
Table 4. List of significantly changed genes in both Illumina and Affymetrix platforms	48
Table 5. Total number of neurons in the BLA of sham and CCI animals.....	75
Table 6. Total Number of GAD67 ⁺ Interneurons in the BLA of sham and CCI animals	76
Table 7. Total number of interneurons in the CA1 region of sham and CCI animals	106

LIST OF FIGURES

- Figure 1. Hippocampal anatomy and circuit.** (A) Schematic illustration of the hippocampal formation anatomy showing the DG, CA3 and CA1 and their connectivity (modified from (204)). (B) Diagram showing hippocampal circuit. Note the unidirectional flow of information. Axons from neurons located in the EC form the perforant pathway, which projects mainly to granule cells in the DG but also projects to pyramidal cells in the CA3 and CA1. Mossy fibers (axons from dentate granule cells) project to CA3, whose axons will form the Schafer collaterals and make synapse on the dendrites of pyramidal cells in the CA1. Axons from CA1 projects back to EC. 8
- Figure 2. Anatomy of amygdala.** The amygdala is divided in five main nuclei: central nucleus (Ce – red), medial nucleus (Me – Yellow), cortical nucleus (CO – purple), accessory basal nucleus (AB – orange), basolateral nucleus (BLA – green) and lateral nucleus (La – blue). Each nucleus is further subdivided is smaller nuclei. CE is subdivided into CEc (central nucleus, capsular subdivision), CEI (central nucleus, lateral subdivision) and CEm (central nucleus, medial subdivision). Me is subdivided into Md (medial nucleus, dorsal subdivision) and Mv (medial nucleus, ventral subdivision). CO is subdivided into COa (cortical nucleus, anterior subdivision) and Cop (cortical nucleus, posterior subdivision). AB is subdivided into BMmc (basomedial nucleus, magnocellular subdivision) and BMpc (basomedial nucleus, parvocellular subdivision). BLA is subdivided into Bi (basal nucleus, intermediate subdivision) and Bpc (basal nucleus, parvocellular subdivision). LA is subdivided into Ld (lateral nucleus, dorsal subdivision), Lvm (lateral nucleus, ventromedial subdivision) and Lvl (lateral nucleus, ventrolateral subdivision). BOT, bed nucleus of the olfactory tract; In, intercalated nuclei; Pir, piriform cortex. Modified from (154).....12
- Figure 3. Amygdalar connections.** Arrows show projections from one amygdalar nucleus to the other and also connections that each nucleus establishes with cortical and subcortical brain regions.13
- Figure 4. Neurometabolic cascade following mTBI.** Neurometabolic cascade following traumatic injury. (A) Mechanical injury leads to membrane rupture and breakdown. (B) Glutamate and potassium leak through ruptured membrane and their extracellular concentration increase. (C) Increased activity of Na/K pumps to restore homeostasis. (D) Hyperglycolysis to generate more ATP, which serve as fuel for ionic pumps. (E) Lactate accumulation. (F) Simultaneously, excessive glutamate leads to overactivation of glutamate receptors, which leads to increased intracellular concentration of Ca^{2+} . (G) Excessive lactate and Ca^{2+} leads impaired oxidative phosphorylation and mitochondrial dysfunction. (H) Decreased ATP production, which leads to energy crisis. (I) Increased Ca^{2+} concentration also leads to activation of lipases, proteases, phosphatases and nucleases, which results cellular damage and activation of the apoptotic pathway. (J) Free radical production as result of increased Ca^{2+} concentration and mitochondrial dysfunction. (K) Increased

Ca ²⁺ concentration also leads to neurofilament compaction and microtubule disassembly. (L) Accumulation of vesicles and organelles leads to axonal swelling and eventual axotomy (105).	17
Figure 5. Characterization of injury severity caused by CCI. Mild CCI does not cause a significant loss of neurons in the CA1 region 24 hours or 7 days after injury. (A) Photomicrograph of Nissl-stained brain coronal slice. Indicated are the sites of impact and the ipsilateral and contralateral CA1. (B) Representative photomicrographs from Nissl-stained sections showing BLA cells from the ipsilateral (Top) and contralateral (Bottom) sides of sham, 1-day CCI, and 7-day CCI animals, respectively. Total magnification is 630X; scale bar, 50 μ m. (C) Group data (mean \pm SE; n = 8 for each group) of stereological estimation of the total number of Nissl-stained neurons in the CA1. There were no significant differences in neuronal number between sham and 1-day or 7-day CCI, on either ipsilateral or contralateral sides, using Student's t-test.....	40
Figure 6. Regulatory networks for CCI-dependent transcripts in rat hippocampal tissue. Transcripts with an abundance of 1.5 or greater in cortically injured (CCI) male rats at 1, 7 and 30 days post-injury compared to sham-operated by microarray analysis (see Table 3) were used as the input for analysis of potential networks using the signal transduction knowledge environment of Ingenuity (http://www.ingenuity.com). A, B, and C are the highest score networks involving the CCI-up-regulated transcripts at day one, seven and 30 respectively. CCI-regulated transcripts are depicted in gray and linked components in white. Circular lines above symbols indicate auto-regulation; connecting lines without arrows indicate direct protein interaction; dashed and solid arrows indicate indirect (e.g. regulation of mRNA levels) and direct (e.g. enzymatic) activation.....	52
Figure 7. Chemokine transcripts up-regulation in hippocampal tissue from the ipsilateral (i.d.) dorsal or contralateral (c.d.) dorsal side of sham-operated (Sham) or cortically injured (CCI) male rats at 1, 7 and 30 days post-injury. Ccl2 (A, i.d. and C, c.d.) and Ccl7 (B, i.d. and D, c.d.) mRNA levels, determined by qRT-PCR, are expressed as fold increase over corresponding control values and represent means \pm SEM of 3 samples (animals) for each condition. *p<0.05; vs. the corresponding control (Student's t test).....	53
Figure 8. Intermediary and longer-term transcriptome changes after CCI. Cd74 (A), C3 (B), RT1-Da (C) and Klf4 (D) mRNA levels, determined by qRT-PCR, are expressed as fold increase over corresponding control values and represent means \pm SEM of 3 samples (animals) for each condition. *, P<0.05; **, P<0.01; vs. the corresponding control (Student's t test).	54
Figure 9. Mild TBI increases anxiety-like behaviors in the open field test. No differences in time spent in the center of the open field were found between CCI and sham animals. However, CCI rats spent significantly less time in the center of the open field 7- and 30-days after injury compared to sham animals. Bars show the mean \pm SE of the percentage of time spent in the center. *p < 0.05.....	73
Figure 10. Mild CCI does not cause a significant loss of neurons in the BLA 24 hours or 7 days after injury. (A) Panoramic photomicrograph of Nissl-stained brain slice. Indicated are the sites of impact and the ipsilateral BLA. (B)	

Representative photomicrographs from Nissl-stained sections showing BLA cells from the ipsilateral (Top) and contralateral (Bottom) sides of sham, 1-day CCI, and 7-day CCI animals, respectively. Total magnification is 630X; scale bar, 50 μ m. (C) Group data (mean \pm SE; n = 8 for each group) of stereological estimation of the total number of Nissl-stained neurons in the BLA.75

Figure 11. Delayed loss of GABAergic interneurons in the BLA within the first week after mild CCI. (A) Representative photomicrographs of GAD-67 immunohistochemically stained GABAergic interneurons in the BLA of sham (left), 1-day CCI (middle), and 7-day CCI (right) animals. Total magnification is 630x; scale bar, 50 μ m. (B) group data showing the mean and standard error of the stereologically estimated total number of GAD-67-positive cells in the BLA 1- and 7-days after CCI compared with sham. Only 7-days after CCI was there a significant bilateral reduction in GAD-67-positive cells indicating a delayed loss of GABAergic interneurons. ***p < 0.001; n = 10 for each group.....76

Figure 12. Mild CCI causes a significant decrease in the frequency and amplitude of sIPSCs in the BLA 7-days after CCI. sIPSCs were recorded from pyramidal-shaped neurons in the presence of d-APV (50 μ M), SCH50911 (20 μ M), and GYKI 52466 (50 μ M), at a holding potential of -70 mV. Representative examples of recordings obtained in the BLA are shown in (A) and (B) for Sham and CCI 7-day animals, respectively. (C) Group data showing the change in the percentage frequency and amplitude of sIPSCs from CCI animals relative to Sham animals. The frequency and amplitude, but not the rise time and the decay time constant of the sIPSCs were significantly reduced in the CCI group compared to the sham controls. *p<0.05; **p < 0.01; n = 18 for each group.78

Figure 13. Mild CCI causes a significant decrease in the frequency and amplitude of mIPSCs in the BLA 7-days after CCI. mIPSCs were recorded from pyramidal-shaped neurons in the presence of d-APV (50 μ M), SCH50911 (20 μ M), and GYKI 52466 (50 μ M), TTX (1 μ M) at a holding potential of -70 mV. Representative examples of recordings obtained in the BLA are shown in (A) and (B) for Sham and CCI 7 days animals, respectively. (C) Group data showing the change in the percentage frequency and amplitude of mIPSCs from CCI animals relative to Sham animals. The frequency and amplitude, but not the rise time and the decay time constant of the sIPSCs were significantly reduced in the CCI group compared to the sham controls. The recorded currents were blocked by the GABA_A receptor antagonist bicuculline (data not shown). *p<0.05; **p < 0.01; n = 17 for each group.....80

Figure 14. Surface expression of α_1 , β_2 , and γ_2 GABA_A receptor subunits is reduced in the BLA of CCI animals 7 days after mild CCI. Western blot for subunits of (A) α_1 , (B) β_2 , and (C) γ_2 subunits, respectively, was performed using biotinylated proteins isolated from the ipsilateral and contralateral sides of Sham and CCI 7-day animals. Group data showing the mean \pm SE of the ratio between each subunit and GLUT1 optical densities. Top panel: representative Western blot for α_1 (A), β_2 (B), and γ_2 (C) subunits of GABA_A receptors, respectively. Bottom panel: representative Western blot for GLUT1, used as a loading control. Note that surface expression of GABA_A α_1 , $\beta_{2/3}$ and γ_2 subunits

are reduced in CCI animals when compared to Sham animals. * $p < 0.01$; $n = 3$ for each group.82

Figure 15. Activation of $\alpha 7$ -nAChRs by fast application of the $\alpha 7$ -nAChR specific agonist, choline, in the BLA, shows increased cholinergic conductance 7-days after CCI. (A) Group data showing the mean \pm SE charge transfer in pyramidal-shaped neurons in the BLA from CCI rats 7-days after injury. A significant increase in the mean charge transfer was observed only 7-days after CCI. (B) Representative charge transfer from $\alpha 7$ -nAChRs from sham (left), 1-days CCI (middle), and 7-day CCI (right) animals. Note that the charge transfer through $\alpha 7$ -nAChRs is increased in the BLA at day 7 post injury. (C) Representative $\alpha 7$ -nAChR-mediated currents recorded from sham (left), 1-day CCI (middle), and 7-day CCI (right) animals. Note the significant increase in the amplitude of the $\alpha 7$ -nAChR-mediated current 7-days post CCI. Experiments were recorded in the presence of α -conotoxin A1B (1 μ M), DH β E (10 μ M), atropine sulfate (0.5 μ M), D-AP5 (50 μ M), CNQX (20 μ M), SCH50911 (10 μ M), LY 3414953 (3 μ M), and bicuculline (20 μ M). * $p < 0.05$; $n = 17$ cells for each group.84

Figure 16. Surface expression of $\alpha 7$ subunit of neuronal nicotinic acetylcholine receptor is increased in the BLA of CCI animals 7-days after mild CCI. Western blot was performed using biotinylated proteins isolated from the ipsilateral and contralateral sides of Sham and CCI 7-day animals. Group data showing the mean \pm SE of the ratio between the $\alpha 7$ subunit and GLUT1 optical densities. Top panel: representative Western blot for $\alpha 7$ -nAChRs. Bottom panel: representative Western blot for GLUT1, used as a loading control..* $p < 0.05$; $n = 3$ for each group.....85

Figure 17. Mild TBI leads to memory deficits in the passive avoidance test. CCI rats spent significantly less time to enter the dark chamber 1- and 7-days after injury compared to sham animals. Bars show the mean \pm SE of the percentage of time spent in the center. * $p < 0.05$ 105

Figure 18. Delayed loss of GABAergic interneurons in the CA1 region within the first week after mild CCI. (A) Representative photomicrographs of GAD-67 immunohistochemically stained GABAergic interneurons in the CA1 of sham (left), 1-day CCI (middle), and 7-day CCI (right) animals. Total magnification is 630x; scale bar, 50 μ m. (B) group data showing the mean and standard error of the stereologically estimated total number of GAD-67-positive cells in the CA1 1- and 7-days after CCI compared with sham. Only 7-days after CCI was there a significant bilateral reduction in GAD-67-positive cells indicating a delayed loss of GABAergic interneurons. * $p < 0.05$; *** $p < 0.001$; $n = 10$ for each group. 106

Figure 19. Mild CCI causes a significant decrease in the frequency and amplitude of sIPSCs in the CA1 7-days after CCI. sIPSCs were recorded from pyramidal-shaped neurons in the presence of d-APV (50 μ M), SCH50911 (20 μ M), and GYKI 52466 (50 μ M), at a holding potential of -70 mV. Representative examples of recordings obtained in the BLA are shown in (A) and (B) for Sham and CCI 7-day animals, respectively. (C) Group data showing the change in the percentage frequency and amplitude of sIPSCs from CCI animals relative to

Sham animals. The frequency and amplitude, but not the rise time and the decay time constant of the sIPSCs were significantly reduced in the CCI group compared to the sham controls.....	108
Figure 20. Mild CCI causes a significant decrease in the frequency and amplitude of mIPSCs in the CA1 7-days after CCI. mIPSCs were recorded from pyramidal-shaped neurons in the presence of d-APV (50 μ M), SCH50911 (20 μ M), and GYKI 52466 (50 μ M), TTX (1 μ M) at a holding potential of -70 mV. Representative examples of recordings obtained in the BLA are shown in (A) and (B) for Sham and CCI 7 days animals, respectively. (C) Group data showing the change in the percentage frequency and amplitude of mIPSCs from CCI animals relative to Sham animals. The frequency and amplitude, but not the rise time and the decay time constant of the sIPSCs were significantly reduced in the CCI group compared to the sham controls. The recorded currents were blocked by the GABA _A receptor antagonist bicuculline (data not shown).....	110
Figure 21. Surface expression of α_1, β_2, and γ_2 GABA_A receptor subunits is reduced in the hippocampus of CCI animals 7 days after mild CCI. Western blot for subunits of (A) α_1 , (B) β_2 , and (C) γ_2 subunits, respectively, was performed using biotinylated proteins isolated from the ipsilateral and contralateral sides of Sham and CCI 7-day animals. Group data showing the mean \pm SE of the ratio between each subunit and GLUT1 optical densities. Top panel: representative Western blot for α_1 (A), β_2 (B), and γ_2 (C) subunits of GABA _A receptors, respectively. Bottom panel: representative Western blot for GLUT1, used as a loading control. Note that surface expression of GABA _A α_1 , $\beta_{2/3}$ and γ_2 subunits are reduced in CCI animals when compared to Sham animals. *** $p < 0.001$; $n = 3$ for each group.	112
Figure 22. Activation of α_7-nAChRs by fast application of the α_7-nAChR specific agonist, choline, in the CA1, shows that cholinergic conductance is unaltered 1- and 7-days after CCI. (A) Group data showing the mean \pm SE charge transfer in pyramidal-shaped neurons in the CA1 from CCI rats 7-days after injury. (B) Representative charge transfer from α_7 -nAChRs from sham (left), 1-days CCI (middle), and 7-day CCI (right) animals. (C) Representative α_7 -nAChR-mediated currents recorded from sham (left), 1-day CCI (middle), and 7-day CCI (right) animals. Experiments were recorded in the presence of α -conotoxin Au1B (1 μ M), DH β E (10 μ M), atropine sulfate (0.5 μ M), D-AP5 (50 μ M), CNQX (20 μ M), SCH50911 (10 μ M), LY 3414953 (3 μ M), and bicuculline (20 μ M).	114
Figure 23. Surface expression of α_7 subunit of neuronal nicotinic acetylcholine receptor is increased in the BLA of CCI animals 7-days after mild CCI. Western blot was performed using biotinylated proteins isolated from the ipsilateral and contralateral sides of Sham and CCI 7-day animals. Group data showing the mean \pm SE of the ratio between the α_7 subunit and GLUT1 optical densities. Top panel: representative Western blot for α_7 -nAChRs. Bottom panel: representative Western blot for GLUT1, used as a loading control.. * $p < 0.05$; $n = 3$ for each group.....	115

CHAPTER 1: Introduction

TRAUMATIC BRAIN INJURY

Traumatic brain injury (TBI) occurs when a bump, blow, jolt to the head, or a penetrating head injury causes damage to the brain leading to temporary or permanent brain dysfunction. TBI is a leading cause of hospitalization, mortality and morbidity in the United States, afflicting approximately 1.7 million people annually; of all reported cases, 16.8% require hospitalization, 3% die, and nearly 80% are treated and released from an emergency department (86). Those that survive are likely to develop long-lasting TBI-related neuropsychiatric disorders such as attention deficits, memory difficulties, impaired learning, mood alterations, depression and anxiety (30; 31; 45; 46; 223). Traumatic brain injury is currently a major healthcare concern among military personnel and athletes practicing contact sports. The Department of Defense (DoD) has reported 273,859 cases of TBI from 2000 to 2013 (DoD Numbers), while contact sports result in approximately 300,000 TBI cases per year (147; 278). However, the number of unreported sports-related TBI's may be astronomical. For example, one study, which includes TBIs in which no medical care was sought, considers sports related TBI-related injuries to be as high as 1.6 – 3.0 million cases annually (164). These numbers reveal the significance of continuing research on TBI and its consequences to human health.

Although TBI is highly associated with the development of long-term neuropsychiatric disabilities, the pathological and pathophysiological alterations underlying such conditions are poorly understood. Determining how TBI alters brain function and morphology is the first step towards the development of well-tolerated

pharmacological strategies aiming at preventing and treating the symptoms associated with head injury.

Mild Traumatic Brain Injury

TBI is often classified according to its severity into mild, moderate and severe. Mild TBI (mTBI) is the most common type of head trauma and accounts for 80% of all reported cases. A consensus definition for mTBI has not been established yet; however, the American Congress of Rehabilitation Medicine (ACRM) and the Centers for Disease Control (CDC) have proposed some criteria for diagnosis of mTBI. These definitions differ in a few aspects but they are mostly in accordance. According to ACRM and CDC a patient with mTBI presents with disruption of brain function, as manifested by at least one of the following: (1) loss of consciousness lasting less than 30 minutes; (2) dysfunction of memory for events immediately before or after the accident (posttraumatic amnesia (PTA) not greater than 24 hours; (3) transient alterations in mental state at the time of the accident (e.g. feeling dazed, disoriented, or confused); (4) focal neurological deficits(s) that may or may not be transient (e.g. seizures); and (5) an initial Glasgow Coma Scale (GCS) of 13-15. mTBI patients may present additional symptoms that fall into one of the following categories: (1) physical symptoms of brain injury, (2) cognitive deficits and (3) behavioral and emotional change(s) as summarized in Table 1. The presence of such symptoms may occur in combination or alone and offers additional evidence that an mTBI has occurred (30; 31; 45; 46; 146; 223)

Physical	Cognitive	Behavioral/Emotional
Nausea	Attention deficit	Irritability
Vomiting	Poor concentration	Sadness
Dizziness	Impaired perception	Nervousness
Headache	Confusion	Disinhibition
Impaired balance	Memory deficit	Impulsive behavior
Blurred vision	Forgetfulness	Emotional liability
Sensitivity to light	Impaired Speech	Apathy
Sensitivity to noise	Language deficit	Anxiety
Sleep disturbance	Difficulty completing tasks	Increased Fear
Fatigue	Trouble solving problems	Increased Arousal
Lethargy	Decreased performance	Lack of Motivation
Sensory loss		Lack of Initiative
		Depression

Table 1. Symptoms and signs associated with mTBI. (321)

Despite of the manifestation of all these symptoms, mTBI is usually characterized by the absence of any overt physical damage. Pathological alterations in mTBI patients are particularly difficult to identify using computed tomography (CT) and conventional magnetic resonance imaging (MRI), although MRI is more sensitive (138; 277). Yet, that does not mean that pathological and pathophysiological changes are not taking place after mTBI. It is likely that current imaging techniques are unable to detect TBI-related alterations since new and improved imaging resources such as positron emission tomography (PET) and diffusion tensor imaging (DTI) are revealing that mTBI patients display minor morphological and functional alterations (23).

Long-term Disabilities

Mild TBI patients usually present acute symptoms such as headache, nausea, vomiting, dizziness, irritability, poor concentration and slurred speech. These symptoms usually resolve shortly after injury; however it is estimated that 7-30% of individuals

develop some cognitive, behavioral, neurological or emotional impairments that persist for weeks, months and even years after mTBI (21; 149).

Memory Deficits

Cognitive impairment is among the most common complaint in individuals that sustain an mTBI. Patients usually develop a constellation of symptoms such as poor concentration, attention deficit, distractibility, compromised vigilance, prolonged reaction time and memory impairment as part of the post-concussive syndrome (PCS), which lasts for a short period of time, but resolves within minutes to months after injury (61). However, 5-15% of mTBI patients develop persistent cognitive disabilities that go beyond this period and bring some degree of functional impairment to their daily lives (256).

Memory deficits, which can be detected within minutes after injury and persist up to several years are particularly debilitating in the aftermath of mTBI (24; 28; 191; 283; 299; 301). During the subacute phase following mTBI, patients develop a transient state of confusion and disorientation referred to as posttraumatic amnesia (PTA) (3). Loss of memories acquired prior to the onset of mTBI (retrograde amnesia) and inability to acquire new memories related to the injury (anterograde amnesia) are often observed during this phase (137). Although PTA is considered a transient subacute state, 59% of mTBI patients report persistent difficulties in remembering things (70; 244).

Working memory (WM), the ability of holding information in mind while simultaneously performing another mental operation, is also impaired in patients that sustained mTBI (13; 14; 188). For example, if the patient is interrupted while performing a requested task, he may completely forget to finish the task unless once again reminded

(94). Another common complaint among mTBI patients is forgetting to keep an appointment, which characterizes deficits with prospective memory (212; 291). All those cognitive deficits, even when mild, affect the performance of simple, yet necessary day-to-day tasks.

Anxiety Disorders

The high prevalence of psychiatric disorders after head injury among both the civilian population and military personnel is of increasing concern (29; 92; 134; 199; 200; 212; 234). In particular, anxiety disorders in general have an incidence as high as 24% among individuals that sustain mTBI (199). Anxiety disorders are a broad term encompassing different psychiatric conditions and are characterized by excessive worrying, fear and dread (156; 177; 271). Specific anxiety disorders such as posttraumatic stress disorder (PTSD), generalized anxiety disorders (GAD), obsessive-compulsive disorder (OCD), panic disorder (PD), specific phobia and social phobia are characterized by different arrays of symptoms, but all of them were diagnosed after mTBI (200).

Posttraumatic stress disorder is (PTSD) is by far the most studied type of all anxiety sequelae after mTBI. It is characterized by the re-experience of a traumatic event accompanied by the increased arousal and fear characteristics of anxiety disorders in general (271). The epidemiology of PTSD after mTBI has been extensively studied and incidence rates varies from 13 to 84% (37; 120; 134; 149; 169; 199; 215). Still, some have argued that mTBI and PTSD cannot co-exist. mTBI is often associated with loss of consciousness (LOC) and patients often report difficulty to remember events that happened around the time of the incidence. On the other hand PTSD is characterized by

recollection of a traumatic event accompanied by heightened arousal. Thus, occurrence of retrograde amnesia would protect against the development of PTSD (157; 263; 264). Additionally, a second group acknowledges the comorbidity between mTBI and PTSD, but argue that the precipitating insult for PTSD is the stress associated with the trauma and its aftermath and not the head injury itself (36; 134; 149). All those questions surrounding the occurrence of PTSD and mTBI point to the continuing need of research on this field. Moreover, unraveling the causes underlying the pathology of such impairments will aid the development of new and improved pharmacological interventions aiming to prevent and treat such psychiatric disorders.

HIPPOCAMPUS

The hippocampus is a brain region localized in the medial temporal lobe. It plays a major role in memory consolidation and is also important for spatial memory and navigation (78; 183; 249; 279; 302). Its name is derived from Greek *hippokampus* (*hippos*: horse; *kampos*: sea monster), since the anatomical shape resembles that of a sea horse. Besides its unique shape, the hippocampus also has a particular morphological organization that is not found anywhere else in the brain. Similar to other cortical regions, the hippocampus is composed mainly by pyramidal-shaped cells and smaller interneurons, which are much less in number. However, in the hippocampus pyramidal cells and interneurons are organized into a compact and very well-defined layer.

The hippocampus is composed of three subregions named CA1, CA2 and CA3 (CA is derived from *Cornu Ammonis*: ram's horn), and together with the dentate gyrus (DG), subiculum, pre-subiculum, para-subiculum and entorhinal cortex (EC), it gives rise to the hippocampal formation. Besides its shape and organizations, the hippocampus also

has a particular connectivity and flow of information. Within the neocortex there is reciprocal connections and flow of information between two different regions that synapse with each other. In the hippocampus, however, information flows in a single direction. Information from all sensory modalities arrives in different regions of the EC. Axons from large pyramidal cells in the EC come together and form the perforant pathway, which projects to all regions of the hippocampal formation including CA1, CA2 and CA3 fields of hippocampus (43). The dentate granule cell axons (called mossy fibers) projects to CA3 and pass along the information received from EC. Then, axons from pyramidal cells in the CA3 form the Schafer collaterals and send projections to CA1 field of hippocampus (Figure 1). Axons from CA1 projects back to EC completing the intrinsic circuit within the hippocampal information. Within the hippocampus, this unidirectional series of synapses is called a trisynaptic circuit and each region has a specific role in the information processing. The DG is the entry region, where aberrant or excessive input is filtered. The CA3 field amplifies the signal and projects to the CA1, which transduces processed information back to the cerebral cortex (55). Therefore, as the main output region of the hippocampus, the CA1 field assumes an important role in the trisynaptic circuit and is one of the target areas investigated in this study. Additionally, functional and morphological deficits in the CA1 field impair both consolidation and memory retrieval (18; 19; 52; 85; 96; 207).

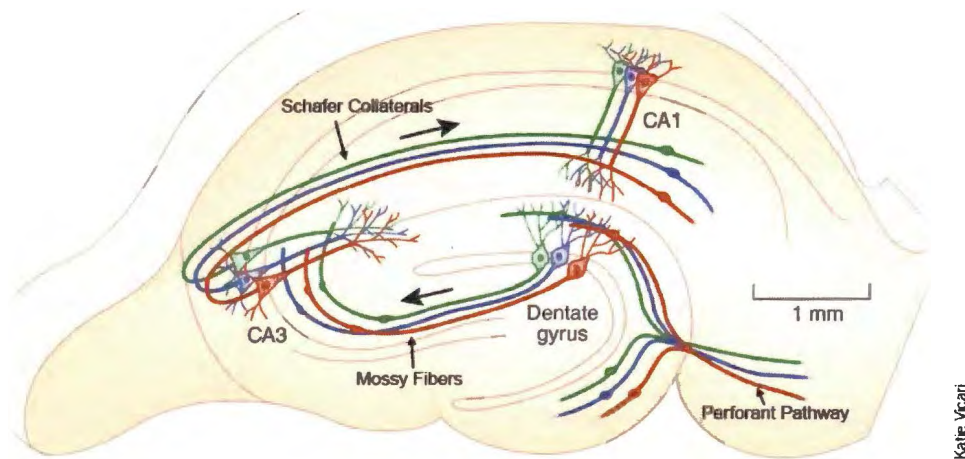
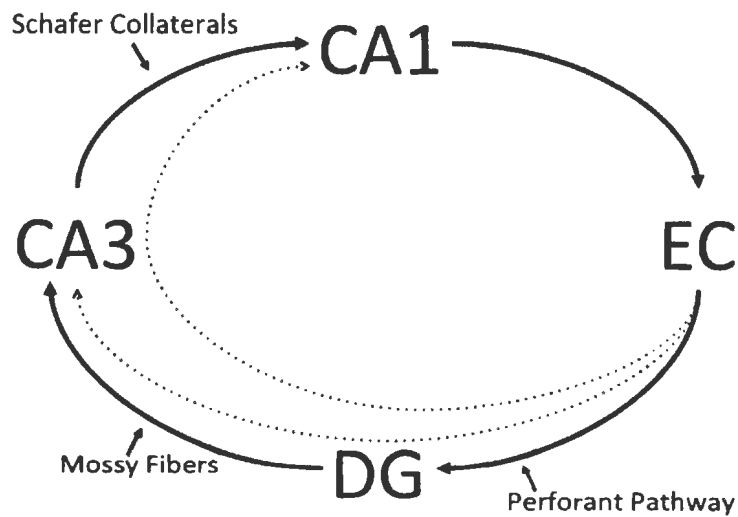
A**B**

Figure 1. Hippocampal anatomy and circuit. (A) Schematic illustration of the hippocampal formation anatomy showing the DG, CA3 and CA1 and their connectivity (modified from (204)). (B) Diagram showing hippocampal circuit. Note the unidirectional flow of information. Axons from neurons located in the EC form the perforant pathway, which projects mainly to granule cells in the DG but also projects to pyramidal cells in the CA3 and CA1. Mossy fibers (axons from dentate granule cells) project to CA3, whose axons will form the Schafer collaterals and make synapse on the dendrites of pyramidal cells in the CA1. Axons from CA1 projects back to EC.

The CA1 region is mainly composed by pyramid-shaped cells intercalated by a population of inhibitory interneurons smaller in size and number. Interneuron population is not homogeneous but rather varies in size, localization and markers expressed (12; 98; 152; 161). Despite their small population, inhibitory interneurons play an important role in the hippocampus physiology. Local GABAergic interneurons synapse onto both the soma and the dendrites of CA1 pyramidal cells and help to control their firing rate, synchronize their activity and modulate synaptic plasticity (8; 122; 124). Because they have such an important role in controlling the output from CA1 pyramidal cells, GABAergic interneurons have been intensively investigated and are the focus of the present study.

Inhibitory GABAergic modulation in the CA1 is mediated by two different receptors: GABA_A and GABA_B. Metabotropic GABA_B receptors mediate a slow response to GABA binding to its agonist site. Their activation results in K⁺ channels opening and K⁺ outflow, which leads to neuronal hyperpolarization. On the other hand, ionotropic GABA_A receptors are permeable to Cl⁻ influx and mediate fast inhibitory responses. They are found at synaptic and extrasynaptic sites and mediate both phasic and tonic inhibition, respectively. These different receptor subtypes work together to ensure proper inhibition in response to both high and low frequency stimulation of GABAergic interneurons.

GABA_A receptors are pentameric structures composed of different subunits (α 1- α 6, β 1- β 3, γ 1- γ 3, δ , ϵ , θ , π and ρ 1- ρ 3) that assemble into a variety of combinations (80). The most common subtype of GABA_A receptor is the α 1 β 2 γ 2, which corresponds to 60% of all GABA_A receptors expressed in the brain and is found both in synaptic and

extrasynaptic localizations (197). This receptor subtype is also the most abundant combination of GABA_A receptor in the hippocampus (80; 197). Hippocampal pyramidal cells and interneurons, however, express a great variety of other GABA_A receptors and their function has been extensively reviewed in (255).

GABAergic and glutamatergic neurotransmission in the hippocampus are both modulated by cholinergic input arriving from the medium septum and diagonal band of Broca (MSDB) (54; 75). Released acetylcholine activates and mediates its effects via muscarinic and nicotinic receptors present on both principal cells and interneurons. However, acetylcholine nicotinic receptors (nAChRs) are particularly important in the regulation of excitability, plasticity and cognitive functions (123; 141; 166; 241; 330). Administration of nicotine and other nicotinic receptors agonists in animals and humans has long been shown to improve memory, whereas nicotinic antagonists can lead to impairments in memory function (167; 211; 257). Acetylcholine nicotinic receptors are pentameric assemblies of homologous subunits, which comprise $\alpha 1$ to $\alpha 10$ and $\beta 2$ to $\beta 4$. Different combinations of such subunits result in individual nAChR with unique functional and structural properties (88; 209). In the hippocampus the most common nicotinic receptors assemblies are $(\alpha 4)_2(\beta 2)_3$, $(\alpha 3)_2(\beta 4)_4$, and $(\alpha 7)_5$ (82; 341) with the $\alpha 7$ being the most prevalent. $\alpha 7$ -containing nicotinic acetylcholine receptors ($\alpha 7$ -nAChRs) are highly permeable to Ca^{2+} and are expressed both pre and postsynaptically. Presynaptically, activation of $\alpha 7$ -nAChRs and subsequent Ca^{2+} influx promote neurotransmitter release; postsynaptically it facilitates the induction of synaptic plasticity such as long-term potentiation (LTP) (193). The result of nAChRs activation on synaptic plasticity associates well with the nicotine effect on memory performance since LTP is

the cellular correlate to learning and memory. Activation of nAChRs and in particular $\alpha 7$ -nAChRs also plays an important role in the regulation of excitability by specifically modulating GABAergic activity in the hippocampus (112).

AMYGDALA

The amygdala is an almond-shaped structure located deep in the temporal lobe and plays a major role in the processing and modulation of emotional behavior. In particular, fear and aggressive behavior are closely associated with amygdalar function. Despite its small size, it is densely innervated and establishes reciprocal connections with the cerebral cortex and the thalamus. Therefore, information from all sensory modalities arrives in the amygdala where they are assessed for their emotional significance. The amygdala is also connected to subcortical regions, in particular the hippocampus, and therefore plays a major role in the consolidation of long-term memory of associative learning.

More than ten different nuclei form the amygdala (Figure 2). Information coming into the amygdala synapses in the basolateral complex; from here efferent fibers project medially to the centromedial amygdala, the main output group (259). The basolateral complex is further divided into lateral, basolateral, and the accessory basal nuclei (160). Excitatory input from the hippocampus, hypothalamus, thalamus, frontal, parietal and olfactory cortices arrives to the basolateral nucleus (BLA) via the external capsule. Reciprocal connections from BLA ultimately end in the hippocampus, frontal cortex, thalamus, striatum and nucleus accumbens (Figure 3) (259).

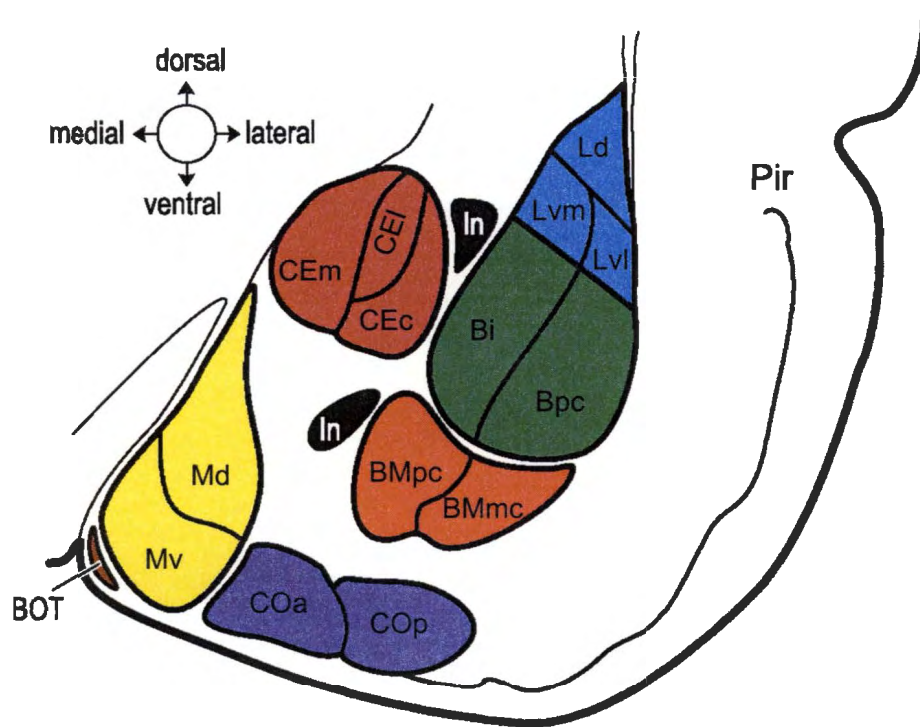


Figure 2. Anatomy of amygdala. The amygdala is divided in five main nuclei: central nucleus (Ce – red), medial nucleus (Me – Yellow), cortical nucleus (CO – purple), accessory basal nucleus (AB – orange), basolateral nucleus (BLA – green) and lateral nucleus (La – blue). Each nucleus is further subdivided in smaller nuclei. CE is subdivided into CEc (central nucleus, capsular subdivision), CEI (central nucleus, lateral subdivision) and CEm (central nucleus, medial subdivision). Me is subdivided into Md (medial nucleus, dorsal subdivision) and Mv (medial nucleus, ventral subdivision). CO is subdivided into COa (cortical nucleus, anterior subdivision) and Cop (cortical nucleus, posterior subdivision). AB is subdivided into BMmc (basomedial nucleus, magnocellular subdivision) and BMpc (basomedial nucleus, parvocellular subdivision). BLA is subdivided into Bi (basal nucleus, intermediate subdivision) and Bpc (basal nucleus, parvocellular subdivision). LA is subdivided into Ld (lateral nucleus, dorsal subdivision), Lvm (lateral nucleus, ventromedial subdivision) and Lvl (lateral nucleus, ventrolateral subdivision). BOT, bed nucleus of the olfactory tract; In, intercalated nuclei; Pir, piriform cortex. Modified from (154).

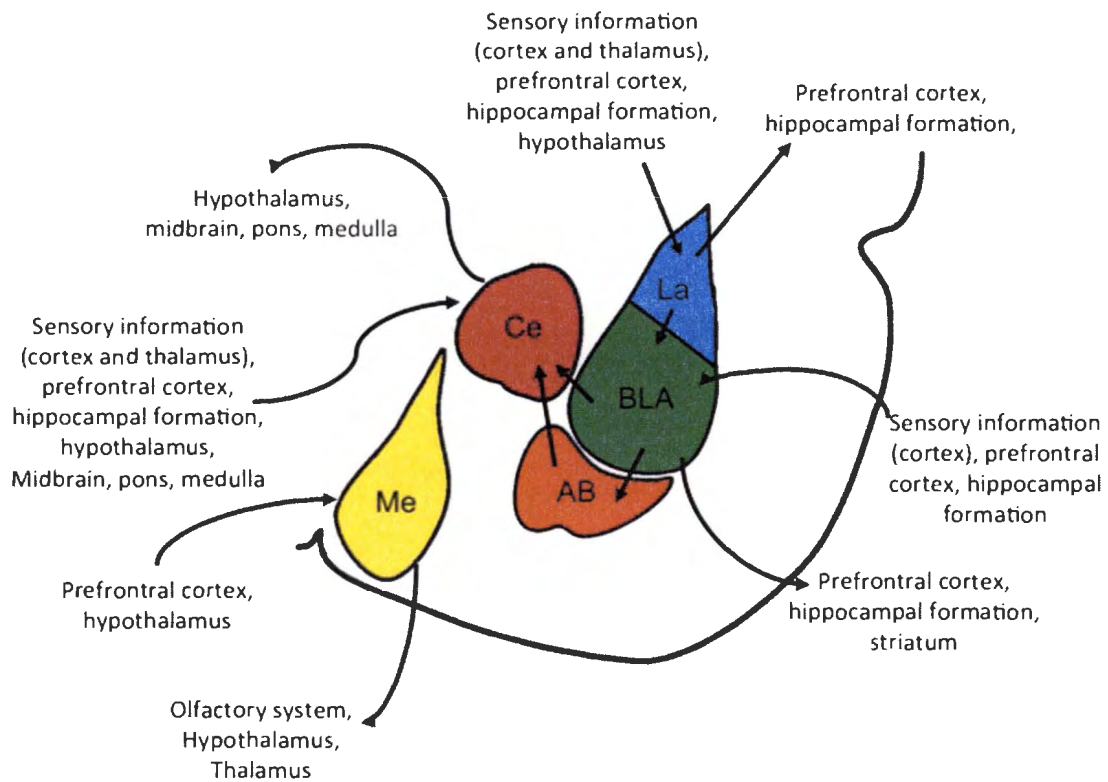


Figure 3. Amygdalar connections. Arrows show projections from one amygdalar nucleus to the other and also connections that each nucleus establishes with cortical and subcortical brain regions.

The major cell types in the BLA are called principal cells and are equivalent to hippocampal and cortical pyramidal neurons. They are pyramidal or semi-pyramidal shaped neurons and synthesize the excitatory neurotransmitter glutamate (294). Interneurons are also present in the BLA and although they correspond to only 15-20% of the neuronal population (189), they are very efficient at regulating principal cell excitability due to high frequency spike discharge (25; 163; 318; 319; 326). Therefore, principal cells within the BLA fire at a very low rate (220) and single interneurons can powerfully inhibit the activity of excitatory principal neurons (326).

Similar to the hippocampus, the BLA is densely innervated by cholinergic fibers arriving from the nucleus basalis magnocellularis, a collection of neurons in the substantia innominate of the basal forebrain (44; 208). Cholinergic fibers arriving in the BLA synapse on both glutamatergic principal cells and GABAergic interneurons through activation of muscarinic and nicotinic receptors (206; 213; 288; 300). $\alpha 7$ -nAChRs are particularly important in the regulation of excitability in the BLA. Presynaptically they facilitate the release of glutamate and postsynaptically they directly modulate neuronal activity of principal cells and interneurons. Interestingly, activation of $\alpha 7$ -nAChRs in the BLA increases both glutamatergic and GABAergic activity but favors inhibition over excitation (228).

NEUROCHEMICAL AND CELLULAR MECHANISMS OF NEUROPATHOLOGY OF MTBI

Functional deficits observed after TBI are not the result of cell death as a direct consequence of mechanical injury to the brain. Rather, complex neuropathological process that involves both primary and secondary injury mechanisms takes place and accounts for TBI-associated functional impairments. Primary injury occurs when a biomechanical force is transferred to the brain resulting in immediate shearing and tearing of blood vessels and brain tissue (32). The primary injury immediately gives way to secondary injury mechanisms by triggering a series of neurochemical cascades that extend over a period of days to months (Figure 4) (26; 105; 168). Disruption of neuronal and axonal cell membranes leads to outflow of intracellular content, such as potassium and glutamate (145; 289). Increased extracellular concentration of potassium has deleterious effects on cellular homeostasis. In an effort to restore the electrochemical gradient the Na/K pump increases its demand for ATP, which results in enhanced glucose

metabolism in a scenario where this need cannot be met due to impaired blood flow (39; 186; 268; 287). The resulting energy crisis hinders the brain from effectively responding to TBI and may be responsible for some postconcussive symptoms. Excessive amounts of extracellular potassium also lead to neuronal depolarization, which in turn favors further glutamate release (145). Moreover, excessive K^+ triggers the reverse transport of glutamate through excitatory amino acid (EAA) transporters on glial cells resulting in a massive increase in the extracellular concentration of this neurotransmitter (42; 181).

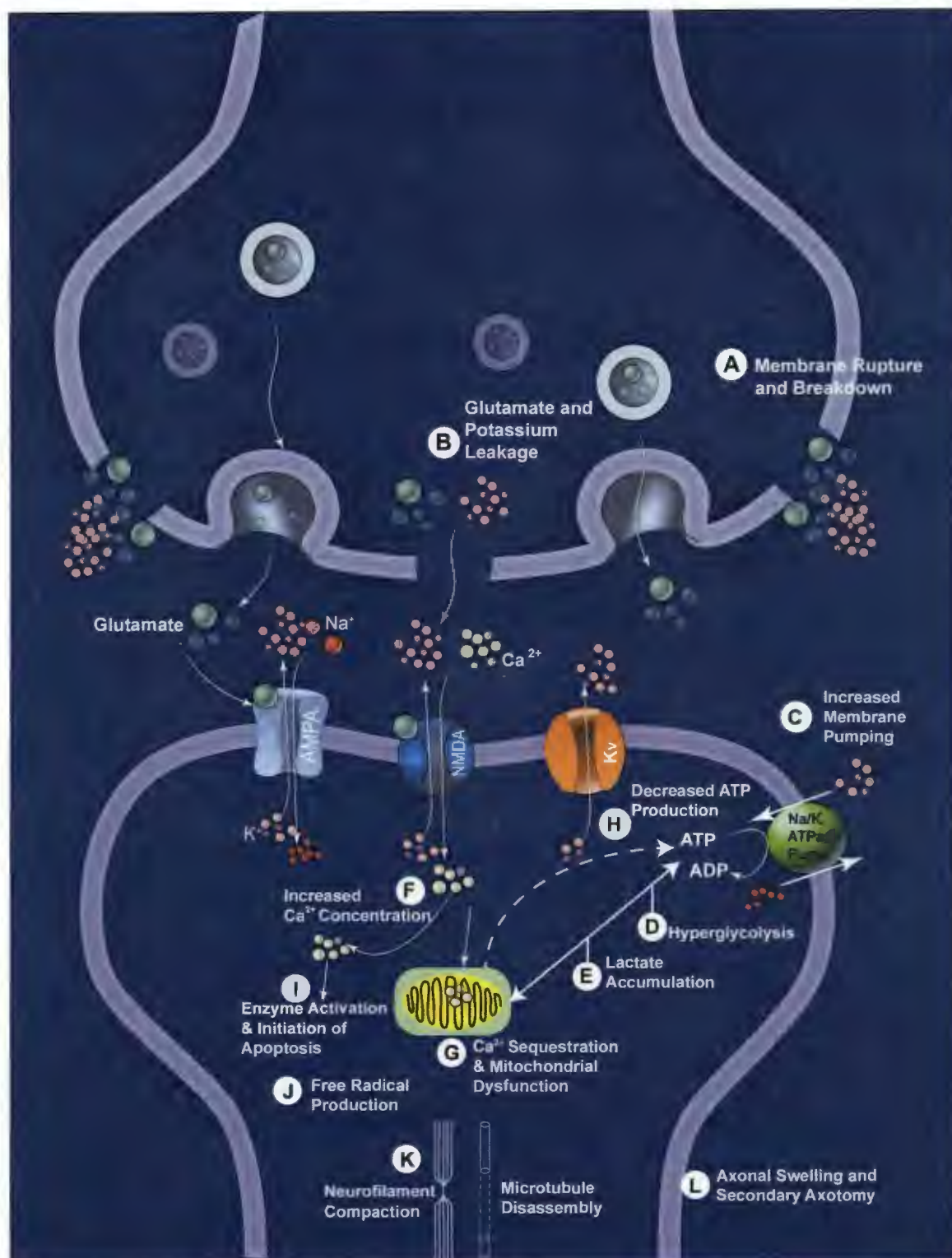


Figure 4. Neurometabolic cascade following mTBI. Neurometabolic cascade following traumatic injury. (A) Mechanical injury leads to membrane rupture and breakdown. (B) Glutamate and potassium leak through ruptured membrane and their extracellular concentration increase. (C) Increased activity of Na/K pumps to restore homeostasis. (D) Hyperglycolysis to generate more ATP, which serve as fuel for ionic pumps. (E) Lactate accumulation. (F) Simultaneously, excessive glutamate leads to overactivation of glutamate receptors, which leads to increased intracellular concentration of Ca^{2+} . (G) Excessive lactate and Ca^{2+} leads impaired oxidative phosphorylation and mitochondrial dysfunction. (H) Decreased ATP production, which leads to energy crisis. (I) Increased Ca^{2+} concentration also leads to activation of lipases, proteases, phosphatases and nucleases, which results cellular damage and activation of the apoptotic pathway. (J) Free radical production as result of increased Ca^{2+} concentration and mitochondrial dysfunction. (K) Increased Ca^{2+} concentration also leads to neurofilament compaction and microtubule disassembly. (L) Accumulation of vesicles and organelles leads to axonal swelling and eventual axotomy (105).

Abnormal release of glutamate is also part of the secondary mechanisms of injury that greatly contributes to TBI-related neuropathology (Figure 4). It leads to hyperactivation of N-methyl-D-aspartate (NMDA) and non-NMDA glutamate receptors, which in turn results in network hyperexcitability (145). This intense excitation spreads to brain regions other than the site of primary injury and is followed by a rebound suppression of neuronal activity. This phenomenon is termed spreading cortical depression and may be responsible for cognitive dysfunctions such as loss of consciousness and amnesia observed after TBI (83; 119; 186; 282; 286). Overactivation of glutamate receptors (91; 216), along with activation of voltage-gated calcium channels by potassium-triggered membrane depolarization both contribute to the massive influx of intracellular calcium (261; 290). Perturbation of calcium homeostasis has deleterious effects within the cell, including compromising microtubule and neurofilament stability, which impair axonal traffic, connectivity and transmission (225; 229; 230). In addition,

oxidative phosphorylation in mitochondria is also impaired resulting in reactive oxygen species (ROS) generation (308; 328). Other free radicals are also generated within the cell characterizing a state of oxidative stress (1). Activation of lipases, proteases, phosphatases and nucleases is also elicited by calcium and further contribute to the cellular damage triggered by TBI (105). Collectively, these cascades culminate in inflammation, necrosis and apoptosis, which are pathological hallmarks of TBI.

Neuroinflammation plays a critical role in secondary injury mechanisms and largely contributes to neurodegeneration, neurological impairments and may also be important for recovery after TBI. Injured tissue releases an array of factors including ATP, glutamate, growth factors and cytokines, which in turn promote microglia recruitment and activation (64; 173). In addition, TBI leads to blood-brain barrier (BBB) breakdown; therefore, peripheral immune cells such as macrophages, lymphocytes and neutrophils can also migrate to the site of injury and contribute to the neuroinflammatory response initiated after injury. Activated microglia and immune cells synthesize and release a variety of neurotoxic substances such as chemokines, cytokines, nitric oxide, ROS and reactive nitrogen species (RNS) that contribute to neuronal death and dysfunction (27; 99; 111). Additionally, the release of pro-inflammatory cytokines and other soluble factors by microglia may activate astrocytes leading to formation of astrogliosis (337). Activated microglia and astrocytes are thought to play a dual role in the brain recovery after injury, having both beneficial and harmful functions. Reactive astrogliosis helps the restoration of BBB function and regulation of extracellular glutamate level, which can reduce excitotoxicity after injury (40; 267; 337). Fusion of activated microglia processes at the site of injury forms a containment area between

healthy and injured tissues in an attempt to stop the spreading of ongoing degeneration (64). Moreover both reactive astrogliosis and activated microglia release substances, such as anti-inflammatory cytokines and neurotrophic factors that grant neuroprotection and aid repair after injury (162). On the other hand, reactive astrogliosis inhibits axon regeneration and adds to the already high production of pro-inflammatory cytokines by activated microglia, which leads to cell death (41; 248; 337).

Cell death following TBI occurs in two different waves and has been detected in the underlying cortex, hippocampus, dentate gyrus, thalamus, striatum, corpus callosum and cerebellum (2; 103; 159; 250; 327). During the first wave, which occurs immediately after TBI, neurons die as a consequence of mechanical damage of brain tissue by necrosis caused by excitotoxicity, metabolic impairment and/or membrane disruption (165). Apoptosis then takes place and gives rise to a second wave of cell death from days to years after the occurrence of TBI. This delayed neuronal loss and is activated by both intrinsic and extrinsic factors and depends on energy availability to take place (33; 57; 69; 127).

Although neurodegeneration has been detected in several brain regions following TBI, the temporal lobe is particularly vulnerable to damage due to its anatomical location. It lies over the greater wing of sphenoid bone and therefore is easily damaged when the brain slides against the bone due to acceleration and deceleration forces. It is estimated that 75% of patients that sustained mTBI display some abnormality in the temporal lobe. Moreover, this specific vulnerability is highly correlated to acute and chronic conditions presented by mTBI patients such as cognitive and emotional complaints (297).

ANIMAL MODELS OF TBI

A variety of animal models are available to study TBI. Each one has its own strengths and weaknesses that are summarized in Table 2. These models have been developed in an attempt to improve our knowledge of the molecular cascades triggered by TBI and the resulting pathological and pathophysiological alterations. A brief description of the most widely used models are provided bellow with a concentrated focus on the controlled cortical impact (CCI) model, which is used in the present work.

Model	Strengths	Weaknesses
<i>Weight-drop models</i>		
Feeney's	Biomechanics of injury mechanism are similar to those seen in human TBI	Need for craniotomy; high mortality rate
Shohami's	Device is easy to operate; neurological severity score can be used with model at 1h post-injury to evaluate neurological impairment	Not highly reproducible
Marmarou's	Biomechanics of injury mechanism are similar to those seen in human TBI	Not highly reproducible; high mortality rate following injury without ventilation
<i>Fluid percussion injury models</i>		
Middle	Highly reproducible; allows fine tuning of injury severity	Need for craniotomy; high mortality rate
Lateral	Highly reproducible; allows fine tuning of injury severity	Need for craniotomy; high mortality rate
<i>Controlled cortical impact</i>	Highly reproducible; allows fine tuning of injury severity; low mortality rate	Need for craniotomy
<i>Blast injury</i>	Biomechanics of injury mechanism are similar to those seen in human TBI	Needs standardization

Table 2. Commonly used animal models of TBI.
Modified from (327)

Fluid Percussion Injury

In the fluid percussion injury (FPI) models a craniotomy is performed either centrally around the midline between Bregma and lambda (midline FPI) (74; 192), or over the parietal lobe (lateral FPI) between Bregma and lambda (292). Injury is then produced by the release of a pendulum that strikes the piston of fluid reservoir. Pressure is generated against the intact dura and through the craniotomy fluid flows into the epidural space, leading to compression of the brain tissue (74; 192; 292). In the original FPI model, the only adjustable parameter was the pendulum height, which was directly associated with injury severity. Improvements to this model were made allowing for control of impact pressure and dwell time, thus reducing variation (327).

Weight-drop

In weight-drop models, a rat (87) or a mouse (50) is anesthetized and then has its skull exposed (with or without craniotomy) to a free falling, guided, weight. The severity of brain injury can be easily adjusted by changing the height and mass of the weight used for injury (201; 327).

There are a few variations of the weight-drop model of TBI. In Fenney's weight-drop model the weight is delivered to the intact dura, which causes cortical contusion (87). Shohami's group, on the other hand, proposed a model for closed head injury (CHI) in which the falling weight is released over an intact skull (269; 273). Similarly to Shohami's model, Marmarou et al. proposed another weight-drop model without craniotomy in which a stainless steel disc is mounted to skull to prevent its fracture (95; 182). This model was developed to specifically mimic the injury caused by acceleration/deceleration in TBI's caused by falls and motor vehicles accidents.

Blast-induced TBI

There is incidence of military personnel exposed to a blast being diagnosed with TBI without showing any external injury (22; 317). Therefore several animal models that specifically mimic this modality of TBI have been developed (51; 178; 246; 316). In such models the animal is usually placed inside a shocking tube that generates shock waves comparable to open-field blast waves.

Controlled Cortical Impact

In the controlled cortical impact (CCI) model, a craniotomy is performed in the exposed skull of an anesthetized animal. The exact location of the craniotomy varies between studies but it is usually placed over the parietal bone between Bregma and lambda. A pneumatic or electromagnetic device drives a rigid impactor onto the exposed, intact dura causing a deformation of the underlying cortex (71). The mechanical parameters of the injury (size of impactor, dwell time, depth and velocity of the impact) can be adjusted to generate deformation of different severities that range from mild to severe (97; 106; 258; 320). The ability to control such parameters gives high reproducibility to CCI model and together with low mortality rate is one of the biggest advantages of this model.

The CCI model successfully mimics a variety of alterations observed in humans such as epidural and subdural haematoma, cortical tissue loss, white and gray matter damage and blood-brain barrier dysfunction (71; 171; 172; 276). Neurodegeneration resulting from CCI is not limited to the site of injury and was detected in vulnerable areas such as the underlying cortex, hippocampus, dentate gyrus, thalamus, striatum and corpus callosum. Some studies even observed damage in the contralateral hemisphere and

suggested that this may be the consequence of anterograde and retrograde degeneration of fibers in the callosum and commissural pathway (106; 115; 116; 276). The severity of such pathological changes varies accordingly to the initial cortical deformation caused by the impact. Therefore, CCI may result in mTBI without major structural alteration as well as in severe injury characterized by widespread histopathological damage (71; 106; 115; 116).

Controlled cortical impact has been shown to efficiently induce cognitive and psychiatric impairments in animals. Anxiety-like behaviors (320; 332) and cognitive deficits (72; 73; 97; 320) were observed in animals exposed to CCI, which may last up to one year after TBI, similar to what is observed in mTBI patients. The severity of cognitive deficits is highly related to the depth of deformation and velocity of impact, which is not observed regarding psychiatric impairments (97; 320). Although it is well established that mild models of TBI, in particular CCI, are sufficient to lead to cognitive and psychiatric disorders, the pathological and pathophysiological changes in specific brain regions associated with such impairments are yet to be determined. The amygdala and hippocampus are two target structures to be investigated. First, because they are both localized within the temporal lobe, a region that is more susceptible to damage after TBI (297) and second, because they have demonstrated to play a major role in the pathology of anxiety and cognitive disorders (as previously described), often observed in mTBI patients.

THESIS PROPOSAL

The present work seeks to understand the functional and morphological alterations that occur in the amygdala and hippocampus and underlie the development of psychiatric and cognitive impairments associated with mTBI. **Our long-term goal** is to develop effective and well-tolerated pharmacological strategies for ameliorating symptoms associated with mTBI. **Our central hypothesis is that mTBI alters neuronal excitability in the amygdala and hippocampus and induces permanent morphological changes in these brain regions that lead to the development of anxiety and cognitive impairments.** To test our hypothesis, we propose the use of the CCI model of traumatic brain injury. Exposure to CCI leads to long-term behavioral, anatomical, and functional changes that are consistent with the signs and symptoms of mTBI seen in humans and rodents. Our specific aims are:

Specific Aim 1: To identify changes in gene expression, in the hippocampus, 1, 7 and 30 days after CCI. Alterations in gene expression in the hippocampus may be an underling cause of the acute neuropathology and long-lasting cognitive and psychiatric deficits following mTBI. Here we propose to identify alterations in hippocampal transcriptome after mTBI by microarray analysis and quantitative RT-PCR.

Specific Aim 2: To identify pathophysiological alterations in the GABAergic system, in the amygdala and hippocampus, 1 and 7 days after CCI exposure. Central Nervous System homeostasis relies primarily on the balance between excitatory and inhibitory synaptic transmission within the brain. An increase in glutamatergic and/or a decrease in GABAergic transmission could lead to hyperexcitability, which underlie

neuropsychiatric comorbidities after TBI. Here, we propose to study the pathophysiological alterations in the amygdala and hippocampus that result in neuronal hyperexcitability after CCI. By means of whole-cell recording in amygdalo-hippocampal slices, we will determine changes in GABAergic synaptic transmission caused by CCI-induced brain injury.

Specific Aim 3: To determine morphological and structural alterations underlying TBI-induced hyperexcitability in the amygdala and hippocampus 1 and 7 days after CCI. Using design-based stereology we will investigate morphological alterations in two brain areas: the hippocampus and amygdala. Since loss of GABAergic interneurons would tip the balance between excitation and inhibition, leading to hyperexcitability, we will be particularly interested in examining the pathological alterations of these inhibitory cells. Using design-based stereology combined with GAD67 immunohistochemistry, we will determine the extent of loss of interneurons relative to the total neuronal loss in these brain regions after CCI.

Specific Aim 4: To identify abnormalities in hippocampus-dependent and amygdala-dependent behavioral tasks at 1 and 7 days after CCI. The long-term consequences of mTBI include neuropsychiatric conditions highly associated with hippocampus and amygdala damage. To date, there is no consistent study showing how a hyperexcitable amygdala can alter behavior in rodents after mTBI. To accomplish this aim, acoustic startle reflex, open field and passive avoidance paradigms will be used to test for changes in amygdala-dependent and hippocampus-dependent behavior after CCI.

The accomplishment of the aims described above will lead to a better understanding of the mechanisms underlying the pathology and pathophysiology of

neuropsychiatric disorders associated with TBI and may help with the development of new pharmacological approaches for treating and preventing the development these illnesses.

CHAPTER 2: Temporal course of changes in gene expression suggests a cytokine-related mechanism for long-term hippocampal alteration after controlled cortical impact

ABSTRACT

Mild traumatic brain injury (mTBI) often has long-term effects on cognitive function and social behavior. Altered gene expression may be predictive of long-term psychological effects of mTBI, even when acute clinical effects are minimal, or transient. Controlled cortical impact (CCI), which causes concussive but non-penetrant trauma to underlying brain resulting in persistent changes in hippocampal synaptic function was used as a model of mTBI. The hippocampal transcriptomes of sham-operated or injured male rats at 1, 7 and 30 days post-injury were examined using microarrays comprising a comprehensive set of expressed genes, subsequently confirmed by quantitative RT-PCR.

Transcripts encoding the chemokines Ccl2 and Ccl7, inflammatory mediators Lcn2 and Timp1, immunocyte activators Ccr5 and Fcgr2b, the MHC II immune response-related genes Cd74 and RT1-Da, the complement component C3, and the transcription factor Klf4 were identified as early (Ccl2, Ccl7, Lcn2, Timp1), intermediate (Ccr5, Fcgr2b, Cd74, RT1-Da, C3) and late (Klf4) markers for the bilateral hippocampal response to CCI.

Ccl2 and Ccl7 transcripts were up-regulated within 24 hours after CCI, and their elevation subsided within one week of injury. Other transcriptional changes occurred later and were more stable, some persisting for at least one month, suggesting that short-term inflammatory responses trigger longer-term alteration in the expression of genes previously associated with injury, ageing, and neuronal function in the brain. These transcriptional responses to mTBI may underlie long-term changes in

excitatory/inhibitory neuronal imbalance in hippocampus leading to the long-term behavioral consequences of mTBI.

INTRODUCTION

Traumatic brain injury (TBI) has a high incidence in both the civilian and military populations, albeit distributed somewhat differently between age and gender. The CDC (Center for Disease Control and Prevention) estimates that each year 1.7 million people in the United States sustain a TBI. Most TBI occurs as a result of falls (35.2% of total), followed by vehicular accidents (17.3%) in the civilian population (60) and as a result of injuries from both penetrating and non-penetrating ordnance among soldiers. A significant fraction of TBI (up to 80%) is considered mild (mTBI) and is the result of concussive non-penetrating insult such as that caused by blast overpressure following exposure to improvised explosive devices, or by a high-impact blow to the head. Mild TBI (mTBI) is characterized by a brief period of unconsciousness, with no signs of brain injury upon neuroimaging, but is associated with subsequent cognitive, emotional, or memory dysfunction. Mild TBI is an hypothesized cause of post-traumatic stress disorder (PTSD) in both civilian (121) and military (134) populations.

Models for mTBI are not easily established, and they include focused exposure to pressurized air (blast overpressure; BoP) (48); actual blast exposure (254), closed head injury (CHI) (93), fluid percussion in which injury is administered by a column of liquid (74) and controlled cortical injury (CCI). The CCI model aims to overcome the limitations of closed head injury, including lack of reproducibility of actual impact effects due to irregularities in rodent cranial surface features, by the administration of a partially penetrating injury to the surface of the brain via an aperture in the skull. In CCI, injury is administered by a metal piston (71) to the cortical surface. Methodological considerations may favor one model or the other to address a specific research question.

The major concern about the applicability of each type of CCI is that it represents a continuum of penetrating (to the region of the brain closest to the source of impact) and non-penetrating (regions of the brain distant from the site of impact) insult to the brain. It is therefore critical to specify whether the sequelae of injury examined are direct (i.e. modeling TBI) or indirect (i.e. modeling mTBI).

In the study described here, we have employed metal piston CCI (which we will henceforth refer to simply as CCI) as a model for mTBI as transmitted to the hippocampus. We have first established that the degree of insult is indeed non-penetrating to the hippocampus, and then examined altered expression of all known transcripts encoded within the hippocampus at one, seven and 30 days after injury. The patterns of altered gene expression, and their bilaterality after unilateral CCI, suggest that CCI is indeed an appropriate model for mTBI. They further indicate that neuroinflammatory mechanisms after concussive injury might contribute to long-term changes in the brain leading to impairment in the hippocampus, a major brain center for memory and cognitive processing.

MATERIALS AND METHODS

Animals

Experiments were performed using male Sprague–Dawley rats (Taconic Farms, Rockville, MD, USA), 5–6 weeks old, weighing 150–200 g at the start of the experiments. Animals were pair-housed until the day of the surgery and then housed individually in an animal facility approved by the Association for Assessment and Accreditation of Laboratory Animal Care, in an environmentally controlled room (20–23°C, 12-h light/dark cycle, lights on 7:00 AM), with food and water available ad

libitum. All animal use procedures were in accordance with the National Institutes of Health Guide for the Care and Use of Laboratory Animals, and were approved by the Animal Care and Use Committee of the Uniformed Services University of the Health Sciences. All efforts were made to minimize the number of animals used and their suffering

Controlled Cortical Impact (CCI) surgery

Following five days of acclimatization, the rats were submitted to unilateral cortical contusion using the controlled cortical impact (CCI) model of traumatic brain injury. The animals were anesthetized with isoflurane (2.5%) delivered by nose cone, the skull shaved and the head placed in a stereotaxic frame. The skull was exposed using a small surgical incision over the scalp. A 4.0 mm hole was drilled in the skull at 3.0 mm lateral from the midline and 4.0 mm posterior to bregma over the left tempoparietal cortex. The overlying portion of bone was carefully removed with no disruption of the dura. Each animal received a single impact of 2.0 mm depth of deformation using an impact tip of 3 mm in diameter with an impact velocity of 3.5 m/sec and a dwell time of 200 ms. After the impact, the bone was replaced and fixed using bone wax, and the incision was closed with absorbable sutures. After surgery the animals received Ringer's solution (5 mL) subcutaneously for rehydration. A group of sham injured rats underwent identical craniotomy procedures without CCI injury. Body temperature was maintained at 37 ± 0.5 °C using a heating pad coupled to a rectal probe.

Fixation and Tissue Processing

Rats subjected to CCI or sham surgery were used for histological studies as follows. One, seven or 30 days after the surgery, rats were deeply anesthetized using

Nembutal (75–100 mg/kg, i.p.) and transcardially perfused with phosphate buffered saline (PBS, 100 ml) followed by 4% paraformaldehyde (250 ml). The brains were removed and post-fixed in 4% paraformaldehyde overnight at 4 °C, then transferred to a solution of 30% sucrose in PBS for 72 h, and frozen in Dry Ice before storage at -80 °C until sectioning. A series of sections containing the rostrocaudal extent of the amygdala was cut at 40 µm intervals on a sliding microtome (Leica Microsystems SM2000R) as previously described (89; 90). Every fifth section was placed in a cryoprotectant solution (30% ethylene glycol and 30% glycerol in 0.05 M sodium phosphate buffer) and stored at -20 °C until processing. Free-floating sections were collected from the cryoprotectant solution, and washed three times for 5 min each. Slices were mounted on a slide, air-dried overnight and processed for Nissl staining with cresyl violet. The sections shown in Figure 2 are representative of sections examined from two CCI animals at one, seven and 30 days, and one sham animal at one, seven and 30 days. Eight CCI and eight sham animals euthanized at seven days post-surgery were used to collect the data for quantitative assessment of cell number in the CA1 region of the hippocampus (see *Stereological Quantification*, below).

Stereological Quantification.

CA1 is the part of the hippocampus in closest proximity to the area of cortical impact in our CCI model, and was therefore used as a representative sub-domain of the hippocampus in which valid assessment of cell number within the entire region, as a function of injury, could be obtained using design-based stereology in Nissl-stained sections (89). Sections were viewed with a Zeiss (Oberkochen, Germany) Axioplan 2ie

fluorescent microscope with a motorized stage, interfaced with a computer running StereoInvestigator 9.0 (MicroBrightField, Williston, VT). The CA2 region was identified on slide-mounted sections and delineated for each slide of each animal, under a 2.5X objective, based on the atlas of Paxinos and Watson (222). All sampling was done under a 63X oil immersion objective. Nissl-stained neurons were distinguished from glial cells by their larger size and pale nuclei surrounded by darkly stained cytoplasm containing Nissl bodies. The total number of Nissl-stained neurons was estimated by using the optional fractionator probe, and, along with the coefficient of error (CE) were calculated by using StereoInvestigator 9.0 (MicroBrightField). The CE was calculated using MicroBrightField software according to the equations of Gundersen et al ($m=1$)(113) and Schmitz and Hof (second estimation)(266). For Nissl-stained neurons in the CA1, a 1-in-10 series of sections was analyzed (seven sections on average). The counting frame was 20 X 20 μm , the counting grid was 250 X 250 μm , and the dissector height was 10 μm . Nuclei were counted when the cell body came into focus within the dissector, which was placed 2 μm below the section surface. Section thickness was measured at every counting site (average mounted section thickness 25.7 μm). An average of 234 neurons per hemisphere per rat were counted. Eight rats per group were analyzed, and the average CE was 0.07 for both Gundersen et al. and Schmitz-Hof equations.

RNA Extraction, Microarray Procedure and Analysis

Left and right hemispheric dorsal hippocampus was removed from the brains of 200 gram male rats subjected to CCI or sham surgery (24 experimental animals comprising six groups—CCI day 1, CCI day 7, CCI day 30, sham day 1, sham day 7 and

sham day 30—with n=3 per group for Affymetrix array and n=4 per group for Illumina array). Tissues were snap frozen on Dry Ice and stored until RNA isolation. Total RNA was extracted using an ultrasonic processor (GE 130PB, Hielscher Systems) and a commercial kit (RNAqueous, Ambion) according to the manufacturer's instructions and quantified by spectrophotometry. RNA was processed for Illumina and Affymetrix array after Bioanalyzer (Agilent, Inc.) determination of quantity and quality. All samples used had RNA integrity number greater than 7.3; Illumina RatRef-12 Expression BeadChip (Cat# BD-27-303) and Affymetrix GeneChip Rat Gene 1.0 ST (Cat# 901173) arrays were used for hybridization.

Samples for Illumina microarray were processed by preparing biotinylated cRNA using an Illumina Total Prep RNA Amplification Kit (Ambion, Austin, TX). Briefly, 5 µg of total RNA from the ipsilateral dorsal hippocampus was converted to double stranded cDNA using T7-oligo (dT) primers, followed by an in vitro transcription (IVT) reaction to amplify biotinylated cRNA as described in the manufacturer's instructions (Illumina Inc., San Diego, CA). The biotinylated cRNA was hybridized to a RatRef-12 Expression BeadChip platform that contains 22,523 probes (Illumina Inc.). The hybridization, washing, and scanning were performed according to the manufacturer's instructions. The chips were scanned using an Illumina Bead Chip Scanner.

For Affymetrix microarray chips processing samples were prepared according to Affymetrix protocols (Affymetrix, Inc). 300 ng of total RNA from the ipsilateral dorsal hippocampus was used per labeling reaction, in conjunction with the Affymetrix-recommended protocol 'One-Cycle Target Labeling and Control Reagents'. Hybridizations were performed with three sets of arrays with labeled RNA from either

untreated samples (Sham) or from treated samples (CCI). The hybridization cocktail containing the fragmented and labeled cDNAs was added to the Affymetrix GeneChip, and chips were washed and stained by the Affymetrix Fluidics Station using the standard format and protocols as described by Affymetrix. The probe arrays were stained with streptavidin phycoerythrin solution (Molecular Probes, Carlsbad, CA) and enhanced by using an antibody solution containing 0.5 mg/mL of biotinylated anti-streptavidin (Vector Laboratories, Burlingame, CA). An Affymetrix Gene Chip Scanner 3000 was used to scan the probe arrays.

The Affymetrix and Illumina scanned arrays were analyzed using Partek Genomic suite following the vendors' recommendations. For Affymetrix arrays, 'Robust Multichips Analysis' (RMA) normalization was used followed by Student's t test to determine significantly up or down regulated genes. A subset of genes was selected whose expression was altered after CCI at least or greater than 1.5 fold ($p \leq 0.05$, Student's t test, $n = 4$ for each group for Illumina array, $n = 3$ for each group for Affymetrix array) at one, seven and 30 days post-injury, and annotated using the latest annotation files from <http://www.affymetrix.com>.

Bioinformatic Analysis

Using Ingenuity Pathway Analysis tool (IPA) (<http://www.ingenuity.com/>), the transcripts up-regulated 1.5-fold or more after CCI in rat hippocampal tissue, were clustered based on their functions. Genes were also clustered based on their distribution in significant canonical pathways. Both indirect and direct networks were built using the default settings to identify interacting gene products.

qRT-PCR

Microarray results were validated by quantitative reverse transcription-polymerase chain reaction (qRT-PCR) using the same RNA samples as those used for the microarray. Approximately 2 µg of total RNA from both ipsilateral and contralesional dorsal hippocampus was submitted to DNase I (RNase-free; Invitrogen) digestion and reverse transcribed using random hexamers pdN6 (Invitrogen) and SuperScript II RNase H⁻ reverse transcriptase (Invitrogen). Splign (<http://www.ncbi.nlm.nih.gov/sutils/splign/splign.cgi?textpage=online@level=form>) was used to identify the exon and intron boundaries. Then Gene-specific forward and reverse primers, listed in Table 3 were designed using Primer 3 input (http://frodo.wi.mit.edu/cgi-bin/primer3/primer3_www.cgi) across exon-exon junctions. Amplicon specificity was confirmed by single, sharp melting curves, and predicted amplicon size by gel electrophoresis, at the end of qRT-PCR. qRT-PCR was performed in a premade reaction mix in the presence of the transcribed cDNA and 10 nM of each specific primers, using the SYBR green chemistry and an iCycler real-time detection system (Bio-Rad, Hercules, CA). Fold changes in mRNA levels were determined by normalizing against a non-variable control transcript, Gapdh, using the $\Delta\Delta C_t$ method (176).

Statistical analysis

For comparisons between two groups a t-test was performed. A p value of <0.05 was taken as statistically significant.

Genes		Primers	
Symbol	Name	Forward	Reverse
Ccl2	chemokine (C-C motif) ligand 2	5'-CCAGAAACCAGCCAACCTCTC-3'	5'-CCGACTCATTGGGATCATCT-3'
Ccl7	chemokine (C-C motif) ligand 7	5'-GCATGGAAGTCTGTGCTGAA-3'	5'-CCGTCCTACCCCTTAGGAC-3'
Cd74	CD74 molecule, major histocompatibility complex, class II invariant chain	5'-AAGAAGTCCCTGGAGGAGAA-3'	5'-GTGTAAGAAGGGCTGAGGAG-3'
C3	complement component 3	5'-ACATCTCCATGATGACTGGC-3'	5'-ACTGGTGGACTTTGAAGGAC-3'
RT1-Da	RT1 class II, locus Da	5'-CACTTGGAGACCTGGTGATA-3'	5'-TGGTCGGGGGAAAGATAGAA-3'
Klf4	kruppel-like factor 4 (gut)	5'-GTGCCCCAAGATTAAGCAAG-3'	5'-GTGACAGTCCCTGCTGTTCA-3'
Bdnf	brain-derived neurotrophic factor	5'-AGCCGAACCTTCTCACATGAT-3'	5'-TGGTCATCACTCTTCTCACC-3'
Ccr5	chemokine (C-C motif) receptor 5	5'-AGAAGGTGAGACATCCGTTT-3'	5'-TACCAGAGAGTAGAGTGCGG-3'
Fcgr2b	Fc fragment of IgG, low affinity IIb, receptor (CD32)	5'-GTTGCCCGTATTGACGATTG-3'	5'-GAGCTTCAGGATGCTTGAGA-3'
Gapdh	glyceraldehyde-3-phosphate dehydrogenase	5'-AGACAGCCGCATCTTCTTGT-3'	5'-CTTGCCGTGGGTAGAGTCAT-3'

Table 3. List of Primers for qRT-PCR

RESULTS

Analysis of TBI severity

To characterize the injury severity caused by our CCI conditions (velocity 3.5 m/s and deformation level 2.0 mm) Nissl staining was performed on coronal brain slices and design-based stereology used to count neurons in ipsilateral and contralateral CA1, the region of the hippocampus in closest proximity to the area of cortical impact in our CCI model. Our results shows that the hippocampus did not show signs of injury or deformation, compared to the sham, either ipsilateral or contralateral to the site of injury induced in cortex by CCI in either gross aspect (Figure 5A), at high power (Figure 5B) or upon neuronal quantification using blinded, computer-assisted stereology (Figure 5C). These data indicate that the CCI conditions used here result in a model for mild traumatic brain injury, a head trauma that usually does not present with discernible cell death in the brain (274).

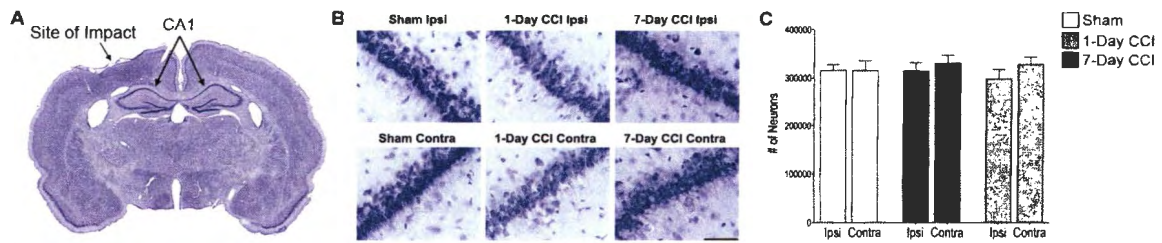


Figure 5. Characterization of injury severity caused by CCI. Mild CCI does not cause a significant loss of neurons in the CA1 region 24 hours or 7 days after injury. (A) Photomicrograph of Nissl-stained brain coronal slice. Indicated are the sites of impact and the ipsilateral and contralateral CA1. (B) Representative photomicrographs from Nissl-stained sections showing BLA cells from the ipsilateral (Top) and contralateral (Bottom) sides of sham, 1-day CCI, and 7-day CCI animals, respectively. Total magnification is 630X; scale bar, 50 μ m. (C) Group data (mean \pm SE; n = 8 for each group) of stereological estimation of the total number of Nissl-stained neurons in the CA1. There were no significant differences in neuronal number between sham and 1-day or 7-day CCI, on either ipsilateral or contralateral sides, using Student's t-test.

Transcriptome Response to CCI

To assess the effect of CCI injury on hippocampal neurons gene transcription we analyzed gene expression changes using two different platforms, a rat microbead Illumina array targeting the 3' ends of approximately 22,000, and a rat gene chip Affymetrix array containing approximately 27,000 genes represented by about 20 probes spread across the full length of the gene. The use of two separate microarray platforms, with differential probe and detection technologies, allowed us to identify with high confidence those transcripts, which were unchanged by CCI (i.e. those transcripts whose abundance was unchanged in *either* microarray platform). Transcripts whose abundance was significantly changed by CCI, but less than 1.5 fold, were discarded (not evaluated) since this represents the group of genes with the highest likelihood of both false positive and false negative results. Transcripts whose abundance was significantly changed by

CCI at one, seven and 30 days post-injury with change magnitude 1.5-fold or more, on either array, were selected for further analysis (Table 4: greatest fold-change in either array is listed).

Gene Name	Symbol	Fold change Day One
chemokine (C-C motif) ligand 2	Ccl2	5.4
chemokine (C-C motif) ligand 7	Ccl7	4.4
TIMP metalloproteinase inhibitor 1	Timp1	2.2
serpin peptidase inhibitor, clade A (alpha-1 antiproteinase, antitrypsin), member 3	Serpina3n	2.2
lipocalin 2	Lcn2	2.1
olfactory receptor 736	Olr736	2.1
cyclin-dependent kinase 1	Cdk1	2.0
cyclin A2	Ccna2	2.0
ring finger protein 213	Rnf213	2.0
PDZ binding kinase	Pbk	1.9
nucleolar and spindle associated protein 1	Nusap1	1.9
NS5A (hepatitis C virus) transactivated protein 9	Ns5atp9	1.8
thyrotropin-releasing hormone	Trh	1.8
olfactory receptor 1421	Olr1421	1.8
t-complex-associated testis expressed 4	Tcte4	1.8
family with sequence similarity 111, member A	Fam111a	1.8
ribonucleotide reductase M2	Rrm2	1.7
TRAF4 associated factor 1	Traf4af1	1.7
activin A receptor, type IC	Acvr1c	1.7
budding uninhibited by benzimidazoles 1 homolog beta (yeast)	Bub1b	1.7
asparaginase homolog (S. cerevisiae)	Aspg	1.7
family with sequence similarity 43, member B	Fam43b	1.6
caspase recruitment domain family, member 11	Card11	1.6
olfactory receptor 486	Olr486	1.6
kinesin family member 11	Kif11	1.6
cadherin 26	Cdh26	1.6
hepatocyte nuclear factor 4, alpha	Hnf4a	1.6
olfactory receptor 1388	Olr1388	1.6
aurora kinase B	Aurkb	1.6
dedicator of cytokinesis 1	Dock1	1.6
vomeroneasal 2, receptor 26	Vom2r26	1.6
heat shock 27kDa protein 1	Hspb1	1.6
5-hydroxytryptamine (serotonin) receptor 3A	Htr3a	1.6
olfactory receptor 1689	Olr1689	1.5
Fc fragment of IgG, low affinity IIIa, receptor (CD16a)	Fcgr3a	1.5
carbohydrate (N-acetylgalactosamine 4-O) sulfotransferase 9	Chst9	1.5
lactase-like	Lctf	1.5
ankyrin repeat domain 23	Ankrd23	1.5
insulinoma-associated 2	Insm2	1.5
kinesin family member 9	Kif9	1.5
gelsolin	Gsn	1.5
toll-like receptor 11	Tlr11	1.5
cyclin B2	Ccnb2	1.5
minichromosome maintenance complex component 3	Mcm3	1.5
germ cell-less homolog 1 (Drosophila)-like	Gmcl1l	1.5
laminin, alpha 2	Lama2	-1.5
olfactory receptor 24	Olr24	-1.5
copine family member IX	Cpne9	-1.5
transmembrane protein 140	Tmem140	-1.5

olfactory receptor 1236	Olr1236	-1.5
thrombospondin 2	Thbs2	-1.5
AI2-like domain 1	A2ld1	-1.6
claudin 22	Cldn22	-1.6
complement component 1, q subcomponent-like 2	C1ql2	-1.6
nescient helix loop helix 1	Nhlh1	-1.6
matrix metalloproteinase 14 (membrane-inserted)	Mmp14	-1.6
enhancer of mRNA decapping 4	Ede4	-1.6
charged multivesicular body protein 4C	Chmp4c	-1.6
apolipoprotein L 9a	Apol9a	-1.6
extracellular matrix protein 2, female organ and adipocyte specific	Ecm2	-1.6
insulin-like 6	Ins16	-1.6
piggyBac transposable element derived 2	Pgbd2	-1.6
growth differentiation factor 15	Gdf15	-1.6
coiled-coil domain containing 129	Ccdc129	-1.7
Fc fragment of IgE, high affinity I, receptor for; alpha polypeptide	Fcer1a	-1.7
ATP-binding cassette, subfamily G (WHITE), member 3-like 3	Abcg313	-1.7
collagen, type VIII, alpha 2	Col8a2	-1.7
neurotrophin 3	Ntf3	-1.7
olfactory receptor 1652	Olr1652	-1.7
methyltransferase like 11B	Mettl11b	-1.7
solute carrier family 13 (sodium/sulfate symporters), member 4	Slc13a4	-1.7
5-hydroxytryptamine (serotonin) receptor 5B, pseudogene	Htr5b	-1.7
synuclein, alpha interacting protein	Sncap	-1.8
claudin 1	Cldn1	-1.8
mitochondrial ribosomal protein S21	Mrps21	-1.8
insulin-like growth factor binding protein 2, 36kDa	Igfbp2	-1.9
apolipoprotein L, 3	Apol3	-2.0
RT1 class I, locus M6, gene 1	RT1-M6-2	-2.2
WD repeat domain 46	Wdr46	-2.5

Gene Name	Symbol	Fold change Day Seven
CD74 molecule, major histocompatibility complex, class II invariant chain	Cd74	5.6
Fc receptor-like S, scavenger receptor	Fcrls	4.7
complement component 3	C3	4.2
myxovirus (influenza virus) resistance 1	Mx1	3.9
RT1 class II, locus Da	RT1-Da	3.7
Fc fragment of IgG, low affinity IIb, receptor (CD32)	Fcgr2b	3.3
solute carrier family 3, member 1	Slc3a1	2.8
protein tyrosine phosphatase, receptor type, C	Ptpcr	2.6
interferon gamma inducible protein 47	Ifi47	2.6
macrophage expressed 1	Mpeg1	2.5
integrin, alpha M	Itgam	2.5
heparan sulfate (glucosamine) 3-O-sulfotransferase 2	Hs3st2	2.4
schlafen 8	Slfn8	2.4
EF-hand calcium binding domain 1	Efcab1	2.4
interferon-induced protein 44-like	Ifi44l	2.4
protein tyrosine phosphatase-like A domain containing 2	Ptplad2	2.4
glycoprotein (transmembrane) nmb	Gpnmb	2.3
egf-like module containing, mucin-like, hormone receptor-like 1	Emr1	2.3
chemokine (C-C motif) receptor 5	Ccr5	2.3
killer cell lectin-like receptor subfamily A, member 1	Klra1	2.3
family with sequence similarity 46, member A	Fam46a	2.3
sodium channel, voltage-gated, type VII, alpha	Scn7a	2.3
CD84 molecule	Cd84	2.3
ribonuclease T2	Rnaset2	2.3
ubiquitin specific peptidase 18	Usp18	2.2
FYN binding protein	Fyb	2.2
meiosis-specific nuclear structural 1	Mns1	2.2

radical S-adenosyl methionine domain containing 2	Rsad2	2.1
membrane-spanning 4-domains, subfamily A, member 6A	Ms4a6a	2.1
receptor (chemosensory) transporter protein 4	Rtp4	2.1
CD180 molecule	Cd180	2.1
serpin peptidase inhibitor, clade G (C1 inhibitor), member 1	Serpig1	2.1
F11 receptor	F11r	2.1
2'-5' oligoadenylate synthetase-like 2	Oasl2	2.1
annexin A3	Anxa3	2.1
lymphocyte antigen 86	Ly86	2.1
CD4 molecule	Cd4	2.1
oxidized low density lipoprotein (lectin-like) receptor 1	Olr1	2.1
complement component 3a receptor 1	C3ar1	2.0
myxovirus (influenza virus) resistance 2	Mx2	2.0
complement component 1, q subcomponent, A chain	C1qa	2.0
phospholipase D family, member 4	Pld4	2.0
CD68 molecule	Cd68	2.0
ephrin-A5	Efna5	2.0
enkurin, TRPC channel interacting protein	Enkur	2.0
interferon regulatory factor 8	Irf8	2.0
heat shock protein 1	Hspb1	2.0
2' -5' oligoadenylate synthetase 11	Oas1i	2.0
tripartite motif-containing 30A	Trim30	2.0
toll-like receptor 3	Tlr3	2.0
5-hydroxytryptamine (serotonin) receptor 2C	Htr2c	2.0
interferon induced with helicase C domain 1	Ifih1	2.0
epithelial stromal interaction 1 (breast)	Epsti1	2.0
schlafen family member 5	Slfn5	2.0
integrin, beta 2	Itgb2	2.0
NCK-associated protein 1-like	Nckap11	2.0
lectin, galactoside-binding, soluble, 3 binding protein	Lgals3bp	2.0
chemokine (C-X-C motif) ligand 16	Cxcl16	2.0
toll-like receptor 7	Tlr7	1.9
TYRO protein tyrosine kinase binding protein	Tyrobp	1.9
dual adaptor of phosphotyrosine and 3-phosphoinositides	Dapp1	1.9
CD53 molecule	Cd53	1.9
pleckstrin	Plek	1.9
G protein-coupled receptor 34	Gpr34	1.9
TIMP metalloproteinase inhibitor 1	Timp1	1.8
coiled-coil domain containing 113	Ccdc113	1.8
cytochrome b-245, beta polypeptide	Cybb	1.8
2'-5'-oligoadenylate synthetase 1A	Oas1a	1.8
lysozyme 2	Lyz2	1.8
lysosomal protein transmembrane 5	Laptm5	1.8
G protein-coupled receptor 183	Gpr183	1.8
galactosidase, beta 1	Glb1	1.8
mediator complex subunit 7	Havcr2	1.8
CD300 molecule-like family member g	Cd300lg	1.8
dedicator of cytokinesis 8	Dock8	1.8
tec protein tyrosine kinase	Tec	1.8
proteasome (prosome, macropain) subunit, beta type, 9 (large multifunctional peptidase 2)	Psmb9	1.8
interleukin 1 receptor-like 1	Il1rl1	1.8
gamma-aminobutyric acid (GABA) A receptor, beta 2	Gabbr2	1.8
unc-93 homolog B1 (C. elegans)	Unc93b1	1.8
nuclear antigen Sp100	Sp100	1.8
purinergic receptor P2Y, G-protein coupled, 12	P2ry12	1.8
2'-5' oligoadenylate synthetase 1B	Oas1b	1.8
alpha-2-macroglobulin	A2m	1.8
ribosomal protein L39	Rpl39	1.8
leucine rich repeat containing 31	Lrrc31	1.8
myosin IF	Myo1f	1.8

complement factor H	Cfh	1.8
complement component 1, s subcomponent	C1s	1.8
CD200 receptor 1	Cd200r1	1.8
leucine-rich repeats and IQ motif containing 1	Lrriq1	1.8
kelch-like 6 (Drosophila)	Klhl6	1.7
interferon, gamma-inducible protein 30	Ifi30	1.7
differential display clone 8	Ddc8	1.7
aldo-keto reductase family 1, member C19	Akr1c19	1.7
sperm associated antigen 6	Spag6	1.7
caspase 4, apoptosis-related cysteine peptidase	Casp4	1.7
RT1 class II, locus Ba	RT1-Ba	1.7
spermatogenesis associated 6	Spata6	1.7
colony stimulating factor 1 receptor	Csf1r	1.7
CD63 molecule	Cd63	1.7
GDNF family receptor alpha 2	Gfra2	1.7
sphingosine-1-phosphate receptor 3	S1pr3	1.7
protein S (alpha)	Pros1	1.7
hemoglobin, beta	Hbb-b1	1.7
CD37 molecule	Cd37	1.7
adenylate kinase 7	Ak7	1.7
chemokine (C-C motif) receptor 2	Ccr2	1.7
SP140 nuclear body protein	Sp140	1.7
lymphocyte cytosolic protein 1 (L-plastin)	Lcp1	1.7
complement component 1, q subcomponent, B chain	C1qb	1.7
C-type lectin domain family 4, member A3	Clec4a3	1.7
DEAD (Asp-Glu-Ala-Asp) box polypeptide 60	Ddx60	1.7
ubiquitin specific peptidase 43	Usp43	1.7
Rho GDP dissociation inhibitor (GDI) beta	Arhgdib	1.7
amyloid beta (A4) precursor protein-binding, family B, member 1 interacting protein	Apbb1ip	1.7
C-type lectin domain family 5, member A	Clec5a	1.7
protein kinase C, theta	Prkcq	1.7
signal transducer and activator of transcription 1, 91kDa	Stat1	1.7
leucine rich repeat containing 34	Lrrc34	1.7
poly (ADP-ribose) polymerase family, member 9	Parp9	1.7
DEAD (Asp-Glu-Ala-Asp) box polypeptide 58	Ddx58	1.7
complement component 1, r subcomponent	C1r	1.7
solute carrier family 15, member 3	Slc15a3	1.6
caspase 1, apoptosis-related cysteine peptidase (interleukin 1, beta, convertase)	Casp1	1.6
transmembrane protein 176A	Tmem176a	1.6
ABO-family member 5	Ggta1	1.6
thioredoxin-related transmembrane protein 4	Tmx4	1.6
interleukin 18 (interferon-gamma-inducing factor)	Il18	1.6
ethanolamine kinase 2	Etnk2	1.6
leucine zipper, putative tumor suppressor 1	Lzts1	1.6
5'-nucleotidase domain containing 3	Nt5dc3	1.6
hexokinase 2	Hk2	1.6
proteolipid protein 2 (colonic epithelium-enriched)	Plp2	1.6
ankyrin-repeat and fibronectin type III domain containing 1	Ankfn1-ps1	1.6
GLI pathogenesis-related 2	Glpr2	1.6
neuron navigator 3	Nav3	1.6
complement component 4B (Chido blood group)	C4-2	1.6
IKAROS family zinc finger 1 (Ikaros)	Ikzf1	1.6
gamma-aminobutyric acid (GABA) A receptor, gamma 1	Gabrg1	1.6
RT1 class II, locus DMb	RT1-DMb	1.6
membrane-spanning 4-domains, subfamily A, member 11	Ms4a11	1.6
cytochrome P450, family 4, subfamily F, polypeptide 18	Cyp4f18	1.6
integrin, alpha L	Itgal	1.6
src kinase associated phosphoprotein 2	Skap2	1.6

ADP-ribosylation factor-like 11	Arl11	1.6
Fc fragment of IgE, high affinity I. receptor for; gamma polypeptide	Fcer1g	1.6
transforming growth factor, beta receptor 1	Tgfbr1	1.6
EF-hand calcium binding domain 7	Efcab7	1.6
granulin	Gm	1.6
neurotensin receptor 1 (high affinity)	Ntsr1	1.6
legumain	Lgmn	1.6
Niemann-Pick disease, type C2	Npc2	1.6
G protein-coupled receptor 65	Gpr65	1.6
C-type lectin domain family 7, member A	Clec7a	1.6
olfactory receptor 237	Olr237	1.6
cytohesin 4	Cyth4	1.6
growth arrest and DNA-damage-inducible, alpha	Gadd45a	1.6
toll-like receptor 2	Tlr2	1.6
colony stimulating factor 3 receptor (granulocyte)	Csf3r	1.6
inositol polyphosphate-5-phosphatase, 145kDa	Inpp5d	1.6
CD244 molecule, natural killer cell receptor 2B4	Cd244	1.6
dedicator of cytokinesis 2	Dock2	1.6
interleukin 13 receptor, alpha 1	Il13ra1	1.6
CD9 molecule	Cd9	1.6
KN motif and ankyrin repeat domains 1	Kank1	1.6
soc-2 suppressor of clear homolog (C. elegans)	Shoc2	1.6
protein tyrosine phosphatase, non-receptor type 6	Ptpn6	1.6
serine peptidase inhibitor, Kunitz type 1	Spint1	1.6
nuclear factor (erythroid-derived 2)-like 2	Nfe2l2	1.6
IK cytokine, down-regulator of HLA II	Ik	1.6
C-type (calcium dependent, carbohydrate recognition domain) lectin, superfamily member 6	Clecsf6	1.6
sema domain, immunoglobulin domain (Ig), short basic domain, secreted, (semaphorin) 3D	Sema3d	1.6
Fc fragment of IgG, low affinity IIa, receptor (CD32)	Fcgr2a	1.6
interleukin 10 receptor, beta	Il10rb	1.6
fatty acid binding protein 7, brain	Fabp7	1.6
tripartite motif containing 5	Trim5	1.6
urotensin 2	Uts2	1.6
hematopoietic prostaglandin D synthase	Hpgds	1.6
v-yes-1 Yamaguchi sarcoma viral related oncogene homolog	Lyn	1.6
AF4/FMR2 family, member 2	Aff2	1.6
poly (ADP-ribose) polymerase family, member 14	Parp14	1.6
NLR family, pyrin domain containing 3	Nlrp3	1.6
RAB20, member RAS oncogene family	Rab20	1.6
F-box protein 39	Fbxo39	1.6
N-acylethanolamine acid amidase	Naaa	1.6
triggering receptor expressed on myeloid cells 2	Trem2	1.6
solute carrier family 39 (zinc transporter), member 10	Slc39a10	1.6
galactosylceramidase	Galc	1.6
guanylate binding protein 2, interferon-inducible	Gbp2	1.6
ubiquitin-conjugating enzyme E2I	Ube2i	1.6
Ras association (RalGDS/AF-6) domain family member 4	Rassf4	1.5
coiled-coil domain containing 40	Ccdc40	1.5
transmembrane protein 176B	Tmem176b	1.5
RT1 class II, locus Bb	RT1-Bb	1.5
transforming growth factor, beta receptor II	Tgfbr2	1.5
hexosaminidase B (beta polypeptide)	Hexb	1.5
serpin peptidase inhibitor, clade B (ovalbumin), member 9	Serpinb9	1.5
plexin B2	Plxn2	1.5
lysine-rich coiled-coil 1	Krcc1	1.5
C-type lectin domain family 2, member G	Clec2g	1.5
FK506 binding protein 14, 22 kDa	Fkbp14	1.5
coiled-coil domain containing 111	Ccdc111	1.5
solute carrier family 12 (sodium/potassium/chloride transporters), member 2	Slc12a2	1.5

Bruton agammaglobulinemia tyrosine kinase	Btk	1.5
magnesium transporter 1	Magt1	1.5
cathepsin D	Ctsd	1.5
solute carrier family 2 (facilitated glucose/fructose transporter), member 5	Slc2a5	1.5
dynein, axonemal, light chain 1	Dnal1	1.5
moesin	Msn	1.5
interferon-induced protein 44	Ifi44	1.5
RAB3B, member RAS oncogene family	Rab3b	1.5
calcyphosine 2	Caps2	1.5
cullin 4B	Cul4b	1.5
transcobalamin II	Tcn2	1.5
tetratricopeptide repeat domain 25	Ttc25	1.5
cyclin-dependent kinase 6	Cdk6	1.5
lectin, galactoside-binding, soluble, 3	Lgals3	1.5
cholinergic receptor, muscarinic 2	Chrm2	1.5
family with sequence similarity 46, member C	Fam46c	1.5
tetraspanin 8	Tspan8	1.5
complement component 1, q subcomponent, C chain	C1qc	1.5
vomerionasal 1 receptor 51	V1ra14	1.5
toll-like receptor 4	Tlr4	1.5
WAP four-disulfide core domain 6B	Wfdc6b	1.5
septin 9	Sept9	1.5
B-cell linker	Blnk	1.5
RAS guanyl releasing protein 3 (calcium and DAG-regulated)	Rasgrp3	1.5
olfactory receptor 1177	Olr1177	1.5
tumor necrosis factor (ligand) superfamily, member 10	Tnfsf10	1.5
coagulation factor X	F10	1.5
transmembrane protein 123	Tmem123	1.5
tripartite motif containing 71	Trim71	1.5
retinal pigment epithelium 65	Rpe65	1.5
solute carrier organic anion transporter family, member 1b3	Slc1b2	-1.5
olfactory receptor 1222	Olr1222	-1.5
collagen, type XVIII, alpha 1	Col18a1	-1.5
complement component 1, q subcomponent-like 2	C1ql2	-1.5
MHC I like leukocyte 1	Mill1	-1.5
galanin receptor 2	Galr2	-1.5
neuromedin B receptor	Nmbr	-1.5
microRNA 138-2	Mir138-2	-1.5
elastin	Eln	-1.5
cornichon homolog 3 (Drosophila)	Cnih3	-1.5
olfactory receptor 1382	Olr1382	-1.5
phospholipase C, epsilon 1	Plce1	-1.5
vomerionasal 2 receptor, 13	Vom2r13	-1.6
alpha-2u globulin PGCL1	Obp3	-1.6
olfactory receptor 1662	Olr1662	-1.6
microRNA 128-1	Mir128-1	-1.6
kelch-like 14 (Drosophila)	Klhl14	-1.6
microRNA 1185-2	Mir154	-1.6
EF-hand domain (C-terminal) containing 2	Efhc2	-1.6
ets variant 3-like	Etv3l	-1.6
olfactory receptor 1366	Olr1366	-1.6
olfactory receptor 781	Olr781	-1.6
T-box 20	Tbx20	-1.6
nuclear receptor subfamily 4, group A, member 1	Nr4a1	-1.6
MLF1 interacting protein	Mif1ip	-1.6
olfactory receptor 1304	Olr1304	-1.6
olfactory receptor 1375	Olr1375	-1.6
POU class 3 homeobox 1	Pou3f1	-1.6
ischemia related factor vof-21	Vof21	-1.6

epithelial stromal interaction 1 (breast)	Epsti1	-1.6
microRNA 95	Mir421	-1.6
prodynorphin	Pdyn	-1.6
microRNA 1185-2	Mir377	-1.7
bone morphogenetic protein 4	Bmp4	-1.7
N-deacetylase/N-sulfotransferase (heparan glucosaminyl) 3	Ndst3	-1.7
fibrinogen C domain containing 1	Fibcd1	-1.7
olfactory receptor 1227	Olr1227	-1.7
thrombopoietin	Thpo	-1.8
potassium channel, subfamily K, member 9	Kcnk9	-1.8
5-hydroxytryptamine (serotonin) receptor 1B	Htr1b	-1.9
lin-28 homolog A (C. elegans)	Lin28a	-1.9
5-hydroxytryptamine (serotonin) receptor 5B, pseudogene	Htr5b	-2.0
chymosin	Cym	-2.0
olfactory receptor 850	Olr850	-2.1
G protein-coupled receptor 151	Gpr151	-3.0
POU class 4 homeobox 1	Pou4f1	-3.3
Gene Name	Symbol	Fold change Day 30
ribosomal protein L30	Rpl30	15.6
CD74 molecule, major histocompatibility complex, class II invariant chain	Cd74	2.4
CART prepropeptide	Cartpt	2.1
protein kinase C, delta	Prkcd	2.1
complement component 3	C3	2.0
cyclin-dependent kinase inhibitor 2B (p15, inhibits CDK4)	Cdkn2b	1.9
solute carrier family 18 (vesicular monoamine), member 2	Slc18a2	1.8
olfactory receptor 1273	Olr1273	1.8
SCAN domain containing 3, pseudogene 2	Scand3-ps2	1.8
olfactory receptor 1689	Olr1689	1.7
neuropilin (NRP) and tolloid (TLL)-like 1	Neto1	1.7
opsin 1 (cone pigments), long-wave-sensitive	Opn1mw	1.6
olfactory receptor 1619	Olr1619	1.6
5-hydroxytryptamine (serotonin) receptor 2C	Htr2c	1.6
heat shock protein 1	Hspb1	1.6
SCY1-like 1 (S. cerevisiae)	Scyl1	1.6
sperm motility kinase 2B	Smok2a	1.6
Fc fragment of IgG, low affinity IIb, receptor (CD32)	Fcgr2b	1.6
arginine vasopressin receptor 2	Avpr2	1.6
macrophage expressed 1	Mpeg1	1.6
olfactory receptor 744	Olr744	1.6
serpin peptidase inhibitor, clade G (C1 inhibitor), member 1	Serping1	1.6
aurora kinase B	Aurkb	1.6
microsomal glutathione S-transferase 1	Mgst1	1.5
kelch-like 4 (Drosophila)	Klhl4	1.5
ArfGAP with coiled-coil, ankyrin repeat and PH domains 2	Acap2	1.5
gamma-aminobutyric acid (GABA) receptor, theta	Gabrq	1.5
ATPase, H+ transporting, lysosomal accessory protein 1-like	Atp6ap1l	1.5
small proline-rich protein 3	Sprr3	1.5
C-type lectin domain family 4, member C	Clec4b2	1.5
activin A receptor, type IC	Acvr1c	1.5
estrogen receptor binding site associated, antigen, 9	Ebag9	-1.5
tubulin, beta 6	Tubb6	-1.5
napsin A aspartic peptidase	Napsa	-1.5
calcineurin B homologous protein 2	Chp2	-1.5
complement component 6	C6	-1.5
membrane protein, palmitoylated 6 (MAGUK p55 subfamily member 6)	Mpp6	-1.5
olfactory receptor 88	Olr88	-1.5
tetraspanin 8	Tspan8	-1.5
tumor necrosis factor receptor superfamily, member 8	Tnfrsf8	-1.5

poly(A) binding protein interacting protein 1	Paip1	-1.5
GA binding protein transcription factor, alpha subunit 60kDa	Gabpa	-1.6
ribosomal protein L10-like	Rpl10l	-1.6
NAD(P)H dehydrogenase, quinone 2	Nqo2	-1.6
origin recognition complex, subunit 4	Orc4	-1.6
olfactory receptor 1164	Olr1164	-1.6
5-hydroxytryptamine (serotonin) receptor 5A	Htr5a	-1.6
EGF-like, fibronectin type III and laminin G domains	Egflam	-1.6
neuroepithelial cell transforming 1	Net1	-1.6
olfactory receptor530	Olr530	-1.6
vomerolnasal 1 receptor 70	Vom1r30	-1.6
Wilms tumor 1 interacting protein	Wtip	-1.6
DUF729 domain containing 1	Dufd1	-1.6
vomerolnasal 1 receptor 81	Vom1r81	-1.6
microRNA 100	Mir100	-1.6
piggyBac transposable element derived 2	Pgbd2	-1.7
UDP-N-acetyl-alpha-D-galactosamine:polypeptide N-acetylgalactosaminyltransferase-like 6	Galnt16	-1.7
ATP-binding cassette, subfamily G (WHITE), member 3-like 3	Abcg313	-1.7
thyrotropin-releasing hormone receptor	Trhr	-1.7
flavin containing monooxygenase 3	Fmo3	-1.7
microRNA let-7a-1	Mirlet7f-1	-1.7
Kruppel-like factor 4 (gut)	Klf4	-1.7
iroquois homeobox 5	Irx5	-1.7
olfactory receptor 260	Olr260	-1.8
Kruppel-like factor 2 (lung)	Klf2	-1.8
keratin 33A	Krt33b	-1.8
solute carrier family 36 (proton/amino acid symporter), member 2	Slc36a2	-1.9
cadherin 12, type 2 (N-cadherin 2)	Cdh12	-1.9
mesothelin	Msln	-2.2
carboxypeptidase X (M14 family), member 2	Cpxm2	-2.4
family with sequence similarity 180, member A	Fam180a	-2.5
proteoglycan 4	Prg4	-3.2
chemokine (C-C motif) ligand 19	Ccl19	-3.3
coagulation factor C homolog, coxlin (Limulus polyphemus)	Coch	-3.5
nuclear protein, transcriptional regulator, 1	Nupr1	-3.8
troponin T type 2 (cardiac)	Tnnt2	-4.1

Table 4. List of significantly changed genes in both Illumina and Affymetrix platforms

Using IPA analysis, the genes changed in each condition (listed in Table 3) were tiled according to their function. Our results show that by day one about a third of the up-regulated genes fell into a cluster related to inflammatory response. Among these, two chemokines Ccl2 and Ccl7 known to be increased in the central nervous system in several neurodegenerative diseases (59; 242) were highly up-regulated (more than 5-fold) at one day post-CCI. Chemokines are a family of structurally related cytokines that activate and recruit leukocytes into areas of inflammation (101; 174; 338).

Both microarrays also show that lipocalin 2 (Lcn2) and tissue inhibitor of metalloproteinase-1 (Timp1) mRNA were significantly up-regulated 24 hours after CCI. Both transcripts encode acute phase proteins up-regulated via various pro-inflammatory stimuli, including TNF- α (101; 174). Lcn2 is induced by TNF- α in cortical neurons solely via its type 1 receptor, and is significantly decreased in cerebrospinal fluid (CSF) of patients with mild cognitive impairment (MCI) and AD and increased in brain regions associated with AD pathology in human brain (210).

By day seven and 30 the set of transcripts characteristic of acute inflammation response is no longer up-regulated and instead a new set of genes associated with complement system, dendritic cell maturation, T cell differentiation and with major histocompatibility complex II (MHC II) pathway, such as complement components (C3, Serping1), immune cell-activating factors (Ccr5, Fcgr2b) and MHC II components (Rt1-Da and Cd74) were up-regulated in the CCI animals compared to Sham. Along with prolonged elevation of MHC II-related transcripts, there occurs a stably altered expression of mRNAs encoding several neuron-specific transcripts, such as regulator of axon guidance (Nav3), neuropeptide CART (Cartpt), monoamine transporter VMAT2 (Slc18a2), and GABAergic receptors (Gabrg1, Gabrb2) (Table 3), with implications for the balance of excitatory and inhibitory transmission in hippocampus.

The clustering of the down-regulated genes, on the other hand, seems to be more disparate. It is noteworthy that several transcripts that are down-regulated after one day of injury, such as those encoding laminin alpha 2, thrombospondin 2, nescient helix loop helix 1, growth differentiation factor 15, neurotrophin 3 (Ntf3), and synuclein alpha interacting protein, are involved in development and function of the nervous system. At

day seven and 30 transcripts encoding transcription factors such as Pou3f1 and Pou4f1 (day seven) or Nupr1 Klf4, Klf2 and Gabpa (day 30) are mainly tiled in a cluster related to cell survival/death.

IPA was used to determine whether the sets of transcripts that were increased at days one, seven and 30 after CCI were related within any known signaling networks. At day one, a group of NF- κ B-responsive genes made up the most prominent cohort of regulated transcripts, with several being known targets of signaling by TNF- α acting through the TNFR1 receptor (Figure 6A; TNF- α -responsive genes indicated with bold arrows). At day seven, the high-scoring network was also associated with inflammation and revealed prominent contributions to gene regulation via signaling through Stat1, ERK, and Irf8 (Figure 6B). By day 30, no inflammation-associated networks were significantly represented, and the network scoring highest was one for cell-cell interaction (Figure 6C).

A



B



B



Figure 6. Regulatory networks for CCI-dependent transcripts in rat hippocampal tissue. Transcripts with an abundance of 1.5 or greater in cortically injured (CCI) male rats at 1, 7 and 30 days post-injury compared to sham-operated by microarray analysis (see Table 3) were used as the input for analysis of potential networks using the signal transduction knowledge environment of Ingenuity (<http://www.ingenuity.com>). A, B, and C are the highest score networks involving the CCI-up-regulated transcripts at day one, seven and 30 respectively. CCI-regulated transcripts are depicted in gray and linked components in white. Circular lines above symbols indicate auto-regulation; connecting lines without arrows indicate direct protein interaction; dashed and solid arrows indicate indirect (e.g. regulation of mRNA levels) and direct (e.g. enzymatic) activation.

Analysis of mRNA levels in hippocampus following TBI

We then confirmed the validity of positive microarray results by measuring independently, with qRT-PCR, the effect of CCI on Ccl2 and Ccl7 mRNA expression. As observed with microarray, our results show that transcriptome changes after CCI were multiphasic. Within 24 hours after CCI, levels of transcripts Ccl2, Ccl7 were elevated, and were no longer up-regulated by day seven and 30. Significantly, up-regulation of both Ccl2 and Ccl7 occurred on both sides of the injured brain, suggesting a response to global concussive injury, rather than local unilateral physical impact at the site of injury (Figure 7A-D). To assess the intermediate and later effect of CCI we expanded the quantification to genes that significantly changed at seven (Cd74, C3 and Rt1-Da) and 30 days (Cd74, C3 and Klf4) and measured the mRNA changes of these transcripts by qRT-PCR (Figure 8). Our data show that Cd74, C3 and Rt1-Da are significantly stimulated, in a range from 9- to 20-fold, seven days post injury (Figure 8A, B and C) and remain persistently up-regulated at 30 days post CCI (Figure 8A and B), while Klf4 mRNA levels are significantly down-regulated (Figure 8D). Transcripts for Ccr5 and Fcgrb2 were also significantly up-regulated at day 7 after CCI (data not shown).

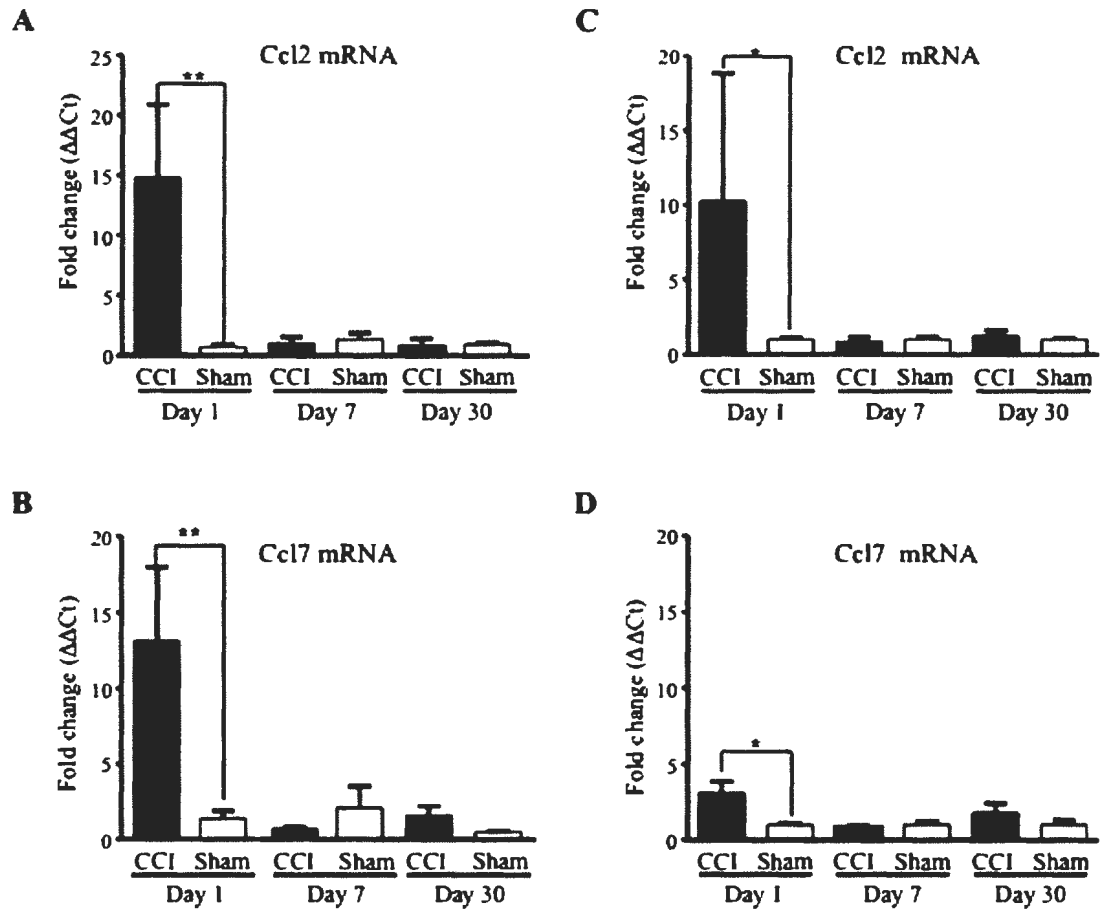


Figure 7. Chemokine transcripts up-regulation in hippocampal tissue from the ipsilateral (i.d.) dorsal or contralateral (c.d.) dorsal side of sham-operated (Sham) or cortically injured (CCI) male rats at 1, 7 and 30 days post-injury. Ccl2 (A, i.d. and C, c.d.) and Ccl17 (B, i.d. and D, c.d.) mRNA levels, determined by qRT-PCR, are expressed as fold increase over corresponding control values and represent means \pm SEM of 3 samples (animals) for each condition. * $p < 0.05$; vs. the corresponding control (Student's t test).

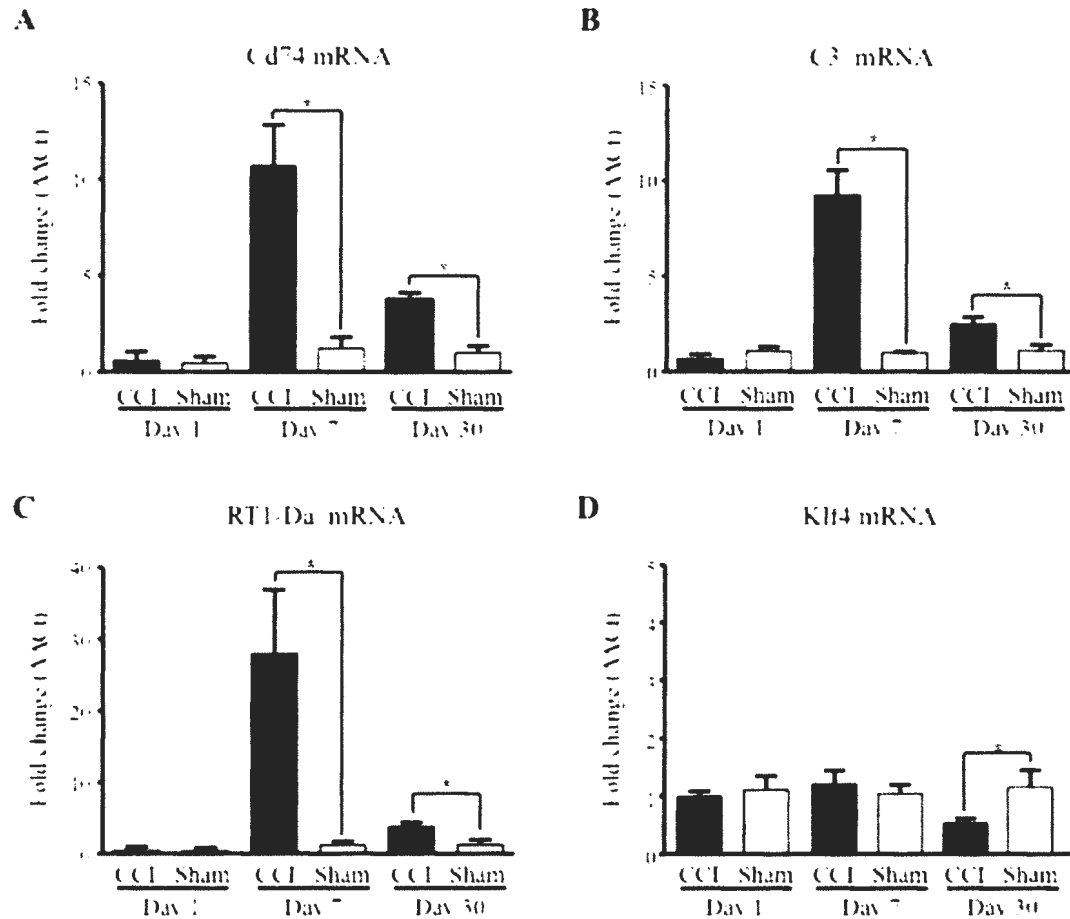


Figure 8. Intermediary and longer-term transcriptome changes after CCI. Cd74 (A), C3 (B), RT1-Da (C) and Klf4 (D) mRNA levels, determined by qRT-PCR, are expressed as fold increase over corresponding control values and represent means \pm SEM of 3 samples (animals) for each condition. *, $P < 0.05$; **, $P < 0.01$; vs. the corresponding control (Student's t test).

We examined in particular the expression of transcripts from the BDNF gene, as BDNF expression has been implicated in recovery from various insults to the hippocampus (275). The BDNF transcript is one that is expressed via multiple promoters in CNS and thus it is possible that a specific BDNF transcript from one of these, in a particular cell type in hippocampus, would be elevated but that this increase would be

lost in measurement of total BDNF mRNA changes after CCI. Since gene expression can be examined in single-exon detail using the data obtained from the Affymetrix array platform, this analysis was also performed. No single 5' or 3' untranslated exons of the BDNF gene were elevated in hippocampus after CCI.

DISCUSSION

The present study highlights the hippocampal transcriptome changes that can occur after an acute exposure to mild traumatic brain injury. mTBI is the most common form of traumatic brain injury worldwide and is defined as a biomechanically induced brain injury characterized by the absence of gross anatomic lesions and without causing any neuronal loss (35; 298; 311). Our data shows that the energy of impact applied in our model of CCI provokes a mild deformation of the rat cortex with the impact lesion fairly localized to the immediate cortical area, and without structurally affecting other areas of the brain such as the hippocampus. Thus, CCI under these conditions appears to be an appropriate model for mTBI as manifested clinically. The results from our study show that mTBI pathophysiology involves alterations in the expression levels of transcripts coding for molecules involved in immune response, intracellular signaling, and cell death and cell survival. This is consistent with the likely complex signaling events that occur after mTBI, that are likely to involve, at least initially, inflammatory events.

TBI has been reported to cause elevation in mRNA encoding the neurotrophin BDNF in hippocampus (130; 185), consistent with a contribution to survival and morphological plasticity of hippocampal neurons by this neurotrophic molecule (329). In our study, no changes in the abundance of BDNF mRNA occurred following mTBI, although we cannot rule out very transient alterations immediately after TBI. These results highlight a qualitative difference between the expression profile following mild, compared to moderate or severe (332), TBI. On the other hand, microarray analysis indicated that transcripts for neurotrophin-3 (Ntf3) are decreased within one day of CCI,

suggesting the possibility that decreased expression of this neurotrophin may be a part of the deleterious sequelae of mTBI.

Neuroinflammation is implicated in the cognitive deficits that accompany neurodegenerative conditions and brain insults (e.g., TBI and sepsis) (34; 63; 110; 151). This damage can be progressive, evolving from hours to days after the initial trauma. It may be associated with compromise of the blood brain barrier, permitting extravasation of circulating neutrophils, monocytes and lymphocytes into the brain parenchyma. Inflammatory factors released by these infiltrating immune cells as well as resident microglia can increase cell death and secondary tissue damage but also lead to less obvious changes in brain function (165; 339). The pro-inflammatory cytokines interleukin-1, TNF- α , and interleukin-6 have been reported to be involved in TBI, and are released within minutes after challenge (165; 203; 339), triggering inflammatory reactions by up-regulation of adhesion molecules, release of chemotactic chemokines, and activation of inflammatory cells (47). Our microarray analysis did not show any increase in pro-inflammatory cytokine mRNAs in hippocampus, perhaps because these genes are very transiently expressed in mTBI. However, transcripts encoding mediators such as Ccl2, Ccl7, Lcn2 and Timp1, known to be involved in acute inflammation under the control of TNF- α , are substantially increased after CCI. Importantly, increases in the mRNAs encoding these inflammatory factors were elevated bilaterally after CCI, further confirming that unilateral cortical impact is likely transmitted via a concussive energy transfer as occurs typically in mTBI, rather than via spreading of inflammatory signaling directly from the site of the impact injury due to

penetration of the blood brain barrier, glial activation, or macrophage infiltration specifically at that location.

Ccl2 and Ccl7 (also called MCP-1 and MCP-3, for monocyte/macrophage chemoattractant proteins) are reported to be produced by astrocytes, and in some cases neurons, within the injured brain (125; 243; 293). In chronic degenerative diseases, they may be associated with recruitment of mononuclear cell infiltrates into the brain (194; 242; 315). However here, the return to normal levels of the bilateral increase of Ccl2 and Ccl7 mRNA levels within a week after injury suggests a short-term inflammatory response with subsequent triggering of longer-term alteration of brain function.

The expression of a discrete set of inflammatory mediators is increased, but only after several days, in CCI/mTBI. These include the neuroinflammatory markers Cd74 and the MHC II-associated genes C3, Ccr5, Fcgr2b, and Rt1-Da. This pattern of expression suggests that up-regulation of these genes by earlier chemokine expression may represent a mechanism whereby a transient insult is registered as a permanent, or at least long-term, effect on the hippocampus. It is noteworthy that each of these transcripts is reported to be increased in the ageing hippocampus (303). A linkage between the expression of Cd74 and MHC II-associated transcripts, and regulation of transcription factors such as Klf4 and other neuron-specific transcripts in hippocampus (this study) on the one hand, and functional alterations in inhibitory neurotransmission in hippocampus and amygdala, on the other (5), has yet to be established.

This study suggests an underlying mechanism for long-term effects on hippocampal function mediated by endogenous chemokine expression in hippocampus.

Although the initial mediator of this effect has not been identified, the strong up-regulation of the chemokines Ccl2 and Ccl7, in addition to Lcn2 and Timp1 suggests regulation via NF- κ B, likely in response to TNF- α in neurons and/or astrocytes as noted in other studies (38; 210; 293). This is consistent with the report that injury associated with TBI is ameliorated by administration of an inhibitor of TNF- α biosynthesis, 3,6-dithiothalidomide (15). Further investigation of this potential cytokine/chemokine cascade in propagation of damage caused by concussive injury to the brain is a promising avenue for understanding and treatment of the long-term sequelae of mild traumatic brain injury.

ACKNOWLEDGEMENTS

We thank Charisse Winston (NIMH-IRP Technical IRTA) and Dr. Babru Samal (NIMH Bioinformatics Core Specialist), for contributions to early phases of this work, and Dr. Abdel Eklahloun (Core Manager, NIHGRI-NIMH-NINCDS Microarray Core Facility) for invaluable assistance and consultation throughout the duration of these experiments. The contributions of Djida Ait-Ali, who participated in the project as a Henry J. Jackson Research Fellow are acknowledged here in lieu of co-authorship for which her written acquiescence could not be obtained. Work reported here was funded in part by the NIMH Intramural Research Program, and by a grant from the Department of Defense administered through the Center for Neuroscience and Regenerative Medicine.

CHAPTER 3: Reduced GABAergic Inhibitory Transmission in the BLA and the Development of Anxiety-like Behaviors After mTBI

ABSTRACT

Traumatic brain injury (TBI) is a major public health concern affecting a large number of professional athletes and civilians. Individuals suffering from a TBI risk developing anxiety disorders, yet the pathophysiological alterations that result in the development of anxiety disorders have not yet been elucidated. One region often damaged by a TBI is the basolateral amygdala (BLA); hyperactivity within the BLA is associated with increased expression of anxiety and fear, yet the functional alterations that lead to BLA hyperexcitability after TBI have not yet been elucidated. We assessed the functional alterations in inhibitory synaptic transmission in the BLA and one mechanism that modulates excitatory synaptic transmission, the α_7 containing nicotinic acetylcholine receptor (α_7 -nAChR), after mTBI, to shed light on the mechanisms that contribute to increased anxiety-like behaviors. Seven days after a mild controlled cortical impact (CCI) injury, animals displayed significantly greater anxiety-like behavior. This was associated with a significant loss of GABAergic interneurons and significant reductions in the frequency and amplitude of spontaneous and miniature GABA_A-receptor mediated inhibitory postsynaptic currents (IPSCs). Decreases in the IPSC amplitude were associated with reduced surface expression of $\alpha 1$, $\beta 2$, and $\gamma 2$ GABA_A receptor subunits. However, significant increases in the surface expression and current mediated by α_7 -nAChR, were observed, signifying increases in the excitability of principal neurons within the BLA. These results suggest that mTBI causes not only a significant reduction in inhibition in the BLA, but also an increase in neuronal

excitability, which may contribute to hyperexcitability and the development of anxiety disorders.

INTRODUCTION

Traumatic brain injury (TBI) is a major public health concern in the United States. There are approximately 1.8 million brain injuries annually (86), 90% of which may be classified as mild since patients do not display any clear morphological or functional abnormalities following injury (23; 312). TBI is also a healthcare concern among athletes with approximately 300,000 cases per year (147; 278). While most patients recover fully from mild TBI (mTBI), approximately 10-15% of patients have persistent cognitive, behavioral, and emotional complaints (20; 149; 170; 187). Of increasing concern is the prevalence of anxiety disorders after mTBI. Recent reports suggest that approximately 23% of individuals that sustain mTBI are at risk for developing anxiety disorders, and, particularly in the military, mTBI significantly increases the risk of developing posttraumatic stress disorder (PTSD) (134; 195).

Although clinical profiles of TBI are variable, mild and moderate TBI have been frequently localized to medial temporal lobe regions including the amygdala and are associated with long-term psychiatric symptoms (143; 297; 333). The amygdala is a limbic structure deep within the temporal lobe that is involved in processing emotion and regulating behavioral and physiological responses to stressors (36; 149). Amygdalar hyperactivity has been observed in the majority of functional neuroimaging studies investigating anxiety disorders (135). In addition, after blast induced TBI, bilateral amygdalar hyperactivity has been observed in U.S. soldiers (184). Thus, amygdalar dysfunction after a TBI, and in particular, neuronal hyperexcitability and hyperactivity in

the basolateral nucleus of the amygdala (BLA), may be a key feature in the pathology of anxiety disorders, including PTSD in TBI victims (66; 81; 134; 237; 272). Although it is well established that anxiety disorders are more prevalent after mTBI, no study to date has identified the functional and morphological alterations that take place in the BLA underlying hyperexcitability after mTBI.

The purpose of this study is to examine alterations in inhibitory synaptic transmission in the BLA after mTBI that contribute to increased hyperactivity and subsequently, the development of anxiety-like behaviors. To this end, we have examined whether a mild controlled cortical impact (CCI) reduces GABA_A receptor mediated inhibitory postsynaptic currents (IPSCs) in the BLA via interneuronal death or alterations in the surface expression of the $\alpha 1$, $\beta 2$, or $\gamma 2$ GABA_A receptors subunits. In addition, we have determined the effects of CCI on the surface expression and activity of $\alpha 7$ -containing nicotinic acetylcholine receptors ($\alpha 7$ -nAChRs), which are present on somatodendritic regions of glutamatergic neurons in the BLA (153), are involved in presynaptically facilitating glutamate release (16), and have previously been found to induce anxiogenic effects (219). Our results suggest that mTBI increases anxiety-like behaviors, and that this may occur by injury-related deficits to inhibitory synaptic transmission. In addition, increased surface expression and ionic flow through $\alpha 7$ -nAChRs on glutamatergic neurons may also contribute to hyperexcitability within the BLA and to long lasting increases in anxiety-like behavior.

EXPERIMENTAL PROCEDURES

Animals

Experiments were performed using 5-6 week old male, Sprague–Dawley rats (Taconic Farms, Rockville, MD, USA). Animals were housed in pairs until the day of the surgery and then housed individually in an environmentally controlled room (20-23°C, ~44% humidity, 12-h light/12-h dark cycle [350-400 lux], lights on at 6:00 am), with food (Harlan Teklad Global Diet 2018, 18% protein rodent diet; Harlan Laboratories; Indianapolis, IN) and water available *ad libitum*. Cages were cleaned weekly and animal handling was minimized to reduce animal stress (231). All animal experiments were conducted following the Guide for the Care and Use of Laboratory Animals (Institute of Laboratory Animal Resources, National Research Council) and were in accordance with the guidelines and approved by the Uniformed Services University of the Health Sciences Institutional Animal Care and Use Committees (IACUC). All efforts were made to minimize the number of animals used and any pain or distress associated with these experiments.

Controlled Cortical Impact Injury

A unilateral cortical contusion using the controlled cortical impact (CCI) model of traumatic brain injury was administered using a previously established protocol (171). Briefly, animals were anesthetized with isoflurane (2.5%) and had their heads shaved and placed in the stereotaxic frame. Core body temperature of the animals was maintained at 36-37°C using a heating pad and D.C. Temperature Control System (FHC, Bowdoin, ME). Without damaging the underlying dura mater, the skin was retracted, and a 4.0 mm craniotomy – 3.0 mm lateral to the midline and 4.0 mm posterior to the bregma over the

left tempoparietal cortex – was performed. In these experiments, the contact velocity was set to 3.5 m/sec with a dwell time of 200 ms and the amount of deformation was set to 2.0 mm using a 3.0 mm diameter impact tip. These parameters have been shown to result in mild traumatic brain injury, i.e. causing no immediate trauma-induced cell death in areas contralateral to the impact, or even ipsilateral and subjacent to the cortical impact area (6). Following injury, the skullcap was replaced and fixed using bone wax (Ethicon, Sommerville, NJ) and the incision was closed with absorbable sutures (Stoelting, IL). The animals received subcutaneously buprenorphine (50 μ L) for pain alleviation and Ringer's solution (5 mL) for rehydration after surgery. Sham-treated controls received the craniotomy, but no CCI injury.

Behavioral Analysis

Open Field Test.

Anxiety-like behavior was assessed using an open field apparatus (40 x 40 x 20 cm clear Plexiglas arena) (10; 84). Animals were acclimated to the apparatus in the first session. On the test day, rats were placed in the center of the open field and activity was measured and recorded for 20 min, using an Accuscan Electronics infrared photocell system (Accuscan Instruments Inc., Columbus, OH). Data were automatically collected and transmitted to a computer equipped with "Fusion" software (from Accuscan Electronics, Columbus, OH). Locomotion (distance traveled in cm), total movement time, and time spent in the center of the open field were analyzed. Anxiety was measured as the ratio of the time spent in the center over the total movement time and expressed as a percentage of the total movement time, as previously described (10).

Immunohistochemistry

Fixation and Tissue Processing.

Seven (7) days after CCI, animals were deeply anesthetized using nembutal (75–100 mg/kg, i.p.) and transcardially perfused with phosphate buffered saline (PBS, 100 ml) followed by 4% paraformaldehyde (250 ml). Brains were removed and post-fixed in 4% paraformaldehyde overnight at 4°C, then transferred to a solution of 30% sucrose in PBS for 72 hours, and frozen with dry ice before storage at -80°C until sectioning. Sectioning was performed as previously described (89; 90). A 1-in-5 series of sections containing the rostrocaudal extent of the amygdala was cut at 40 µm on a sliding microtome (Leica Microsystems SM2000R). A 1-in-5 series of free-floating sections was collected from the cryoprotectant solution, and washed three times for 5 min each. Slices were mounted on a slide, air-dried overnight and processed for Nissl staining with cresyl violet while the adjacent series of sections were mounted on slides for Fluoro-Jade C (FJC) staining.

GAD-67 Immunohistochemistry.

To label GAD-67 immunoreactive neurons, a 1-in-5 series of free-floating sections was collected from the cryoprotectant solution, washed three times for 5 min each in 0.1 M PBS, and incubated in a blocking solution containing 10% normal goat serum (Millipore Bioscience Research Reagents, Temecula, CA) and 0.5% Triton X-100 in PBS for 1 hour at room temperature. The sections were then incubated with mouse anti-GAD-67 serum (1:1000, MAB5406; Millipore Bioscience Research Reagents), 5% normal goat serum, 0.3% Triton X-100, and 1% bovine serum albumin overnight at 4°C. After rinsing three times for 10 min each in 0.1% Triton X-100 in PBS, the sections were

incubated with Cy3-conjugated goat anti-mouse antibody (1:1000; Jackson ImmunoResearch Laboratories Inc., West Grove, PA) and 0.0001% 4,6-diamidino-2-phenylindole dihydrochloride (Sigma-Aldrich) in PBS for 1 hour at room temperature. After a final rinse in PBS for 10 min, sections were mounted on slides, air-dried for at least 30 min, and coverslipped with ProLong Gold antifade reagent (Invitrogen, Carlsbad, CA).

Stereological Quantification.

Design-based stereology was performed to quantify the total number of neurons in Nissl-stained sections and interneurons in GAD-67-immunostained sections in the BLA (90). Sections were viewed with a Zeiss (Oberkochen, Germany) Axioplan 2ie fluorescent microscope with a motorized stage, interfaced with a computer running StereoInvestigator 8.0 (MicroBrightField, Williston, VT). The BLA was identified on slide-mounted sections and delineated for each slide of each animal, under a 2.5X objective, based on the atlas of Paxinos and Watson (222). All sampling was done under a 63X oil immersion objective. Nissl-stained neurons were distinguished from glia cells by their larger size and pale nuclei surrounded by darkly stained cytoplasm containing Nissl bodies. The total number of Nissl-stained and GAD-67-immunostained neurons was estimated by using the optional fractionator probe, and, along with the coefficient of error (CE), were calculated by using StereoInvestigator 8.0 (MicroBrightField). The CE was calculated by the software according to the equations of Gundersen et al., ($m = 1$; (113)) and Schmitz and Hof (second estimation; (266)).

For Nissl-stained neurons in the BLA, a 1-in-5 series of sections was analyzed (six sections on average). The counting frame was 35 X 35 μm , the counting grid was

190 X 190 μm , and the dissector height was 12 μm . Nuclei were counted when the cell body came into focus within the dissector, which was placed 2 μm below the section surface. Section thickness was measured at every counting site, and the average mounted section thickness was 24.7 μm . An average of 187 neurons per hemisphere per rat were counted, and the average CE was 0.07 for both the Gunderson et al. and Schmitz-Hof equations.

For GABAergic interneurons immuno-labeled for GAD-67 in the BLA, a 1-in-5 series of sections was analyzed (on average six sections). The counting frame was 60 X 60 μm , the counting grid was 100 X 100 μm , and the dissector height was 20 μm . Nuclei were counted when the top of the nucleus came into focus within the dissector, which was placed 2 μm below the section surface. Section thickness was measured at every fifth counting site, and the average mounted section thickness was 24 μm . An average of 210 neurons per side per rat was counted, and the average CE was 0.08 for both the Gunderson et al. and Schmitz-Hof equations.

Amygdala Slice Electrophysiology

Coronal slices containing the amygdala were prepared from rats 1 or 7 days after surgery. The rats were anesthetized with isofluorane and then decapitated. Coronal brain slices (400 μm -thick) containing the amygdala (-2.64 to -3.36 from Bregma) were cut using a vibratome (Leica VT 1200 S; Leica Microsystems, Buffalo Grove, IL), in ice-cold cutting solution consisting of (in mM): 115 sucrose, 70 NMDG, 1KCl, 2 CaCl₂, 4 MgCl₂, 1.25 NaH₂PO₄, 30 NaHCO₃, 25 D-glucose. Slices were transferred to a holding chamber, maintained at 32°C for 25 min, and then at room temperature, in a bath solution containing (in mM): 125 NaCl, 2.5 KCl, 2.0 CaCl₂, 2.0 MgCl₂, 21 NaHCO₃, 1.25

NaH₂PO₄, and 22 D-glucose. Recording solution was the same as the holding bath solution. All solutions were saturated with 95% O₂, 5% CO₂ to achieve a pH near 7.4. Slices were transferred to a submersion-type recording chamber (0.7 mL capacity), where they were continuously perfused with oxygenated ACSF (flow rate about 5 mL/min). Neurons were visualized with an upright microscope (Zeiss Axioskop 2, Thronwood, NY) through a 40x water immersion objective, equipped with a CCD-100 camera (Dage-MTI, Michigan City, IN). All experiments were performed at 32°C. Tight-seal (>1 GΩ) whole-cell recordings were obtained from the cell body of pyramidal-shaped neurons in the BLA region, which were identified on the basis of their electrophysiological properties (259; 260). Current activated by hyperpolarization (I_h current) characteristic of principal neurons was recorded during the first minutes after breaking into the cell. Patch electrodes were fabricated from borosilicate glass and had a resistance of 3.5-4.5 MΩ when filled with solution A containing (in mM): 135 Cs-gluconate, 10 MgCl₂, 0.1 CaCl₂, 1 EGTA, 10 Hepes, 2 Na-ATP, 0.2 Na₃GTP, pH 7.3 (285–290 mOsm) or solution B containing (in mM): 60 Cs-gluconato, 60 KCH₃SO₃, 10 KCl, 10 EGTA, 10 HEPES, 5 Mg-ATP, 0.3 NaGTP, pH 7.2 (280–290 mOsm/kg). Solution A was used in experiments involving bath application of choline and solution B was used to record spontaneous and miniature inhibitory postsynaptic currents (IPSCs). Neurons were voltage-clamped using an Axopatch 200B amplifier (Axon Instruments, Foster City, CA, USA). IPSCs were pharmacologically isolated and recorded at a -70 mV holding potential as inward currents in voltage-clamp mode. Access resistance (15–24 MΩ) was regularly monitored during recordings, and cells were rejected if it changed by 15% during the experiment. Ionic currents and action potentials were amplified and filtered (1 kHz) using the Axopatch

200B amplifier (Axon Instruments, Foster City, CA) with a four-pole, low-pass Bessel filter, were digitally sampled (up to 2 kHz) using the pClamp 10.2 software (Molecular Devices, Sunnyvale, CA), and further analyzed using the Mini Analysis program (Synaptosoft Inc., Fort Lee, NJ) and Origin (OriginLab Corporation, Northampton, MA). The peak amplitude, 10–90% rise time, and decay time constant of IPSCs were analyzed off-line using pClamp 10.2 software and the Mini Analysis Program (Synaptosoft, Inc., Leonia, NJ, USA). Miniature IPSCs (mIPSCs) were analyzed off-line using the Mini Analysis Program (Synaptosoft, Fort Lee, NJ) and detected by manually setting the mIPSC threshold (~1.5 times the baseline noise amplitude) after visual inspection.

Agonists of α_7 -nAChRs were applied by pressure injection. Pressure application was performed with the help of a push–pull experimental arrangement (226), as utilized previously (89). Pressure was applied to the pipette via a Picospritzer (General Valve Division, Parker Hannifin Corp., Fairfield, NJ), set at about 100 MPa (14 psi). A motorizer (Newport, Fountain Valley, CA) was coupled with the approach/withdrawal (push–pull) actuator of a micromanipulator (Burleigh PCS-5000 series; EXFO Photonic Solution Inc., Mississauga, Ontario, Canada). Motorizer movement and duration of application pulses were controlled with a Master-8 digital stimulator (AMPI; Jerusalem, Israel). Ionic currents were amplified and filtered (1 kHz) using an Axopatch 200B amplifier, with a four-pole low-pass Bessel filter, and were digitally sampled (up to 5 kHz). Currents were recorded using pClamp 10.2 software and further analyzed using OriginLab (Northampton, MA) and Mini60 software.

Drugs used were as follows: 6-cyano-7-nitroquinoxaline-2,3-dione (CNQX), an α -amino-3-hydroxyl-5-methyl-4-isoxazole-propionate (AMPA)/kainate receptor

antagonist; d-2-amino-phosphonovalerate (AP-5), an *N*-methyl-d-aspartic acid (NMDA) receptor antagonist; and SCH50911, a GABA_B receptor antagonist (all purchased from Tocris, Ellisville, MO). We also used bicuculline methiodide, a GABA_A receptor antagonist, and tetrodotoxin, a sodium channel blocker (purchased from Sigma-Aldrich, St. Louis, MO).

Biotinylation and Western Blot

Coronal slices containing BLA were prepared as described for electrophysiology experiments. After a 1-hour recovery period in oxygenated ACSF, slices were incubated in ACSF containing 1 mg/ml EZ-Link Sulfo-NHS-SS-Biotin (Pierce, Rockford, IL) for 1 hour on ice, followed by the addition of quench solution (provided in the Pierce Cell Surface Protein Isolation Kit, Cat No. 89881). The BLA was then dissected and tissue sections were transferred to small plastic tubes containing radioimmunoprecipitation assay (RIPA) buffer composed of (in mM) 50 Tris-HCl, pH 7.4, 150 NaCl, 2 EDTA, 50 NaF, 1 Na₃VO₄, 1% Triton X-100, 0.1% SDS, 0.5% Na-deoxycholate, and a Protease Inhibitor Cocktail (Sigma-Aldrich, MO). Samples were sonicated and the homogenates were centrifuged at 14,000 g for 10 min at 4°C. Protein concentrations were measured using the DC Protein Assay Kit (Bio-Rad, CA). Protein (1,500 µg) was then mixed with 400 µL of UltraLink immobilized NeutrAvidin agarose beads (Pierce) for 1 hour at room temperature. The beads were then washed 3 times with 500 µL wash buffer (provided in the kit). Samples were eluted in 400 µL of RIPA buffer containing Protease Inhibitor Cocktail supplemented with 50 mM dithiothreitol and mixed for 1 hour at room temperature followed by centrifugation at 14,000g for 10 min at 4°C. Then, LDS 4x (Invitrogen) was added to protein samples. Biotinylated proteins were resolved by SDS-

PAGE, transferred to nitrocellulose membranes, and probed with the following antibodies Anti-Alpha1 GABA-A Receptor, clone N95/65, 75-136 (1:1000; UC Davis/NIH NeuroMab Facility), Anti-GABA A Receptor Beta 2,3 Chain, clone BD17/MAB341 (1:1000, Millipore, Billerica, MA), Anti-GABA A Receptor Gamma 2, Ab16213 (1:1000, AbCam, Cambridge, MA), Anti-Nicotinic Acetylcholine Receptor ($\alpha 7$ Subunit) M220 (1:1000, Sigma-Aldrich, St. Louis, MO) . The signal from the immunoreactive band was detected by using a gel imaging system (Fuji LAS-3000). Membranes were stripped using ReBlot Plus Strong Antibody Stripping Solution (Millipore, Billerica, MA) and re-probed with Anti-GLUT1 (1:1000, Millipore, Billerica, MA) for loading control. Signal intensity was determined by densitometric scanning using ImageJ. When duplicate conditions were performed in one animal, the ratio values were averaged to obtain an animal average for that condition.

Statistical Analysis

Statistical values are presented as mean \pm standard error (SE). Results from ipsilateral and contralateral sides of sham-operated and traumatized animals were compared using one-way ANOVA followed by Bonferroni post-hoc test in the stereology and Western blot experiments. For open-field experiments, two-way ANOVA followed by Tukey post-hoc test was used. For electrophysiology experiments, either one-way ANOVA followed by Bonferroni post-hoc test or independent t-tests were performed. $p < 0.05$ was considered statistically significant for all statistical analysis. Sample sizes (n) refer to the number of rats, except for the electrophysiology results where “n” refers to the number of slices or recorded cells.

RESULTS

Anxiety-like behaviors increase 7 days after CCI

Rats exposed to mild CCI were tested in the open field apparatus 2 days before and 1, 7 and 30 days after surgery. Prior to surgery, there was no difference in the time spent in the center of the open field in the sham ($12.6 \pm 1.0\%$ of the total movement time) and CCI ($13.1 \pm 2.8\%$ of the total movement time; $p = 0.85$) groups. One day after the surgery, sham ($12.1 \pm 1.3\%$ of the total movement time) and CCI ($10.2 \pm 2.3\%$ of the total movement time) animals also spent similar amount of time in the center of the field ($p = 0.98$). However, 7 days post injury, CCI rats ($6.3 \pm 1.2\%$ of the total movement time) spent significantly less time in the center of the open field compared to sham animals ($12.5 \pm 1.0\%$ of the total movement time; $p = 0.015$; $n = 8$). Sustained increases in anxiety were also observed 30 days post injury as CCI rats ($8.2 \pm 0.6\%$ of the total movement time) spent significantly less time in the open field compared to sham animals ($14.2 \pm 0.7\%$ of the total movement time; $p = 0.02$; $n = 8$; Figure 9).

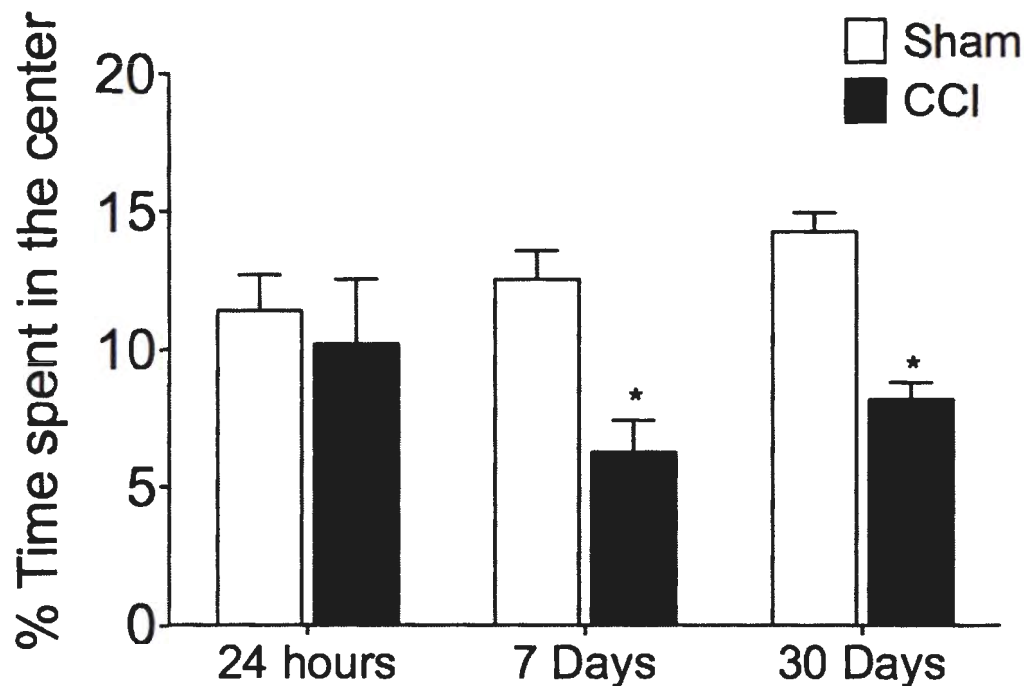


Figure 9. Mild TBI increases anxiety-like behaviors in the open field test. No differences in time spent in the center of the open field were found between CCI and sham animals. However, CCI rats spent significantly less time in the center of the open field 7- and 30-days after injury compared to sham animals. Bars show the mean \pm SE of the percentage of time spent in the center. * $p < 0.05$.

Neuropathology of Principal Neurons and Interneurons in the BLA after CCI

We next examined whether the increase in anxiety was associated with a loss of neurons and interneurons after CCI. Estimation of the total number of neurons in the BLA, using an unbiased stereological method in Nissl-stained sections, revealed that animals that received a CCI did not lose a significant number of total neurons 1- or 7-days after injury compared to age-matched sham injured control animals (Table 5; Figure 10). We next asked whether CCI induced interneuronal death 1- or 7- days after injury, as previous studies have found a significant loss of interneurons after mTBI (336).

Estimation of the total number of interneurons in the BLA, using an unbiased stereological method to quantify GAD67 immunoreactive cells, showed that there was no significant loss of interneurons 1 day after CCI either ipsilateral or contralateral to the site of injury compared to sham controls (Table 6; Figure 11). Similar to the Nissl-stained sections, GAD67-positive cells from 1- and 7-day sham control groups did not display any significant differences and were therefore averaged together (data not shown). However, 7 days after CCI, animals showed a 28.8% reduction ipsilateral and a 23.8% reduction in GAD67-positive cells contralateral to the site of injury, indicating a significant loss in the number of GAD67-positive neurons in the BLA (Table 5; Figure 11B).

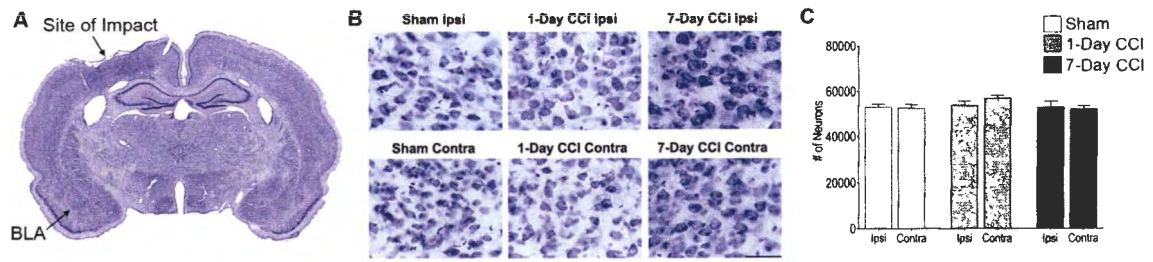


Figure 10. Mild CCI does not cause a significant loss of neurons in the BLA 24 hours or 7 days after injury. (A) Panoramic photomicrograph of Nissl-stained brain slice. Indicated are the sites of impact and the ipsilateral BLA. (B) Representative photomicrographs from Nissl-stained sections showing BLA cells from the ipsilateral (Top) and contralateral (Bottom) sides of sham, 1-day CCI, and 7-day CCI animals, respectively. Total magnification is 630X; scale bar, 50 μ m. (C) Group data (mean \pm SE; $n = 8$ for each group) of stereological estimation of the total number of Nissl-stained neurons in the BLA.

Condition	# of Cells \pm SEM	Compared to	# of Cells \pm SEM
Sham Ipsilateral	52,969 \pm 1,392	CCI 1 day Ipsilateral	52,815 \pm 2,723
		CCI 1 day Contralateral	51,961 \pm 1,608
		CCI 7 days Ipsilateral	53,733 \pm 1,954
		CCI 7 days Contralateral	56,922 \pm 1,257
Sham Contralateral	52,400 \pm 1,741	CCI 1 day Ipsilateral	52,815 \pm 2,723
		CCI 1 day Contralateral	51,961 \pm 1,608
		CCI 7 days Ipsilateral	53,733 \pm 1,954
		CCI 7 days Contralateral	56,922 \pm 1,257

Table 5. Total number of neurons in the BLA of sham and CCI animals

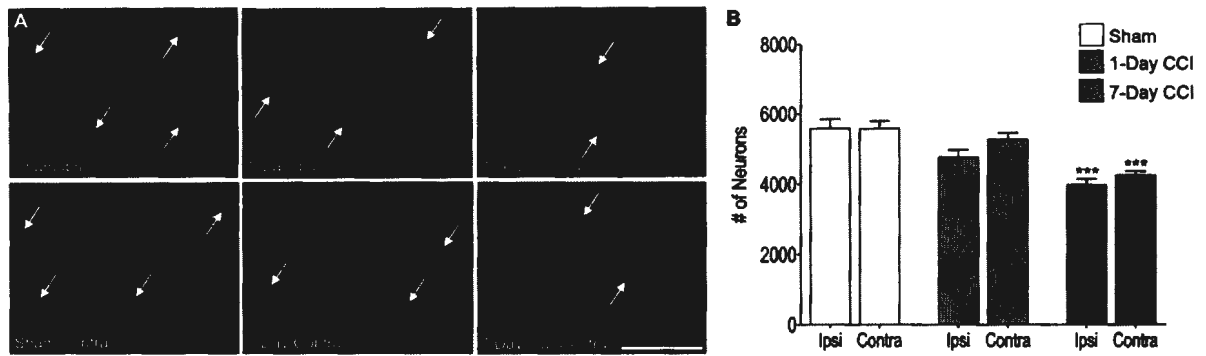


Figure 11. Delayed loss of GABAergic interneurons in the BLA within the first week after mild CCI. (A) Representative photomicrographs of GAD-67 immunohistochemically stained GABAergic interneurons in the BLA of sham (left), 1-day CCI (middle), and 7-day CCI (right) animals. Total magnification is 630x; scale bar, 50 μ m. (B) group data showing the mean and standard error of the stereologically estimated total number of GAD-67-positive cells in the BLA 1- and 7-days after CCI compared with sham. Only 7-days after CCI was there a significant bilateral reduction in GAD-67-positive cells indicating a delayed loss of GABAergic interneurons. *** $p < 0.001$; $n = 10$ for each group.

Condition	# of Cells \pm SEM	Compared to	# of Cells \pm SEM
Sham Ipsilateral	5,590 \pm 258.2	CCI 1 day Ipsilateral	4,763 \pm 209.8
		CCI 1 day Contralateral	5,277 \pm 190.2
		CCI 7 days Ipsilateral	3,980 \pm 172.1***
		CCI 7 days Contralateral	4,254 \pm 106.8**
Sham Contralateral	5,589 \pm 205.1	CCI 1 day Ipsilateral	4,763 \pm 209.8
		CCI 1 day Contralateral	5,277 \pm 190.2
		CCI 7 days Ipsilateral	3,980 \pm 172.1***
		CCI 7 days Contralateral	4,254 \pm 106.8**

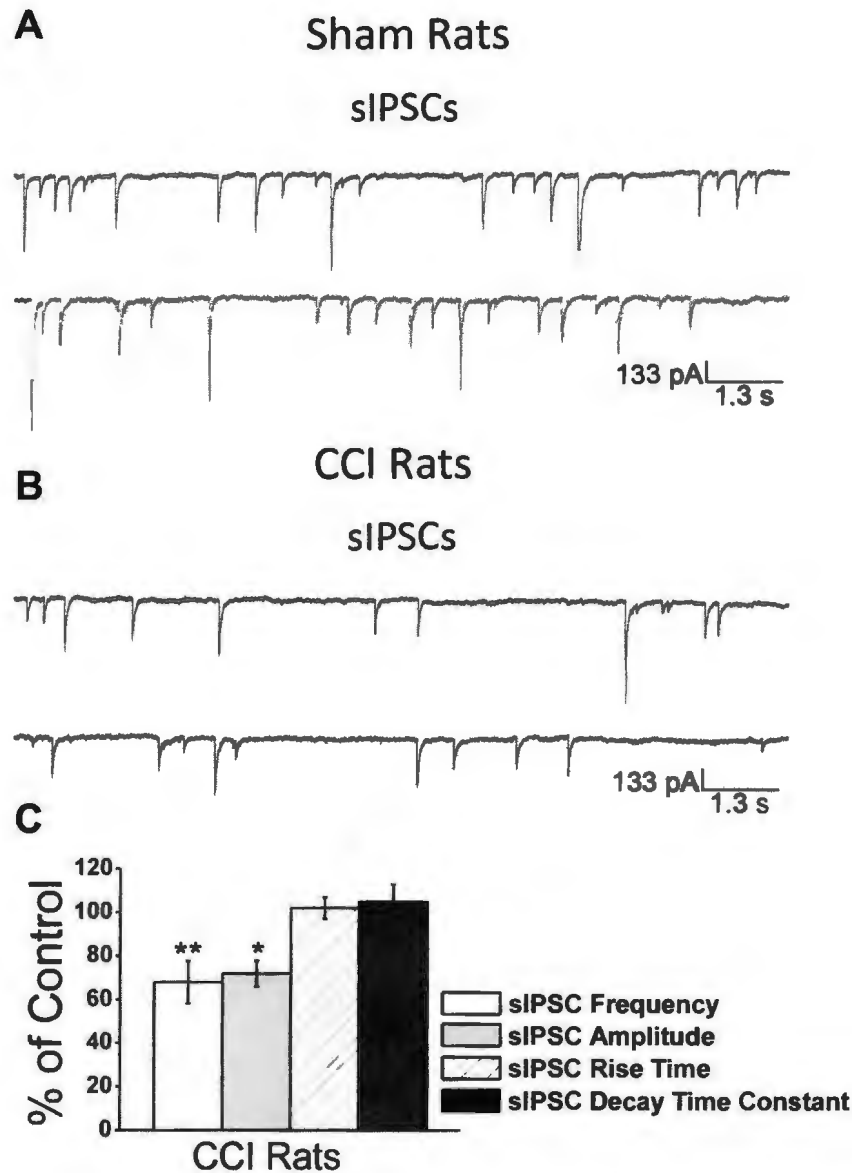
** $p < 0.01$, *** $p < 0.001$

Table 6. Total Number of GAD67⁺ Interneurons in the BLA of sham and CCI animals

Alterations in GABA_A-mediated spontaneous and miniature IPSCs

Whole-cell recordings obtained from BLA neurons were identified on the basis of their size, pyramidal-like shape, firing patterns in response to depolarizing current pulses in the current-clamp mode, and the presence of a current activated by hyperpolarizing voltage-steps (I_h), in the voltage clamp mode. Depolarizing current injections generated variable patterns of accommodating spiking. Four 1 s-long hyperpolarizing pulses starting from V_{hold} -70 to -80 mV and ending with -110 mV elicited nonlinear I_h current in principal neurons (10; 323) (data not shown).

To determine whether CCI impaired inhibitory synaptic transmission, we recorded spontaneous GABA_A receptor-mediated IPSCs (sIPSCs) from principal neurons in the presence of CNQX (20 μ M), D-AP5 (50 μ M), SCH50911 (10 μ M), and LY 3414953 (3 μ M) at a holding potential of -70 mV. Sham animals did not differ in the frequency and amplitude of sIPSCs at either 1- or 7-days after surgery and so we averaged together the amplitude and frequency of all sham animals. We examined the frequency and amplitude of GABA_A receptor-mediated sIPSCs 1- and 7-days after CCI. Compared to sham animals (mean frequency = 2.9 ± 0.7 Hz; mean amplitude = 288 ± 9 pA; $n = 18$), we found no significant difference in the frequency (2.7 ± 1.2 Hz; $n = 18$; $p > 0.05$) and amplitude (293 ± 12 pA; $n = 18$; $p > 0.05$) of GABA_A receptor-mediated sIPSCs 1 day after CCI. However, 7 days after CCI we found a $32 \pm 9.8\%$ reduction in the frequency ($n = 18$; $p < 0.01$) and a $28 \pm 5.9\%$ reduction in the amplitude ($n = 18$; $p < 0.05$) of GABA_A receptor mediated sIPSCs (Figure 12).



Figure

12. Mild

CCI causes a significant decrease in the frequency and amplitude of sIPSCs in the BLA 7-days after CCI. sIPSCs were recorded from pyramidal-shaped neurons in the presence of d-APV (50 μ M), SCH50911 (20 μ M), and GYKI 52466 (50 μ M), at a holding potential of -70 mV. Representative examples of recordings obtained in the BLA are shown in (A) and (B) for Sham and CCI 7-day animals, respectively. (C) Group data showing the change in the percentage frequency and amplitude of sIPSCs from CCI animals relative to Sham animals. The frequency and amplitude, but not the rise time and the decay time constant of the sIPSCs were significantly reduced in the CCI group compared to the sham controls. * $p < 0.05$; ** $p < 0.01$; $n = 18$ for each group.

To determine how CCI impaired inhibitory transmission, we examined the effects

of CCI on miniature IPSCs (mIPSCs), recorded in the presence of CNQX (20 μ M), D-

AP5 (50 μ M), SCH50911 (10 μ M), and LY 3414953 (3 μ M), and TTX (1 μ M) at a holding potential of -70 mV. Recording mIPSCs from principal neurons in the BLA allows us to directly examine whether changes in the probability of quantal release at the presynaptic terminal or internalization of postsynaptic GABA_A receptors contributed to impaired inhibitory synaptic transmission. Sham animals did not differ in the frequency and amplitude of mIPSCs at either 1- or 7-days after surgery and so we averaged together the amplitude and frequency of all sham animals (data not shown). We examined the frequency and amplitude of GABA_A receptor-mediated mIPSCs 1- and 7-days after CCI. Compared to sham animals (mean frequency = 1.5 ± 0.7 Hz; mean amplitude = 59 ± 8 pA; $n = 17$), we found no significant difference in the frequency (1.5 ± 0.4 Hz; $n = 17$; $p > 0.05$) and amplitude (55 ± 10 pA; $n = 17$; $p > 0.05$) of GABA_A receptor-mediated mIPSCs 1 day after CCI. However, 7 days after CCI we found a $35 \pm 5\%$ reduction in the frequency ($n = 17$; $p < 0.01$) and a $22 \pm 4.8\%$ reduction in the amplitude ($n = 17$; $p < 0.05$) of GABA_A receptor mediated mIPSCs 7 days after CCI (Figure 13).

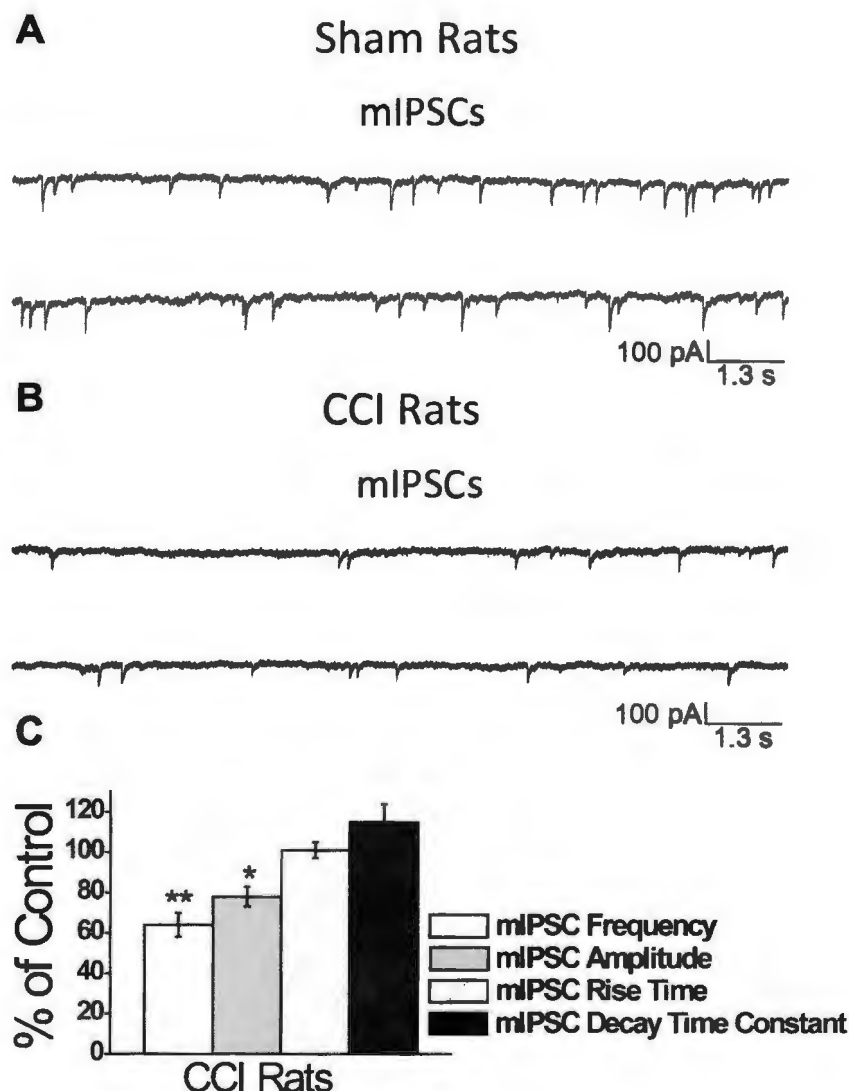


Figure 13. Mild CCI causes a significant decrease in the frequency and amplitude of mIPSCs in the BLA 7-days after CCI. mIPSCs were recorded from pyramidal-shaped neurons in the presence of d-APV (50 μ M), SCH50911 (20 μ M), and GYKI 52466 (50 μ M), TTX (1 μ M) at a holding potential of -70 mV. Representative examples of recordings obtained in the BLA are shown in (A) and (B) for Sham and CCI 7 days animals, respectively. (C) Group data showing the change in the percentage frequency and amplitude of mIPSCs from CCI animals relative to Sham animals. The frequency and amplitude, but not the rise time and the decay time constant of the sIPSCs were significantly reduced in the CCI group compared to the sham controls. The recorded currents were blocked by the GABA_A receptor antagonist bicuculline (data not shown). * $p < 0.05$; ** $p < 0.01$; $n = 17$ for each group.

Reduced membrane expression of GABA_A receptor subunits

Because we found a decrease in both the amplitude and frequency of GABA_A receptor-mediated IPSCs, the latter of which may be a result of the significant loss of interneurons observed 7 days after CCI, we next examined whether internalization of the GABA_A receptor contributed to the reduced amplitude of the IPSC. To determine whether GABA_A receptor subunits are internalized after CCI, we measured CCI-induced changes in surface expression of GABA_A subunits α 1, β 2, and γ 2 from the BLA. Membrane proteins were isolated by biotinylation assay and levels of specific subunits were quantified by Western blot. After densitometric analysis, Western blot membranes were stripped and re-probed for GLUT1. It has been previously demonstrated that expression of GLUT1 is unaltered as opposed to GLUT3 following TBI (117) and therefore was used as a loading control. We found that the surface expression of all three GABA_A subunits were reduced 7 days ($n = 4$) after CCI both ipsilateral (47.3%; $p < 0.001$) and contralateral to the site of impact (52.5%; $p < 0.001$) compared to sham control animals ($n = 4$). Ipsilateral to the side of impact, a 48.3% ($p = 0.002$) reduction of the α 1 subunit, a 51.8% ($p < 0.001$) reduction of the β 2 subunit, and a 43.1% ($p < 0.001$) reduction of the γ 2 subunit, were found, whereas contralateral to the side of impact, 50.2% ($p < 0.001$) reduction of the α 1 subunit, a 47.3% ($p < 0.001$) reduction of the β 2 subunit, and a 60.3% ($p < 0.001$) reduction of the γ 2 subunit, was observed, indicating that the reduced amplitude in the GABA_A receptor-mediated sIPSCs may be due to reductions in the surface expression of GABA_A receptors (Figure 14).

Figure 14. Surface expression of α_1 , β_2 , and γ_2 GABA_A receptor subunits is reduced in the BLA of CCI animals 7 days after mild CCI. Western blot for subunits of (A) α_1 , (B) β_2 , and (C) γ_2 subunits, respectively, was performed using biotinylated proteins isolated from the ipsilateral and contralateral sides of Sham and CCI 7-day animals. Group data showing the mean \pm SE of the ratio between each subunit and GLUT1 optical densities. Top panel: representative Western blot for α_1 (A), β_2 (B), and γ_2 (C) subunits of GABA_A receptors, respectively. Bottom panel: representative Western blot for GLUT1, used as a loading control. Note that surface expression of GABA_A α_1 , $\beta_{2/3}$ and γ_2 subunits are reduced in CCI animals when compared to Sham animals. * $p < 0.01$; $n = 3$ for each group.

Alterations in α_7 -nAChR-mediated currents after mTBI

In the BLA, α_7 -nAChRs have previously been reported to be present on somatodendritic regions of glutamatergic neurons (153) and are involved in presynaptically facilitating glutamate release (16; 142). To determine whether α_7 -nAChRs contributed to the principal cell hyperexcitability, we pressure-applied tricholine citrate (5 mM; 70 ms; 14 psi), while recording from principal neurons of sham control slices ($n = 17$) in the presence of α -conotoxin AulB (1 μ M), DH β E (10 μ M), atropine sulfate (0.5 μ M), D-AP5 (50 μ M), CNQX (20 μ M), SCH50911 (10 μ M), LY 3414953 (3 μ M), and bicuculline (20 μ M) and examined the mean charge transferred, a measurement that reflects the amount of current (charged particles) flowing into the cell by integrating the duration of the open time of ion channels. In current-clamp mode, pressure

application of tricholine citrate onto control slices elicited a brief train of action potentials, while in the voltage clamp mode it induced inward currents. The current induced by tricholine citrate was nearly blocked by 1 μ M α -BgTx. The mean charge transferred through α_7 -nAChRs in sham animals was 715 ± 66 pC ($n = 16$). 1-day after CCI we did not observe any alteration in the mean charge transferred through α_7 -nAChRs (748 ± 63 pC; $n = 16$). However 7-days after CCI, the mean charge transferred was significantly increased (970 ± 80 ; $n = 17$) compared to sham animals. Puff application of tricholine citrate elicited α_7 -nAChR currents that were 35.6% ($p = 0.035$) larger in 7-day CCI compared to sham animals, suggesting an increase in the membrane expression of functional α_7 -nAChRs (Figure 15).

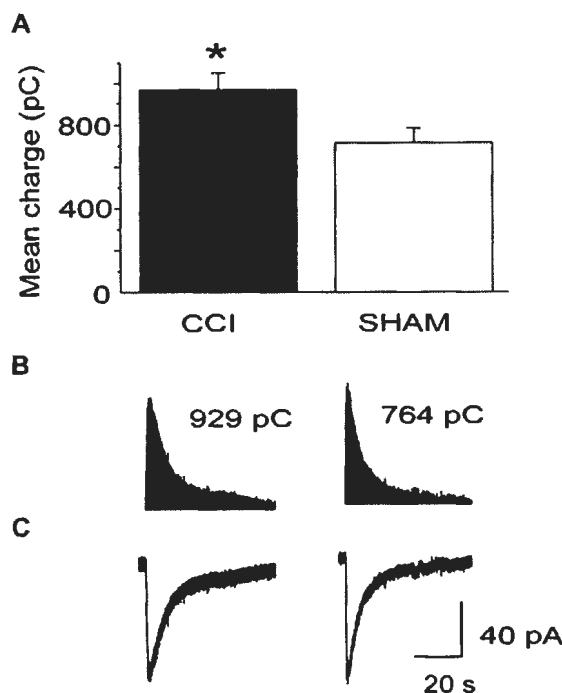


Figure 15. Activation of α_7 -nAChRs by fast application of the α_7 -nAChR specific agonist, choline, in the BLA, shows increased cholinergic conductance 7-days after CCI. (A) Group data showing the mean \pm SE charge transfer in pyramidal-shaped neurons in the BLA from CCI rats 7-days after injury. A significant increase in the mean charge transfer was observed only 7-days after CCI. (B) Representative charge transfer from α_7 -nAChRs from sham (left), 1-days CCI (middle), and 7-day CCI (right) animals. Note that the charge transfer through α_7 -nAChRs is increased in the BLA at day 7 post injury. (C) Representative α_7 -nAChR-mediated currents recorded from sham (left), 1-day CCI (middle), and 7-day CCI (right) animals. Note the significant increase in the amplitude of the α_7 -nAChR-mediated current 7-days post CCI. Experiments were recorded in the presence of α -conotoxin AulB (1 μ M), DH β E (10 μ M), atropine sulfate (0.5 μ M), D-AP5 (50 μ M), CNQX (20 μ M), SCH50911 (10 μ M), LY 3414953 (3 μ M), and bicuculline (20 μ M). * p <0.05; n = 17 cells for each group.

Increased membrane expression of α_7 -nAChRs after CCI

We found that 7 days after CCI, α_7 -nAChR currents are increased by 35.6%. We used biotinylation and Western blot analysis to determine whether the surface expression of α_7 -nAChRs increase after CCI and contributed to an increase in the amplitude of α_7 -nAChR-mediated currents. We found that the surface expression of the α_7 -nAChR was increased by 37.2% ($p < 0.001$) 7 days after CCI ($n = 4$) compared with sham control animals ($n = 8$). In CCI animals the increase in the surface expression of α_7 -nAChRs was 44.2% ($p = 0.017$) on the contralateral site of injury versus 37.2% ($p = 0.049$) ipsilateral to the site of injury (Figure 16).

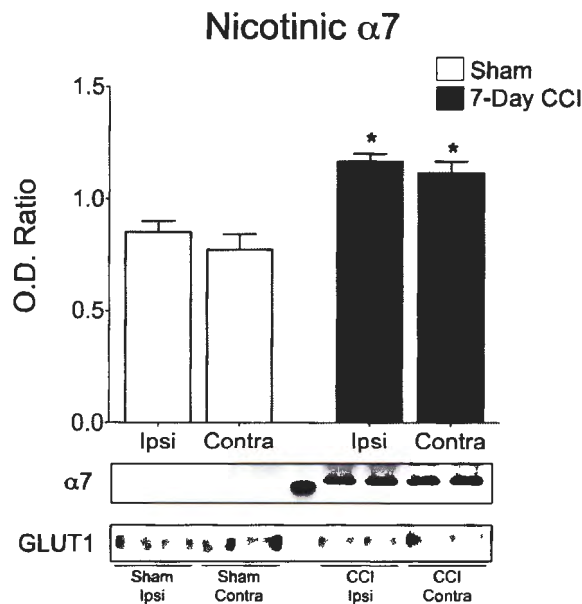


Figure 16. Surface expression of α_7 subunit of neuronal nicotinic acetylcholine receptor is increased in the BLA of CCI animals 7-days after mild CCI. Western blot was performed using biotinylated proteins isolated from the ipsilateral and contralateral sides of Sham and CCI 7-day animals. Group data showing the mean \pm SE of the ratio between the α_7 subunit and GLUT1 optical densities. Top panel: representative Western blot for α_7 -nAChRs. Bottom panel: representative Western blot for GLUT1, used as a loading control..* $p < 0.05$; $n = 3$ for each group.

DISCUSSION

The present study revealed that CCI-induced mTBI caused a long-lasting increase in anxiety-like behaviors. This was accompanied by, and may be the result of reduced GABA_A receptor mediated inhibitory synaptic transmission and increased excitability within the BLA. Reduced inhibitory tonus within the BLA is consistent with a delayed but significant loss of interneurons as compared to the total number of neurons within the BLA, and a significant decrease in the surface expression of $\alpha 1$, $\beta 2$, and $\gamma 2$ GABA_A receptors subunits after mTBI. Interneuronal loss and internalization of GABA_A receptors led to a reduction in the frequency and amplitude of GABA_A-receptor mediated spontaneous and miniature IPSCs, respectively. Additionally, in principal neurons, we observed a significant increase in the charge transferred by $\alpha 7$ -nAChRs. The increase in charge transferred via the $\alpha 7$ -nAChRs was accompanied by an increase in surface expression of $\alpha 7$ -nAChRs in the BLA. Together, reductions in GABAergic inhibitory transmission and increase in $\alpha 7$ -nAChRs function, may contribute to hyperexcitability in the BLA.

Long-lasting increases in anxiety and the development of anxiety disorders have been consistently observed in humans following TBI (67; 235; 325). The recent focus of media attention on sports related injuries has revealed that mild concussions sustained during play increases the incidence of developing neuropsychiatric disorders, including anxiety disorders (77; 126). Similarly, U.S. soldiers exposed to TBI are significantly more likely to report anxiety and anxiety disorders compared to soldiers that did not suffer a TBI (134). Accordingly, anxiety-like behaviors have been observed in animals [present study, (79; 195; 240), using different models of TBI, including fluid percussion

injury (240), blast exposure (79), and mTBI induced by CCI [present study, (195)]. Thus, mTBI may cause functional and morphological alterations in the BLA underlying long-lasting increases in anxiety-like behavior in animals and the manifestation of anxiety disorders in humans.

Although it is apparent that mild TBI increases the prevalence of developing anxiety disorders (200), it has not been excluded that the anxiety may be due to the stress associated with the trauma and its aftermath and not with trauma itself (36; 134; 140; 149). Here, we aimed to investigate the effect of mTBI alone on the development of anxiety disorders. To reduce animal stress and increase the validity of our model, we employed strict stress-mitigating guidelines. These included allowing animals to acclimate to their new environment a minimum of 3 days prior to any experimental procedures, cleaning cages only once per week, minimizing handling pre- and post-surgery (231), and providing medication to alleviate pain. Similar to other experimental procedures (79; 195), animals were administered a general anesthetic prior to surgery. Our results clearly demonstrated that the increase in anxiety-like behaviors 7- and 30-days after mTBI was due to the CCI and not due to uncontrolled stress (79) or the surgery (56). Thus, while stress may be a risk factor for the development of anxiety disorders, mTBI alone clearly caused a delayed increase in anxiety. Stress-mTBI interactions are therefore likely to mutually exacerbate the development of long-term symptoms of anxiety.

Anxiety disorders in humans have often been attributed to neuronal hyperexcitability in the amygdala (236; 309). One of the pharmacological treatments for anxiety includes administration of benzodiazepines, which suggests that GABAergic

inhibitory transmission plays a crucial role in the pathology of anxiety (253). Indeed, recent evidence suggests that deficits in GABAergic inhibition within the BLA may contribute to anxiogenic behaviors in animals (11; 49; 198) and ablation of a specific subpopulation of interneurons in the BLA results in anxiety-like behavior (295). Although one previous study found an upregulation of N-methyl-D-aspartate (NMDA) receptors in the BLA after mTBI (240), no previous study examined the functional alterations to inhibitory synaptic transmission after mTBI and its role in the development of anxiety-like behaviors. Here, we report that mTBI leads to a significant decrease in inhibitory synaptic transmission in the BLA, including reductions in both the frequency and amplitude of mIPSCs. This reduction was consistent with the loss of GABAergic interneurons and decreased expression of GABA_A receptors, both of which are associated with increased anxiety-like behaviors (62; 295). Together with the selective loss of GABAergic neurons, reduced surface expression of GABA_A receptors in the BLA may constitute one mechanism by which mTBI leads to hyperexcitability in the BLA and the subsequent development of anxiety-like behaviors.

Excitability within the BLA is also regulated by activation of α_7 -nAChRs (148; 153). α_7 -nAChRs are highly expressed in the BLA (142; 153), play an important role in modulating glutamatergic synaptic transmission, (16), and induce anxiogenic effects when activated by specific agonists (219). Since α_7 -nAChRs regulate neuronal excitability, we examined whether α_7 -nAChR activation contributed to BLA hyperexcitability after mTBI. Within 7 days of TBI, we found a significant increase in the surface expression of α_7 -nAChRs and associated increases in the current mediated by α_7 -nAChRs on principal neurons. Thus, we show that in addition to a significant loss of

interneurons and reduction in the inhibitory synaptic transmission, an enhancement in the α_7 -nAChRs-mediated transmission contributed to neuronal hyperexcitability and long-lasting increases in anxiety-like behavior.

Is mTBI more than just a focal injury? We induced injury by placing a single mild focal impact to the left parietal cortex, yet pathological and pathophysiological alterations in the BLA, a brain region far from the impact site, was observed on each hemisphere. Thus, our study corroborates with the notion that controlled cortical impact is actually more than a focal brain injury (100; 296). Following the impact, intracranial pressure changes on each side of the brain, though the contralateral side is less affected than the ipsilateral side (53). We speculate that such mechanical alterations trigger a neuropathological cascade throughout the brain that ultimately leads to the pathological and pathophysiological alteration observed. We recently reported that within 24 hours of CCI, chemokines transcripts are upregulated and remains elevated for at least one week (Ait-Ali et al., 2013). Subsequent inflammation takes place and may be the underlying cause for functional and morphological alterations in the BLA on both hemispheres here reported.

In conclusion, the results from this study demonstrated that a mild TBI leads to long lasting increases in anxiety-like behavior. This increase is a result of a significant loss of GABAergic interneurons, reduced surface expression of GABA_A receptors and inhibitory synaptic transmission, and, increases in the surface expression and function of α_7 -nAChRs, which subsequently increase excitability within principal neurons in the BLA. With the high incidence of anxiety disorders being reported after TBI (235), it is essential to understand the pathophysiological mechanisms underlying their development.

Although the results described above suggests that alterations in inhibitory synaptic transmission and cholinergic transmission contribute to increased anxiety, further studies are needed to elucidate the mechanisms leading to pathological and pathophysiological alterations in the BLA after mTBI so that pharmacological therapies may be developed to ameliorate psychiatric conditions following injury.

CHAPTER 4: Specific loss of interneurons and reduced GABAergic inhibitory synaptic transmission in the CA1 field of hippocampus – implications for cognitive impairment after mild traumatic brain injury

ABSTRACT

Patients that suffer mild traumatic brain injury (mTBI) usually do not show any evident damage when submitted to imaging but can develop long-term cognitive impairment such as memory and learning deficits and posttraumatic epilepsy. The hippocampus besides being a key brain region in the pathology of such cognitive and neurological impairments shows a high susceptibility to mTBI-induced damage due to its anatomical localization. In the present study investigated whether mTBI induces pathological and pathophysiological alterations in the CA1 region of the hippocampus that may contribute to the development of neurological deficits. Controlled cortical impact (CCI) was used as a model of mTBI, in which a significant reduction in the total number of neurons in the CA1 was not observed. Still, animals submitted to mTBI showed signs of cognitive impairment in the passive avoidance test. Design-based stereology revealed that the number of GABAergic interneurons is significantly reduced in CA1 7 days after CCI. This interneuronal loss is consistent with a significant reduction in the frequency of spontaneous and miniature GABA_A-receptor mediated inhibitory postsynaptic currents (IPSCs) 7 days after CCI. Moreover reduced amplitude of IPSCs was associated with a significant decrease in the surface expression of $\alpha 1$, $\beta 2$, and $\gamma 2$ subunits of the GABA_A receptor. There were no changes in function and expression of $\alpha 7$ -containing nicotinic acetylcholine receptor ($\alpha 7$ -nAChR) after CCI. Together, these results suggest that mTBI causes a significant reduction in GABAergic inhibitory

transmission in the CA1, which may contribute to changes in hippocampal excitability and the development of cognitive impairment.

INTRODUCTION

Mild traumatic brain injury (mTBI) accounts for more than 80% of all head trauma cases (200). A mild traumatic brain injury is currently defined as brain trauma that results in physiological disruption of brain function by one or more of the following: a) any loss of consciousness up to 30 min; b) posttraumatic amnesia up to 24 hours; c) any alteration of consciousness i.e. dazed feeling, disorientation up to 24 hours; d) transient neurological dysfunction such as a seizure and an intracranial lesion that does not require surgical intervention; and e) a Glasgow Coma Scale of 13-15 performed 30 min or longer after initial injury (30; 31; 45; 46; 223). Symptoms consisting of headache, sleep disturbance, balance problems, fatigue, irritability, memory and concentration problems frequently occur after mTBI. The majority of patients that sustain a mild brain injury recover completely over days to months. Although a minority of patients continue to be symptomatic, the high incidence of this disorder translates into a large number of afflicted individuals. Persistent symptoms of the central nervous system such as memory/concentration difficulties, feeling dazed or “in a fog,” irritability, fatigue, difficulties with concentration/focus, attention, disordered sleep, and neuropsychiatric problems such as anxiety, depression can have devastating effects on patients and families (102; 196; 200; 245; 284).

Learning and memory impairment is frequently reported after mTBI, which is often associated with hippocampus functional impairment (190). In fact, a recent study showed that in those mTBI cases where a standard head CT was normal, less than one-third demonstrated an abnormal brain MRI (Yuh et al., 2013). Located in the temporal lobe, the hippocampus plays a major role in learning and memory and is particularly

susceptible to mTBI-related injury due to its anatomic location (131; 158; 297). Conventional imaging techniques usually do not show any sign of overt morphological damage in the hippocampus and other brain regions (23; 310). However, more sensitive imaging techniques revealed that 75% of mTBI patients have functional abnormalities in the medial temporal lobe including the hippocampus (297). Similarly, stereological analysis of animals exposed to mTBI, do not reveal significant loss of hippocampal neurons (6; 76); yet some studies suggest that alterations in hippocampal function and excitability may result from mild brain injury even in the absence of clear morphological damage (76; 107; 109; 238; 239).

Changes in hippocampal excitability after TBI may result from deficits in the GABAergic inhibitory synaptic transmission (114; 205; 221; 233; 322). Severe TBI leads to reduction of the GABA_A-mediated inhibitory transmission in dentate granule cells (DGCs) in rats (205; 221) and mice (322). Both, evoked (322) and spontaneous (205; 221; 322) miniature inhibitory postsynaptic currents (mIPSC) are less frequent in DGCs after severe TBI, which was associated with loss of parvalbumin-positive interneurons (221). However, the study of mTBI impact in the hippocampal inhibitory GABAergic synaptic transmission is not clear and more studies are needed to elucidate mechanisms that are involved in the functional pathology.

The purpose of the current study is to investigate functional and morphological alterations in CA1 inhibitory synaptic transmission after mTBI. CA1 is the output region within the hippocampal trisynaptic circuit and alterations in this region may have an impact in the functionality of the entire hippocampus. By means of whole-cell patch clamp, we examined whether a mild brain injury induced by a controlled cortical impact

(CCI) impairs GABA_A receptor-mediated inhibitory transmission in the CA1. We also determined whether changes in the inhibitory transmission are associated with alterations in the number of GABAergic interneurons and surface expression of the $\alpha 1$, $\beta 2$, or $\gamma 2$ GABA_A receptor subunits. Additionally, whether the expression and function of $\alpha 7$ -containing nicotinic acetylcholine receptors ($\alpha 7$ -nAChRs) are altered after CCI was also investigated. In conclusion, our results show that mTBI induces deficits in the GABA_A-mediated inhibitory transmission, which may contribute to neuronal hyperexcitability and the development of cognitive deficits.

EXPERIMENTAL PROCEDURES

Animals

Experiments were performed on male Sprague–Dawley rats (Taconic Farms, Rockville, MD, USA), 5– 6 weeks old, weighing 150 – 200 g at the start of the experiments. Animals were housed paired until the day of the surgery and then housed individually in an animal facility that is Association for Assessment and Accreditation of Laboratory Animal Care accredited, in an environmentally controlled room (20 –23 °C, 12-h light/dark cycle, lights on at 6:00 AM), with food (Harlan Teklad Global Diet 2018, 18% protein rodent diet; Harlan Laboratories; Indianapolis, IN) and water *ad libitum*. Cages were cleaned weekly and animal handling was minimized to reduce animal stress (231). All animal use procedures were in accordance with the National Institutes of Health Guide for the Care and Use of Laboratory Animals, and were approved by the Uniformed Services University of the Health Sciences Institutional Animal Care and Use Committees (IACUC). All efforts were made to minimize the number of animals used

and their suffering. All animals were allowed to acclimate in the animal facility for at least 5 days prior to surgery.

Controlled Cortical Impact Injury

A unilateral cortical contusion using the controlled cortical impact (CCI) model of traumatic brain injury was administered using a previously established (171) protocol. Briefly, animals were anesthetized with isoflurane (2.5%) and had their heads shaved and placed in the stereotaxic frame. Core body temperature of the animals was maintained at 36-37°C using a heating pad and D.C. Temperature Control System (FHC, Model Number 40-90-8D, Bowdoin, ME). Without damaging the underlying dura mater, the skin was retracted, and a 4.0 mm craniotomy – 3.0 mm lateral to the midline and 4.0 mm posterior to the bregma over the left tempoparietal cortex – was performed. In these experiments, the contact velocity was set to 3.5 m/sec with a dwell time of 200 ms and the amount of deformation was set to 2.0 mm using a 3.0 mm diameter impact tip. Following injury, the skullcap was replaced and fixed using bone wax (Ethicon, Sommerville, NJ) and the incision was closed with absorbable sutures (Stoelting, IL). The animals received subcutaneously buprenorphine (50 µL) for pain alleviation and Ringer's solution (5 mL) for rehydration after surgery. Sham-treated controls received the craniotomy, but no CCI injury.

Passive Avoidance

One day prior to the controlled cortical impact surgery, animals were submitted to the training session of the passive avoidance test, which provides a measure of contextual memory (hippocampal dependent) and learning. During training, animals were placed into a darkened chamber. After a delay of 60s, a light came on and the door to the other,

still darkened chamber opened. Each animal had up to 300 sec to cross to the dark chamber. Once he did, the door closed, a 0.8 mA shock was delivered through the grid floor for 1 s, and the latency to cross was recorded. Each testing trial performed on the days 1 and 7 days following CCI was identical to the training session, except that the shock was not be delivered if/when the animal crosses into the darkened chamber. Memory occurred if the animal did not cross into the chamber in which it previously was shocked or if the latency to cross is significantly longer during the testing trial than the training trial.

Immunohistochemistry

Fixation and Tissue Processing.

Seven (7) days after CCI, animals were deeply anesthetized using nembutal (75–100 mg/kg, i.p.) and transcardially perfused with phosphate buffered saline (PBS, 100 ml) followed by 4% paraformaldehyde (250 ml). Brains were removed and post-fixed in 4% paraformaldehyde overnight at 4°C, then transferred to a solution of 30% sucrose in PBS for 72 hours, and frozen with dry ice before storage at -80°C until sectioning. Sectioning was performed as previously described (89; 90). A 1-in-5 series of sections containing the rostrocaudal extent of the amygdala was cut at 40 µm on a sliding microtome (Leica Microsystems SM2000R). A 1-in-5 series of free-floating sections was collected from the cryoprotectant solution, and washed three times for 5 min each. Slices were mounted on a slide, air-dried overnight and processed for Nissl staining with cresyl violet.

GAD-67 Immunohistochemistry.

To label GAD-67 immunoreactive neurons, a 1-in-5 series of free-floating sections was collected from the cryoprotectant solution, washed three times for 5 min each in 0.1 M PBS, and incubated in a blocking solution containing 10% normal goat serum (Millipore Bioscience Research Reagents, Temecula, CA) and 0.5% Triton X-100 in PBS for 1 hour at room temperature. The sections were then incubated with mouse anti-GAD-67 serum (1:1000, MAB5406; Millipore Bioscience Research Reagents), 5% normal goat serum, 0.3% Triton X-100, and 1% bovine serum albumin overnight at 4°C. After rinsing three times for 10 min each in 0.1% Triton X-100 in PBS, the sections were incubated with Cy3-conjugated goat anti-mouse antibody (1:1000; Jackson ImmunoResearch Laboratories Inc., West Grove, PA) and 0.0001% 4,6-diamidino-2-phenylindole dihydrochloride (Sigma-Aldrich) in PBS for 1 hour at room temperature. After a final rinse in PBS for 10 min, sections were mounted on slides, air-dried for at least 30 min, and coverslipped with ProLong Gold antifade reagent (Invitrogen, Carlsbad, CA).

Stereological Quantification.

Design-based stereology was performed to quantify the total number of neurons in Nissl-stained sections and interneurons in GAD-67-immunostained sections in the BLA (90). Sections were viewed with a Zeiss (Oberkochen, Germany) Axioplan 2ie fluorescent microscope with a motorized stage, interfaced with a computer running StereoInvestigator 9.0 (MicroBrightField, Williston, VT). The CA1 region was identified on slide-mounted sections and delineated for each slide of each animal, under a 2.5X objective, based on the atlas of Paxinos and Watson (222). All sampling was done under

a 63X oil immersion objective. Nissl-stained neurons were distinguished from glia cells by their larger size and pale nuclei surrounded by darkly stained cytoplasm containing Nissl bodies. The total number of Nissl-stained and GAD-67-immunostained neurons was estimated by using the optional fractionator probe, and, along with the coefficient of error (CE), were calculated by using StereoInvestigator 9.0 (MicroBrightField). The CE was calculated by the software according to the equations of Gundersen et al., (1999) ($m = 1$) (113) and Schmitz and Hof (2000) (second estimation) (266).

For Nissl-stained neurons in the CA1, a 1-in-10 series of sections was analyzed (seven sections on average). The counting frame was 20 X 20 μm , the counting grid was 250 X 250 μm , and the dissector height was 10 μm . Nuclei were counted when the cell body came into focus within the dissector, which was placed 2 μm below the section surface. Section thickness was measured at every counting site, and the average mounted section thickness was 25.7 μm . An average of 234 neurons per hemisphere per rat were counted. Eight rats per group were analyzed, and the average CE was 0.07 for both the Gundersen et al. and Schmitz-Hof equations.

For GABAergic interneurons immuno-labeled for GAD-67 in the CA1, a 1-in-10 series of sections was analyzed (on average seven sections). The counting frame was 50 X 50 μm , the counting grid was 130 X 130 μm , and the dissector height was 20 μm . Nuclei were counted when the top of the nucleus came into focus within the dissector, which was placed 2 μm below the section surface. Section thickness was measured at every fifth counting site, and the average mounted section thickness was 26.3 μm . An average of 257 neurons per side per rat was counted. Eight rats were analyzed per group, and the average CE was 0.08 for both the Gundersen et al. and Schmitz-Hof equations.

Electrophysiological Experiments

Coronal slices were prepared from rats 7 days after surgery. The rats were anesthetized with isoflurane and then decapitated. Brain slices (400 μm -thick) were cut using a vibratome (series 1000; Technical Products International, St. Louis, MO), in ice-cold cutting solution consisting of (in mM): 115 sucrose, 70 NMDG, 1KCl, 2 CaCl_2 , 4 MgCl_2 , 1.25 NaH_2PO_4 , 30 NaHCO_3 , 25 D-glucose. Slices were transferred to a holding chamber, at room temperature, in a bath solution containing (in mM): 125 NaCl, 2.5 KCl, 2.0 CaCl_2 , 2.0 MgCl_2 , 25 NaHCO_3 , 1.25 NaH_2PO_4 , and 22 D-glucose. Recording solution was the same as the holding bath solution. All solutions were saturated with 95% O_2 , 5% CO_2 to achieve a pH near 7.4. Slices were transferred to a submersion-type recording chamber (0.7 mL capacity), where they were continuously perfused with oxygenated ACSF ($\sim 3\text{--}4$ mL/min). Neurons were visualized with an upright microscope (Zeiss Axioskop 2, Thronwood, NY) through a 40x water immersion objective, equipped with a CCD-100 camera (Dage-MTI, Michigan City, IN). All experiments were performed at room temperature (28°C). Tight-seal (>1 G Ω) whole-cell recordings were obtained from the cell body of pyramidal-shaped neurons in the CA1 region, which were identified on the basis of their electrophysiological properties (259; 260). Patch electrodes were fabricated from borosilicate glass and had a resistance of 1.5–5.0 M Ω when filled with a solution containing (in mM): 135 Cs-gluconate, 10 MgCl_2 , 0.1 CaCl_2 , 1 EGTA, 10 Hepes, 2 Na-ATP, 0.2 Na_3GTP , pH 7.3 (285–290 mOsm). Neurons were voltage-clamped using an Axopatch 200B amplifier (Axon Instruments, Foster City, CA, USA). Inhibitory postsynaptic currents (IPSCs) were pharmacologically isolated and recorded at a -70 mV holding potential. Access resistance (5–24 M Ω) was regularly

monitored during recordings, and cells were rejected if it changed by 15% during the experiment. Ionic currents and action potentials were amplified and filtered (1 kHz) using the Axopatch 200B amplifier (Axon Instruments, Foster City, CA) with a four-pole, low-pass Bessel filter, were digitally sampled (up to 2 kHz) using the pClamp 10.2 software (Molecular Devices, Sunnyvale, CA), and further analyzed using the Mini Analysis program (Synaptosoft Inc., Fort Lee, NJ) and Origin (OriginLab Corporation, Northampton, MA). The peak amplitude, 10–90% rise time, and decay time constant of IPSCs were analyzed off-line using pClamp 10.2 software and the Mini Analysis Program (Synaptosoft, Inc., Leonia, NJ, USA). Miniature IPSCs (mIPSCs) were analyzed off-line using the Mini Analysis Program (Synaptosoft, Fort Lee, NJ) and detected by manually setting the mIPSC threshold (~1.5 times the baseline noise amplitude) after visual inspection.

Agonists of α_7 -nAChRs were applied by pressure injection. Pressure application was performed with the help of a push–pull experimental arrangement (226), as utilized previously (89). Pressure was applied to the pipette via a Picospritzer (General Valve Division, Parker Hannifin Corp., Fairfield, NJ), set at about 100 MPa (14 psi). A motorizer (Newport, Fountain Valley, CA) was coupled with the approach/withdrawal (push–pull) actuator of a micromanipulator (Burleigh PCS-5000 series; EXFO Photonic Solution Inc., Mississauga, Ontario, Canada). Motorizer movement and duration of application pulses were controlled with a Master-8 digital stimulator (AMPI; Jerusalem, Israel). Ionic currents were amplified and filtered (1 kHz) using an Axopatch 200B amplifier, with a four-pole low-pass Bessel filter, and were digitally sampled (up to 5

kHz). Currents were recorded using pClamp 10.2 software and further analyzed using OriginLab (Northampton, MA) and Mini60 software.

Drugs used were as follows: 6-cyano-7-nitroquinoxaline-2,3-dione (CNQX), an α -amino-3-hydroxyl-5-methyl-4-isoxazole-propionate (AMPA)/kainate receptor antagonist; d-2-amino-phosphonovalerate (AP-5), an *N*-methyl-d-aspartic acid (NMDA) receptor antagonist; and SCH50911, a GABA_B receptor antagonist (all purchased from Tocris, Ellisville, MO). We also used bicuculline methiodide, a GABA_A receptor antagonist, and tetrodotoxin, a sodium channel blocker (purchased from Sigma-Aldrich, St. Louis, MO).

Biotinylation and Western Blot

Coronal slices containing the hippocampus were prepared as described for electrophysiology experiments. After a 1-hour recovery period in oxygenated ACSF, slices were incubated in ACSF containing 1 mg/ml EZ-Link Sulfo-NHS-SS-Biotin (Pierce, Rockford, IL) for 1 hour on ice, followed by the addition of quench solution (provided in the Pierce Cell Surface Protein Isolation Kit, Cat No. 89881). The hippocampus was then dissected and tissue sections were transferred to small plastic tubes containing radioimmunoprecipitation assay (RIPA) buffer composed of (in mM) 50 Tris-HCl, pH 7.4, 150 NaCl, 2 EDTA, 50 NaF, 1 Na₃VO₄, 1% Triton X-100, 0.1% SDS, 0.5% Na-deoxycholate, and a Protease Inhibitor Cocktail (Sigma-Aldrich, MO). Samples were sonicated and the homogenates were centrifuged at 14,000 g for 10 min at 4°C. Protein concentrations were measured using the DC Protein Assay Kit (Bio-Rad, CA). Protein (1,500 μ g) was then mixed with 400 μ L of UltraLink immobilized NeutrAvidin agarose beads (Pierce) for 1 hour at room temperature. The beads were then washed 3

times with 500 μ L wash buffer (provided in the kit). Samples were eluted in 400 μ L of RIPA buffer containing Protease Inhibitor Cocktail supplemented with 50 mM dithiothreitol and mixed for 1 hour at room temperature followed by centrifugation at 14,000g for 10 min at 4°C. Then, LDS 4x (Invitrogen) was added to protein samples. Biotinylated proteins were resolved by SDS-PAGE, transferred to nitrocellulose membranes, and probed with the following antibodies Anti-Alpha1 GABA-A Receptor, clone N95/65, 75-136 (1:1000; UC Davis/NIH NeuroMab Facility), Anti-GABA A Receptor Beta 2,3 Chain, clone BD17[MAB341 (1:1000, Millipore, Billerica, MA), Anti-GABA A Receptor Gamma 2, Ab16213 (1:1000, AbCam, Cambridge, MA). The signal from the immunoreactive band was detected by using a gel imaging system (Fuji LAS-3000). Membranes were stripped using ReBlot Plus Strong Antibody Stripping Solution (Millipore, Billerica, MA) and re-probed with Anti-GLUT1 (1:1000, Millipore, Billerica, MA) for loading control. Signal intensity was determined by densitometric scanning using ImageJ. When duplicate conditions were performed in one animal, the ratio values were averaged to obtain an animal average for that condition.

Statistical Analysis

Statistical values are presented as mean \pm standard error (SE). Results from ipsilateral and contralateral sides of sham-operated and traumatized animals were compared using One-Way ANOVA followed by Bonferroni post-hoc test in the stereology and Western blot experiments. For open-field experiments, two-way ANOVA followed by Tukey post-hoc test was used. For electrophysiology experiments, either One-way ANOVA followed by Bonferroni post-hoc test or independent t-tests were performed. $p < 0.05$ was considered statistically significant for all statistical analysis.

Sample sizes (n) refer to the number of rats, except for the electrophysiology results where “n” refers to the number of slices or recorded cells.

RESULTS

Memory impairments after mTBI

Rats were exposed to mild TBI and then tested for memory impairments in the passive avoidance context. Prior to surgery all animals were trained in the passive avoidance apparatus and their latency to cross to the dark chamber were recorded. After being randomly assigned to Sham and CCI groups, rats were submitted to CCI surgery and tested in the passive avoidance context 1- and 7- days later. Prior to surgery, the latency to enter the dark chamber did not differ between sham (24 ± 9 sec, $n=8$) and CCI (27 ± 5 sec, $n=8$) rats. One day after the surgery, however, CCI rats spent significantly less time (89.27 ± 25.97 sec; $n=8$) in the bright chamber when compared to Sham rats (218.8 ± 34.24 sec; $n=8$; $p=0.0207$). CCI rats still showed reduced latency to enter the dark chamber (58.52 ± 11.20 sec; $n=8$) when compared to Sham rats (190.6 ± 32.59 sec, $n=8$; $p=0.0171$) 7 days after the surgery (Figure 17).

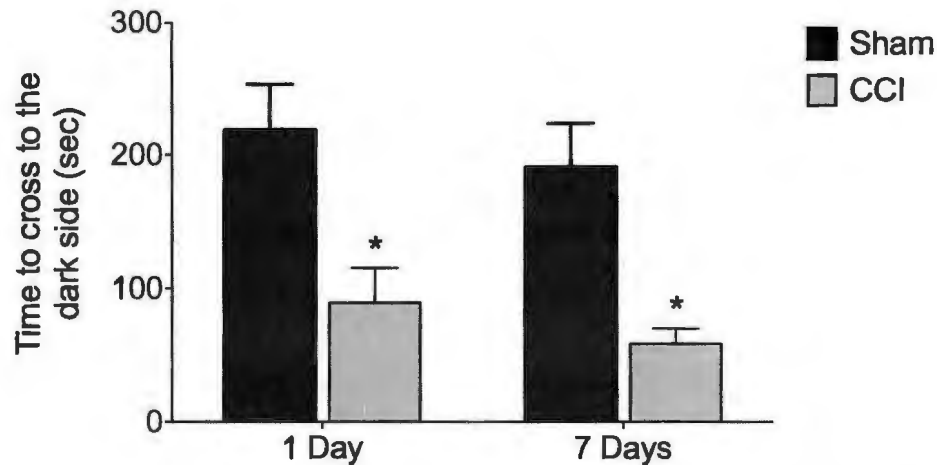


Figure 17. Mild TBI leads to memory deficits in the passive avoidance test. CCI rats spent significantly less time to enter the dark chamber 1- and 7-days after injury compared to sham animals. Bars show the mean \pm SE of the percentage of time spent in the center. * $p < 0.05$.

Loss of GABAergic interneurons

We have recently shown that our CCI model does not cause any significant loss of neurons in the CA1 region of hippocampus, which we have used as a parameter to classify it as mTBI (6). Because CA1 excitability and function are tightly regulated by local interneurons (8; 122; 124) we also investigated whether specific loss of interneurons occurs in the CA1 region after CCI. Design-based stereology revealed that there was no significant reduction in the total number of interneurons 1 day after CCI either ipsilateral or contralateral to the site of injury when compared to sham controls (Table 7). GAD67-positive cells from 1- and 7-day sham control groups did not display any significant differences and were therefore averaged together (data not shown). However, the total number of GAD67-positive cells was reduced by 23.08% ipsilateral and by 14.96% contralateral to the lesion seven days after CCI (Table 7; Figure 18). Our results show

that the interneuronal population is significantly reduced in the CA1 region 7 days after CCI in the absence of any alteration in the total number of neurons.

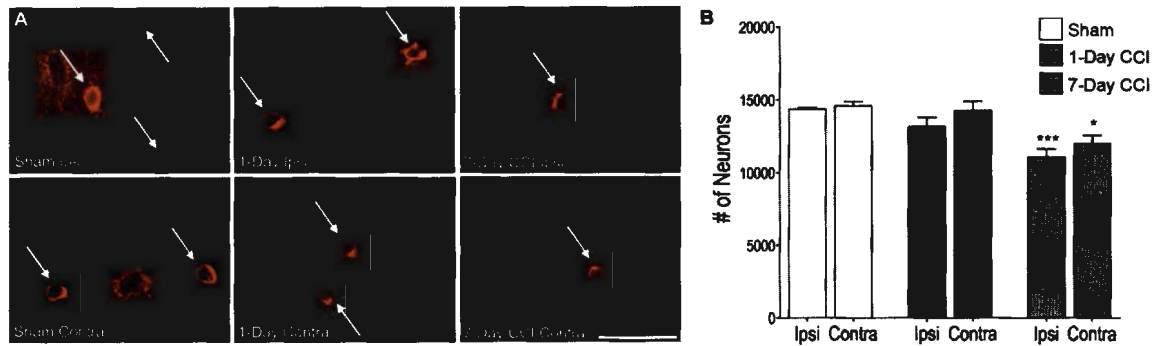


Figure 18. Delayed loss of GABAergic interneurons in the CA1 region within the first week after mild CCI. (A) Representative photomicrographs of GAD-67 immunohistochemically stained GABAergic interneurons in the CA1 of sham (left), 1-day CCI (middle), and 7-day CCI (right) animals. Total magnification is 630x; scale bar, 50 μ m. (B) group data showing the mean and standard error of the stereologically estimated total number of GAD-67-positive cells in the CA1 1- and 7-days after CCI compared with sham. Only 7-days after CCI was there a significant bilateral reduction in GAD-67-positive cells indicating a delayed loss of GABAergic interneurons. *p < 0.05; ***p < 0.001; n = 10 for each group.

Condition	# of Cells \pm SEM	Compared to	# of Cells \pm SEM
Sham Ipsilateral	14,367 \pm 97.7	CCI 1 day Ipsilateral	13,165 \pm 615.3
		CCI 1 day Contralateral	14,262 \pm 621.6
		CCI 7 days Ipsilateral	11,058 \pm 559.3***
		CCI 7 days Contralateral	11,974 \pm 572.1*
Sham Contralateral	14,587 \pm 281.5	CCI 1 day Ipsilateral	13,165 \pm 615.3
		CCI 1 day Contralateral	14,262 \pm 621.6
		CCI 7 days Ipsilateral	11,058 \pm 559.3***
		CCI 7 days Contralateral	11,974 \pm 572.1*

*p < 0.05, ***p < 0.001

Table 7. Total number of interneurons in the CA1 region of sham and CCI animals

Reduced Inhibitory tone in the CA1

Whole-cell recordings were obtained from CA1 pyramidal cells to determine the mTBI-induced alterations in the GABAergic inhibitory synaptic transmission. GABA_A-mediated spontaneous inhibitory post-synaptic currents (sIPSCs) were recorded at a holding potential of -70 mV in the presence of CNQX (20 μM), D-AP5 (50 μM), SCH50911 (10 μM), and LY 3414953 (3 μM), 1 and 7 days after CCI. First, we recorded GABA_A-mediated spontaneous inhibitory postsynaptic currents (sIPSCs) to determine whether mTBI impaired the overall inhibitory synaptic transmission in the CA1 regions. Sham animals did not differ in the frequency and amplitude of sIPSCs at either 1- or 7-days after surgery and so we averaged together the amplitude and frequency of all sham animals (data not shown). One day after the surgery the mean frequency of sIPSCs in the CCI group (3.6 ± 0.7 Hz; $n = 15$) did not differ significantly from sham controls (3.2 ± 0.9 Hz; $n = 15$). Likewise, we found no difference in the mean the amplitude of sIPSCs between sham control (254 ± 8 pA; $n = 15$) and CCI rats (258 ± 10 pA; $n = 15$). However, 7 days after CCI the mean frequency of sIPSCs recorded from CCI rats (2.47 ± 0.5 Hz; $n = 15$) was reduced by $35 \pm 4\%$ ($p < 0.005$) when compared to Sham controls (3.8 ± 1.1 Hz; $n = 15$). Also, we found a $32 \pm 5\%$ reduction ($p < 0.005$) in the mean amplitude of sIPSCs recorded from CCI rats (192 ± 7 pA; $n = 15$) when compared to Sham controls (282 ± 8 pA; $n = 15$). There were no significant differences in the rise and the decay time constant of the sIPSCs in CCI rats and sham controls 1 and 7 days after the surgery (Figure 19).

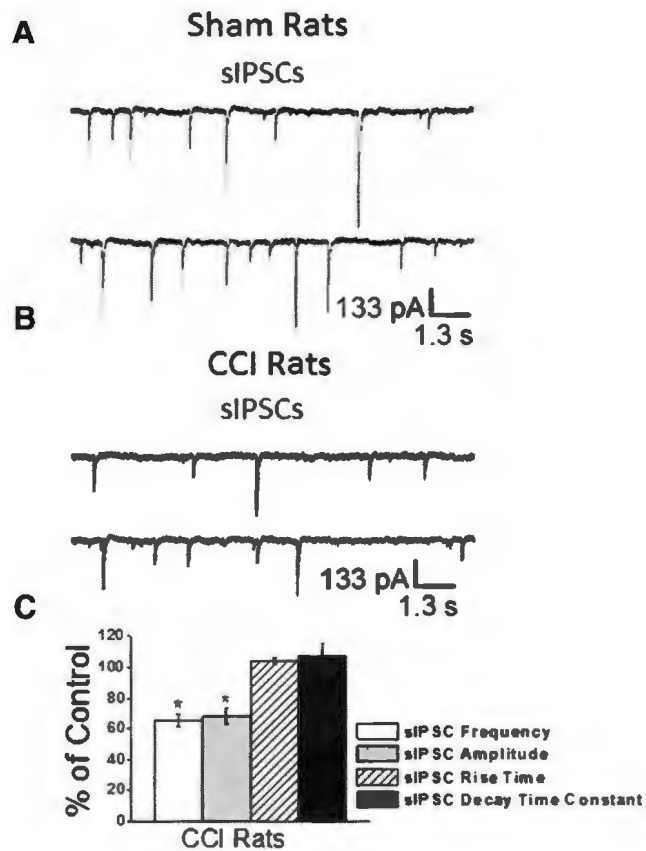


Figure 19. Mild CCI causes a significant decrease in the frequency and amplitude of sIPSCs in the CA1 7-days after CCI. sIPSCs were recorded from pyramidal-shaped neurons in the presence of d-APV (50 μ M), SCH50911 (20 μ M), and GYKI 52466 (50 μ M), at a holding potential of -70 mV. Representative examples of recordings obtained in the BLA are shown in (A) and (B) for Sham and CCI 7-day animals, respectively. (C) Group data showing the change in the percentage frequency and amplitude of sIPSCs from CCI animals relative to Sham animals. The frequency and amplitude, but not the rise time and the decay time constant of the sIPSCs were significantly reduced in the CCI group compared to the sham controls.

To determine whether decreased inhibitory tone in CA1 region is associated with reduced responsiveness of postsynaptic GABA_A receptors, we also recorded miniature inhibitory postsynaptic currents (mIPSCs) 1 and 7 days after the surgery. Action potential-independent mIPSCs were recorded at a holding potential of -70 mV in the presence of CNQX ($20\mu\text{M}$), D-AP5 ($50\mu\text{M}$), SCH50911 ($10\mu\text{M}$), and LY 3414953 ($3\mu\text{M}$), and TTX ($1\mu\text{M}$). The frequency and amplitude of mIPSCs recorded from Sham animal did not differ at either 1- or 7-days after surgery and so we averaged together the amplitude and frequency of all sham animals (data not shown). The frequency and amplitude of mIPSCs recorded from CCI animals (mean frequency = 1.9 ± 0.4 Hz; mean amplitude = 64 ± 3 ; $n = 15$) did not differ from those recorded from Sham controls (mean frequency = 1.7 ± 0.6 ; mean amplitude = 65 ± 4 ; $n = 15$) 1 day after the surgery. However, we found a $29 \pm 3\%$ reduction in frequency (1.34 ± 0.5 Hz; $n = 15$; $p < 0.005$) and a $25 \pm 3\%$ reduction in the amplitude (48 ± 7 pA; $n = 15$; $p < 0.001$) of mIPSCs recorded 7 days after the surgery from CCI rats (Figure 20).

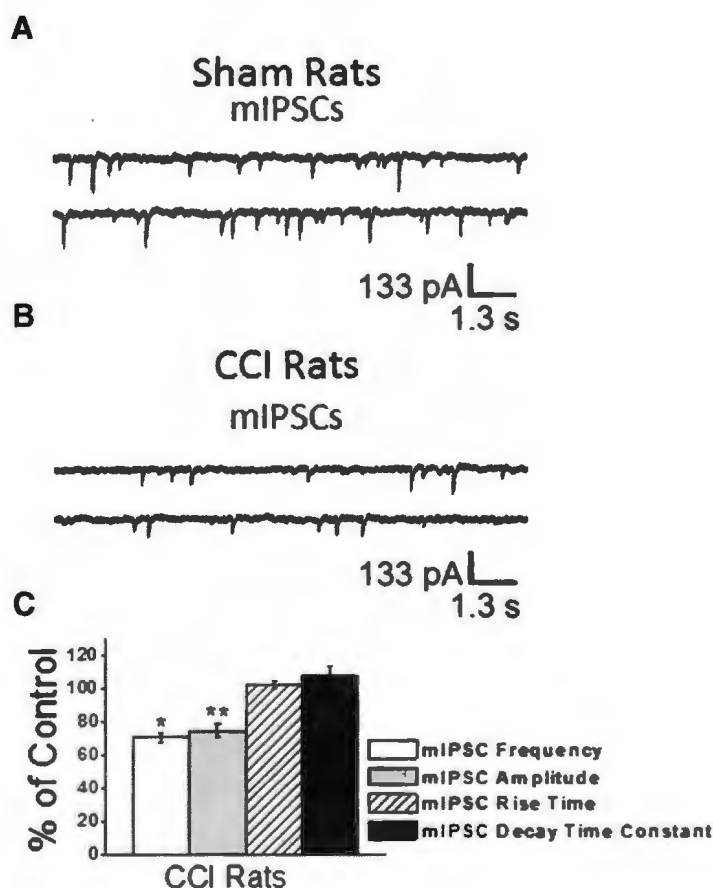


Figure 20. Mild CCI causes a significant decrease in the frequency and amplitude of mIPSCs in the CA1 7-days after CCI. mIPSCs were recorded from pyramidal-shaped neurons in the presence of d-APV (50 μ M), SCH50911 (20 μ M), and GYKI 52466 (50 μ M), TTX (1 μ M) at a holding potential of -70 mV. Representative examples of recordings obtained in the BLA are shown in (A) and (B) for Sham and CCI 7 days animals, respectively. (C) Group data showing the change in the percentage frequency and amplitude of mIPSCs from CCI animals relative to Sham animals. The frequency and amplitude, but not the rise time and the decay time constant of the sIPSCs were significantly reduced in the CCI group compared to the sham controls. The recorded currents were blocked by the GABA_A receptor antagonist bicuculline (data not shown).

Reduced surface expression of GABA_A receptor subunits in the hippocampus

Because reduced amplitude of mIPSCs in CCI rats suggests that the density of postsynaptic GABA_A receptors is reduced we investigated whether mTBI induces changes in the surface expression of GABA_A receptors subunits in the hippocampus. To determine mTBI-induced alterations in the surface expression of $\alpha 1$, $\beta 2$, and $\gamma 2$ subunits of GABA_A receptor, membrane proteins are isolated by a biotinylation assay and quantified by Western blot. After densitometric analysis, Western blot membranes were stripped and re-probed for GLUT1. It has been previously demonstrated that expression of GLUT1 is unaltered following TBI (117). Therefore, surface expression of GLUT1 was used as a loading control. Seven days after the surgery the surface expression of all three GABA_A subunits examined were reduced in CCI animals compared to sham controls. Ipsilateral to the side of injury, a 67.3% ($p < 0.0001$) reduction of the $\alpha 1$ subunit, a 37.4% ($p < 0.0001$) reduction of the $\beta 2$ subunit, and a 61.7% ($p < 0.0001$) reduction of the $\gamma 2$ subunit, were found, whereas 56.8% ($p < 0.0001$) reduction of the $\alpha 1$ subunit, a 44.8% ($p < 0.0001$) reduction of the $\beta 2$ subunit, and a 54.4% ($p < 0.0001$) reduction of the $\gamma 2$ subunit was observed in the hippocampus contralateral to the injury, indicating that the reduced amplitude in the GABA_A receptor-mediated sIPSCs may be due to reduction in the number of GABA_A receptors in the postsynaptic terminal (Figure 21).

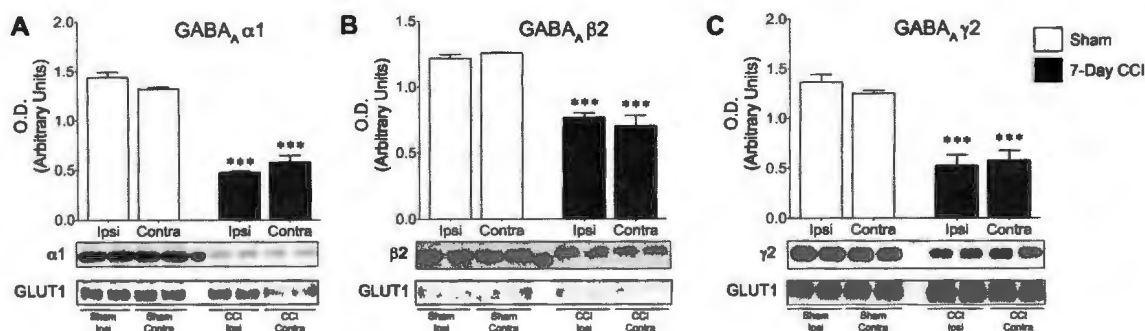


Figure 21. Surface expression of α_1 , β_2 , and γ_2 GABA_A receptor subunits is reduced in the hippocampus of CCI animals 7 days after mild CCI. Western blot for subunits of (A) α_1 , (B) β_2 , and (C) γ_2 subunits, respectively, was performed using biotinylated proteins isolated from the ipsilateral and contralateral sides of Sham and CCI 7-day animals. Group data showing the mean \pm SE of the ratio between each subunit and GLUT1 optical densities. Top panel: representative Western blot for α_1 (A), β_2 (B), and γ_2 (C) subunits of GABA_A receptors, respectively. Bottom panel: representative Western blot for GLUT1, used as a loading control. Note that surface expression of GABA_A α_1 , $\beta_{2/3}$ and γ_2 subunits are reduced in CCI animals when compared to Sham animals. *** $p < 0.001$; $n = 3$ for each group.

Unaltered function and surface expression of α_7 -nAChRs

α_7 -Containing nicotinic acetylcholine receptors (α_7 -nAChRs) play a major role in the regulation of excitability and cognitive function in the hippocampus (123; 141; 166; 241; 330). Therefore, we examined whether mTBI induces alterations in the function and expression of α_7 -nAChRs in the CA1 region. To determine changes in the function of α_7 -nAChRs we pressure-applied tricholine citrate (5 mM; 70 ms; 14 psi), while recording from interneurons of brain slices in the presence of α -conotoxin AulB (1 μ M), DHBE (10 μ M), atropine sulfate (0.5 μ M), D-AP5 (50 μ M), CNQX (20 μ M), SCH50911 (10 μ M), LY 3414953 (3 μ M), and bicuculline (20 μ M). In current-clamp mode, pressure application of tricholine citrate onto control slices elicited a brief train of

action potentials, while in the voltage clamp mode it induced inward currents. The current induced by tricholine citrate was nearly blocked by 1 μ M α -BgTx. The mean charge transferred through α_7 -nAChRs in sham animals was 350 ± 50 pC ($n = 13$). We did not observe any alteration in the mean charge transfer through α_7 -nAChRs in CCI rats 1- (310 ± 30 pC; $n = 5$) or 7- (460 ± 80 pC; $n = 8$) days after surgery compared to sham controls (Figure 22).

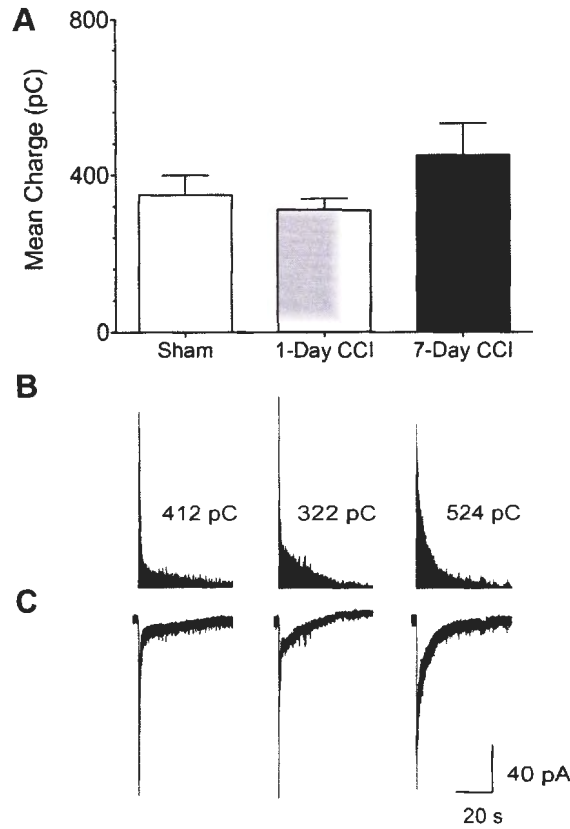


Figure 22. Activation of α_7 -nAChRs by fast application of the α_7 -nAChR specific agonist, choline, in the CA1, shows that cholinergic conductance is unaltered 1- and 7-days after CCI. (A) Group data showing the mean \pm SE charge transfer in pyramidal-shaped neurons in the CA1 from CCI rats 7-days after injury. (B) Representative charge transfer from α_7 -nAChRs from sham (left), 1-days CCI (middle), and 7-day CCI (right) animals. (C) Representative α_7 -nAChR-mediated currents recorded from sham (left), 1-day CCI (middle), and 7-day CCI (right) animals. Experiments were recorded in the presence of α -conotoxin AulB (1 μ M), DH β E (10 μ M), atropine sulfate (0.5 μ M), D-AP5 (50 μ M), CNQX (20 μ M), SCH50911 (10 μ M), LY 3414953 (3 μ M), and bicuculline (20 μ M).

Next, we used biotinylation and Western blot analysis to confirm whether the surface expression of $\alpha 7$ -nAChRs is unaltered after CCI. Accordingly, we found that the surface expression of the $\alpha 7$ -nAChR was unaltered in CCI animals 7 days after surgery when compared with Sham control animals (Figure 23).

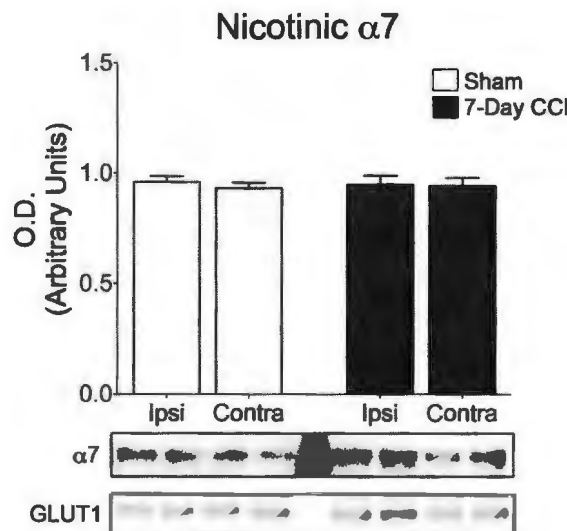


Figure 23. Surface expression of $\alpha 7$ subunit of neuronal nicotinic acetylcholine receptor is increased in the BLA of CCI animals 7-days after mild CCI. Western blot was performed using biotinylated proteins isolated from the ipsilateral and contralateral sides of Sham and CCI 7-day animals. Group data showing the mean \pm SE of the ratio between the $\alpha 7$ subunit and GLUT1 optical densities. Top panel: representative Western blot for $\alpha 7$ -nAChRs. Bottom panel: representative Western blot for GLUT1, used as a loading control..* $p < 0.05$; $n = 3$ for each group.

DISCUSSION

Mild traumatic brain injury can lead to long-lasting cognitive and neuropsychiatric impairment in humans despite the absence of clear morphological damage. The aim of the present study was to investigate the pathological and pathophysiological alterations in the hippocampus, a key brain region in cognitive processes, which may underlie memory deficits after mTBI. In this report, mild traumatic brain injury leads to pathological and pathophysiological alterations in the CA1 subfield of hippocampus that contribute to a significant decrease in the inhibitory GABAergic activity. Rats exposed to mild TBI using the model of CCI also display impaired memory consolidation and memory processes when tested in the passive avoidance context 1 and 7 days after CCI. We also observed a substantial reduction in the frequency and amplitude of action potential-dependent and action potential-independent GABA_A-mediated currents 7 days after mTBI using the model of CCI. Specific loss of inhibitory interneurons in the CA1 was also observed in the CA1 following mTBI. Additionally, surface expression of $\alpha 1$, $\beta 2$ and $\gamma 2$ subunits of the GABA_A receptor were reduced in the hippocampus 7 days after CCI. In contrast, $\alpha 7$ -nAChR function and expression in the CA1 were not altered 7 days after mTBI. All these mTBI-induced pathological and pathophysiological alterations leading to reduced inhibitory tone in the CA1 region of hippocampus are likely to contribute to memory and cognitive deficits observed in CCI rats.

Memory deficits are usually detected early after injury and may persist beyond 1 year after injury (28; 136; 196; 245; 283; 284; 299). Accordingly, here we show that a single exposure to mTBI was sufficient to induce memory deficits in rats 1 and 7 days

after CCI. These results are in lieu with human data where mTBI patients have particular difficulty with recent memory (137). Likewise, our results show that memory consolidation was impaired when tested 1 and 7 days after CCI. Although the mechanisms of memory impairment following mTBI are poorly understood in patients, our data suggests that loss of GABAergic input into CA1 pyramidal neurons may be a contributing factor.

Positive modulation of GABAergic inhibitory synaptic transmission has long been considered to be detrimental to memory formation and consolidation (58; 139; 270; 331; 334). Administration of drugs that enhance GABAergic neurotransmission improved the behavioral and cognitive outcome of rodents after TBI (63; 214). Conversely, administration of bicuculline, a GABA_A receptor antagonist, exacerbated memory deficits induced by TBI (214). Our model of mTBI does not result in significant neuronal loss in the CA1 region (6) but did induce a selective loss of GABAergic inhibitory interneurons. Moreover, we demonstrate that mTBI leads to decreased expression of GABA_A receptors in the hippocampus. Consistently, we observed a significant decrease in inhibitory synaptic transmission in the CA1, including reductions in both the frequency and amplitude of mIPSCs following mTBI. Reduction in the hippocampal GABAergic inhibitory neurotransmission has been previously observed following severe TBI (205; 221; 322). However, to the best of our knowledge this is the first report to show that mTBI leads to reduced inhibition in the CA1 region and that this may be associated with cognitive impairments observed after trauma.

Alpha 7-containing neuronal nicotinic acetylcholine receptors ($\alpha 7$ nAChRs) are widely expressed in the CA1 region of hippocampus and its activation

modulate both GABAergic and glutamatergic transmission (4; 9; 82; 144; 175; 285; 314). Moreover, $\alpha 7$ nAChRs are known to play an important role in several cognitive functions such as attention, learning and memory (324) and $\alpha 7$ nAChR density was reported to be reduced in several brain regions, including hippocampus, following TBI (133; 304-307). In the CA1, the density of $\alpha 7$ nAChRs as determined by [125 I]-Bungarotoxin autoradiography was significantly reduced at 2, 24, 48 and 72 hours following TBI but was back to control levels at day 7 (133; 305; 307). These alterations together with other impairments in the cholinergic system are thought to contribute to cognitive deficits following TBI. In our study we investigated alterations in the function and expression of $\alpha 7$ nAChRs at 1 and 7 days following mTBI. Results showed that the function and expression of $\alpha 7$ nAChRs were unaltered 7 days after mTBI and no significant functional alteration in $\alpha 7$ nAChRs was observed 24 hours after mTBI. The apparent discrepancy between our results and those of Hoffmeister et al.,(2011) (133) may be due to differences in the parameters employed to induce a brain injury by CCI as well as the methodology. We used electrophysiological techniques to quantify $\alpha 7$ nAChRs function specifically on interneurons at 24 hours whereas autoradiographic analysis, which would be expected to quantify the total amount of $\alpha 7$ nAChRs in the CA1 subfield, was used in the previous study (133).

In conclusion, the results from this study demonstrated that a mild CCI leads to a significant reduction in the GABAergic inhibitory synaptic transmission in the CA1 region, which is a result of the selective loss of GABAergic interneurons and reduced surface expression of GABA_A receptor subunits. Here, we propose that decreased inhibition may be the underlying cause of hippocampal dysfunction and

subsequent memory impairments observed after mTBI. Further studies are needed to elucidate how trauma leads to persistent cognitive deficits so that pharmacological therapies may be developed to ameliorate such impairments following TBI.

CHAPTER 5: Discussion and Future Directions

Mild traumatic brain injury accounts for 80% of all reported cases of TBI and is often associated with the development of long-term psychiatric and neurological disorders including anxiety, cognitive impairments and posttraumatic epilepsy. Nevertheless, routine neuro-imaging of these patients usually reveals completely normal brain morphology and thus, the absence of any structural alteration that might explain the neurological symptoms. Accordingly, the present investigation was designed to determine the molecular and cellular mechanisms underlying the development of long-lasting deficits after mTBI. We focused our study on two temporal lobe structures known to be critically involved in TBI-related neurological functions: the hippocampus and amygdala. The hippocampus plays an important role in the pathophysiology of cognitive disorders and posttraumatic epilepsy whereas the amygdala is closely associated with the development of anxiety disorders. The present study employed a model of mTBI that replicates the cognitive and behavioral consequences of mTBI in humans. Specifically, we observed that CCI-induced mTBI leads to memory deficits and increased anxiety-like behaviors in rats. Further, although the delivery of a mechanical impact to the exposed dura produced some damage to the underlying cortex, there was no reduction in the total number of neurons in the BLA and CA1 region of hippocampus, an observation that is consistent with the condition of “mild TBI”. However, at the molecular level we observed that mTBI induced clear pathophysiological alterations including: up-regulation of specific gene transcripts encoding molecules involved in the immune response, intracellular signaling, and cellular death and survival. Functionally, we observed that GABAergic inhibitory synaptic transmission was significantly reduced in both brain

regions; the frequency and amplitude of GABA_A-receptor mediated spontaneous and miniature IPSCs were reduced after CCI. This was consistent with reduced immunoreactivity for GAD67 and a significant decrease in the surface expression of $\alpha 1$, $\beta 2$, and $\gamma 2$ GABA_A receptors subunits after mTBI. Additionally, in the BLA, we observed a significant increase in the function and expression $\alpha 7$ -nAChRs, which was not detected in the CA1. We propose, therefore, that these pathological and pathophysiological alterations may contribute to hyperexcitability in the BLA and CA1 and the development of long-lasting cognitive and behavioral impairments after mTBI.

Mild traumatic brain injury is usually the result of a concussion. This type of injury involves acceleration and deceleration forces that cause the brain “shake” inside the cranium, affecting different brain regions. Despite being mild, concussions are far from being a focal brain injury and a reliable model of mTBI should reproduce this characteristic. The present work showed that a single mild focal impact to the left parietal cortex induced molecular, functional and morphological alterations in brain regions far from the impact site on both brain hemispheres. Therefore, our data showed that CCI is more than just a focal injury, although we did not identify how the injury spread to other brain regions. During the injury a concussive force is transferred to the brain and intracranial pressure changes on each side of the brain, though the contralateral side is less affected than the ipsilateral side (53). We speculate that this increase in pressure disrupts brain homeostasis and may lead to the activation of the neurometabolic cascade detailed in Chapter 1 throughout the brain, which leads to functional and morphological damage. Additionally, it has been shown that anterograde and retrograde degeneration are two important mechanisms that contribute to spread damage following CCI (115; 116).

Moreover, activated microglia may migrate from to site of injury and move along degenerating and intact axons and initiate an inflammatory response in regions far from the site of impact (68). Regardless of the mechanism responsible for the widespread pathophysiological alterations observed, our study corroborates the notion that controlled cortical impact is actually more than a focal brain injury (100; 296).

When a biomechanical force is transferred to the brain, immediate shearing and tearing of blood vessels and brain tissue can occur. Excitotoxicity then takes place leading to neuronal cell death and other pathological alterations (26; 32; 105; 168). In addition to that, the neurometabolic cascade activated after mTBI may ultimately lead to changes in the expression level of genes whose products are involved in metabolism, cell death, cell survival, inflammation among other cellular processes. (108; 128-130; 217). We investigated whether mTBI alters the expression level of neurotrophic factors (NTFs). NTFs are a class of structurally related molecules that play a major role in the growth and survival of developing neurons and the maintenance of mature neurons (17; 65; 179; 180). Unlike previous studies (130; 185) we did not observe any alterations in the expression of BDNF but found a significant reduction of Ntf3. Given the role that NTFs play in neuronal survival, downregulation of Ntf3 after mTBI may favor neuronal death and contribute to deficits observed after mTBI.

Neuroinflammation is a secondary injury mechanism that follows tissue damage and may substantially contribute to the long-term pathology of mTBI and the development of associated neuropsychiatric disorders (47; 118; 203; 247; 265; 340). mTBI leads to a transient increase in the levels of pro-inflammatory cytokines including interleukin-1 (IL-1), tumor necrosis factor- α (TNF- α), and interleukin-6 (IL-6), which

peak within hours after injury in the brain and rapidly return to baseline levels (47; 165; 202; 203; 265; 340). This transient increase explains why our microarray analysis did not show any increase in the levels of pro-inflammatory cytokine mRNAs in the hippocampus. By 24 hours after mTBI, our earliest time point, levels of cytokine mRNAs had returned to control values and were not different from those observed in sham animals. Still, transcripts encoding other inflammatory mediators including: Ccl2, Ccl7, Lcn2 and Timp1, which function downstream to cytokine up-regulation, were considerably up-regulated 24 hours after mTBI. Within a week after injury mRNA levels of these transcripts had returned to control levels. Intriguingly, by 7 and 30 days post-mTBI, a new set of genes associated with chronic inflammation were un-regulated. These included genes encoding messages for the complement system, dendritic cell maturation, T cell differentiation and major histocompatibility complex II (MHC II) pathway. Specifically, complement components, C3 and Serping1; immune cell-activating factors, Ccr5, and Fcgr2b; and MHC II components, Rtl- Da and Cd74 were all up-regulated. The transient increase in chemokine mRNAs followed by up-regulation of this second set of genes suggests that a chronic inflammatory response may take place after mTBI and underlie the longer-lasting neurological consequences of mild brain injury.

Neuronal cell death is a central component of TBI pathology and occurs in two different waves following injury (232; 281). Within hours after TBI neurons die as a direct consequence of primary injury (165) whereas additional cell death can occur over days to years as result of secondary damage to the brain (33; 57; 69; 127; 232; 281). The protracted cell death following TBI occurs by several mechanisms in which inflammation plays a central role (232; 281). Consistent with this hypothesis we observed an up-

regulation of proinflammatory signaling molecules and a significant reduction in GAD67 immunoreactivity in both the BLA and hippocampus regions, suggesting a delayed, specific loss of GABAergic interneurons. Therefore, we speculate that a sustained inflammatory response contributes to interneuronal loss following mTBI. Remarkably, this neuronal loss appears to be specific to the relatively small pool of GABAergic neurons which represent only 10% and 5% of the total neuronal mass of the BLA and CA1, respectively. Accordingly, TBI-induced reductions in the total number of neurons in these regions were small and did not achieve statistical significance.

It should also be noted that the delayed loss of GAD67 immunoreactivity may not reflect the actual death of GABAergic interneurons but rather may involve a prolonged suppression of GAD67 expression. It is known that the expression of GAD67 can be differentially regulated in response to diverse stimuli (132; 155; 224; 262). Thus, a sustained downregulation of GAD67 could underlie pathophysiological alteration that occurs in response to mTBI. Regardless of the cause, the observed reduction in GAD67 immunoreactivity has a major implication to pathophysiology of mTBI. This finding reveals the possibility that loss of GABAergic inhibition may result in a state of neuronal hyper-excitability that underlies the associated symptomology.

Consistent with reductions in the number of cells expressing GAD67, we observed that inhibitory synaptic transmission in the BLA and CA1 was impaired after mTBI. The frequency and amplitude of spontaneous and miniature GABA_A-mediated IPSCs were smaller in both regions following injury. As the former is associated with loss of GAD67 immunoreactivity, the latter suggests that the number of GABA_A receptors is reduced in the postsynaptic membrane. Accordingly, we observed that the surface

expression of the GABA_A subunits $\alpha 1$, $\beta 2$, and $\gamma 2$, which constitute the majority of GABA_A receptors in the brain and are highly expressed in the BLA and CA1 (197), is reduced in both regions following mTBI. Although we did not investigate whether mTBI induces changes in the surface expression of GABA_A subunits other than $\alpha 1$, $\beta 2$, and $\gamma 2$ we can conclude, based on our electrophysiological data, that the stoichiometry of GABA_A receptors does not change after mTBI. Changes in the subunit composition of GABA_A receptors are likely to result in alterations in kinetic parameters (7; 104), which was not observed in our study. We did not identify what triggers reduction in the surface expression of GABA_A receptor subunits, however we suggest that this may be associated with inflammatory reaction. Inflammation has been previously suggested to impair GABAergic inhibitory transmission in the CNS (49; 251; 252; 280; 335). In particular, TNF- α induces internalization of GABA_A receptors and leads to reductions in the frequency and amplitude of mIPSCs (49; 280). Because our data shows that following mTBI there is a prominent activation of the inflammatory response and significant reduction in the frequency and amplitude of sIPSCs and mIPSCs, it is likely that inflammation may play an important role in the development of functional impairments to the GABAergic inhibitory system after mTBI.

Reduced GABAergic inhibitory synaptic transmission can lead to the development of hyperexcitability, which is associated with neuropsychiatric disorders in humans. Amygdalar hyperexcitability, in particular, has often been correlated with anxiety disorders in humans (236; 309) and anxiety-like behaviors in rodents (66). Indeed, upregulation of TNF- α in the BLA leads to deficits in the GABAergic inhibitory synaptic transmission and development of anxiety-like behaviors in animals (49).

Accordingly our data suggests that mTBI-induced reduction in the GABAergic transmission may lead to hyperexcitability in the BLA and the subsequent development of anxiety-like behavior in rats. Our evidence that increases in anxiety-like behavior are associated with deficits to the GABAergic system in the BLA is corroborated by previous studies demonstrating that the selective loss of GABAergic interneurons in the BLA contributes to anxiogenic behaviors (295). Likewise, we propose that impaired inhibition in the CA1 region of the hippocampus may be the underlying cause of memory deficits following mTBI. Loss of parvalbumin-positive interneurons in the CA1 regions has been previously associated with memory deficits (207), which is consistent with our findings. Moreover, administration of drugs that enhance GABAergic activity improves the cognitive outcome after mTBI (63; 214). This is in lieu with our proposal that deficits in the GABAergic inhibitory system in the CA1 region may underlie the development of cognitive impairment after mTBI. GABAergic interneurons are essential for synchronized activity (known as theta rhythm) in the CA1 region and modulation of synaptic plasticity, which are both important for proper memory function (8; 122; 124). Therefore, we speculate that impaired inhibitory synaptic transmission in the CA1 leads to hyperexcitability and functional alterations that underlie the development of cognitive impairment following mTBI.

There are additional mechanisms that modulate excitability in the BLA and CA1 regions. Activation of α_7 -nAChRs, which are highly expressed on both regions, increases the presynaptic release of glutamate and regulate glutamatergic and GABAergic synaptic transmission (9; 82; 142; 144; 148; 153; 227)}. Additionally, activation of α_7 -nAChRs play an important role in the regulation of synaptic plasticity (141; 150) and cognition

(324) as well as in the development of anxiety disorder (218). Therefore, we examined whether alterations in the function and expression of α_7 -nAChRs contributed to BLA and CA1 hyperexcitability and subsequent anxiety-like behaviors and cognitive impairment after mTBI. In the BLA we found a significant increase in the surface expression and function of α_7 -nAChRs 7 days after mTBI, which was not observed in the CA1. Thus, we suggest that increased cholinergic transmission mediated by α_7 -nAChRs contributed to neuronal hyperexcitability in the BLA and the subsequent development of anxiety-like behavior. However, according to our results cognitive impairment observed in rats after mTBI is not due to alterations in the expression and function of α_7 -nAChRs in the CA1.

The present work identified molecular, morphological and functional alterations that take place after mTBI and may contribute to the development of long-lasting neuropsychiatric disorders, however the initial mediator of all alterations discussed herein remains to be determined. We suggest that TNF- α may play an important role in initiating the cascade that resulted in the pathophysiological alterations that followed mTBI. First, binding of TNF- α to its receptor TNFR1 leads to activation of the transcription factor NF- κ B, which ultimately leads to changes in gene expression (313). *Ccl2*, *Ccl7*, *Lcn2* and *Timp1* are some of the genes regulated by NF- κ B in response to TNF- α (38; 210; 293) that are upregulated after mTBI. Second, upregulation of TNF- α in the BLA is associated with reduced GABAergic inhibitory synaptic transmission and the development of anxiety-like behaviors in mice with persistent inflammatory pain (49). Finally, inhibition of TNF- α biosynthesis after mTBI prevents the development of cognitive impairment in mice (15). While we do not propose that TNF- α acts alone to induce all the alterations discussed above, its prominent role in the development of the

changes observed here is consistent with the proposal that this molecule is critical in the pathophysiology of mTBI.

In conclusion, the results from this study demonstrated that mild TBI leads to molecular, functional and morphological alterations in the BLA and CA1, which may underlie the development of anxiety-like behavior and cognitive impairments. A significant loss of GABAergic interneurons and reduced surface expression of GABA_A receptors appears to contribute to a decrease in GABAergic inhibitory synaptic transmission, which in turn, may lead to hyperexcitability in both regions. In the BLA, increases in the surface expression and function of α_7 -nAChRs, contributed to increased excitability within principal neurons in the BLA, which was not observed in the CA1. We concluded that reduced inhibition and subsequent hyperexcitability in the BLA and CA1 is associated with the development of anxiety disorders and cognitive impairment following mTBI. The high incidence of anxiety disorders and cognitive impairment after a mild head trauma points to the urgency to unravel the basic mechanisms underlying the development of these conditions. To date, there is no pharmacological therapy that effectively prevents the psychiatric and cognitive disorders resulting from mTBI. The present finding that the GABAergic system is selectively affected by mTBI indicates that therapies targeting this system should be considered as pharmacological therapies for mTBI. Moreover we speculate that trauma-induced alterations in the GABAergic system may be triggered by upregulation of the cytokine TNF- α . This conclusion is consistent with the report that anti-TNF- α therapy blocks the cognitive impairment after TBI (15), and the anxiety-like behavior observed in mice with persistent inflammatory pain (49). Further investigation of the potential role of this cytokine in the pathological and

pathophysiological alterations observed in mTBI will hopefully lead a better understanding of the mechanisms of injury and may provide new targets for effective pharmacological intervention.

APPENDIX A: Additional Publications

EXPRESSION OF miRNAs AND THEIR COOPERATIVE REGULATION OF THE PATHOPHYSIOLOGY IN TRAUMATIC BRAIN INJURY.

Hu Z, Yu D, **Almeida-Suhett C**, Tu K, Marini AM, Eiden L, Braga MF, Zhu J, Li Z.

PLoS One. 2012;7(6):e39357

Abstract

Traumatic brain injury (TBI) is a leading cause of injury-related death and disability worldwide. Effective treatment for TBI is limited and many TBI patients suffer from neuropsychiatric sequelae. The molecular and cellular mechanisms underlying the neuronal damage and impairment of mental abilities following TBI are largely unknown. Here we used the next generation sequencing platform to delineate miRNA transcriptome changes in the hippocampus at 24 hours and 7 days following TBI in the rat controlled cortical impact injury (CCI) model, and developed a bioinformatic analysis to identify cellular activities that are regulated by miRNAs differentially expressed in the CCI brains. The results of our study indicate that distinct sets of miRNAs are regulated at different post-traumatic times, and suggest that multiple miRNA species cooperatively regulate cellular pathways for the pathological changes and management of brain injury. The distinctive miRNAs expression profiles at different post-CCI times may be used as molecular signatures to assess TBI progression. In addition to known pathophysiological changes, our study identifies many other cellular pathways that are subjected to modification by differentially expressed miRNAs in TBI brains. These pathways can potentially be targeted for development of novel TBI treatment.

PRESYNAPTIC FACILITATION OF GLUTAMATE RELEASE IN THE BASOLATERAL AMYGDALA: A MECHANISM FOR THE ANXIOGENIC AND SEIZUROGENIC FUNCTION OF GLUK1 RECEPTORS.

Aroniadou-Anderjaska V, Pidoplichko VI, Figueiredo TH, **Almeida-Suhett CP**, Prager EM, Braga MF.

Neuroscience. 2012 Sep 27;221:157-69.

Abstract

Kainate receptors containing the GluK1 subunit (GluK1Rs; previously known as GluR5 kainate receptors) are concentrated in certain brain regions, where they play a prominent role in the regulation of neuronal excitability, by modulating GABAergic and/or glutamatergic synaptic transmission. In the basolateral nucleus of the amygdala (BLA), which plays a central role in anxiety as well as in seizure generation, GluK1Rs modulate GABAergic inhibition via postsynaptic and presynaptic mechanisms. However, the role of these receptors in the regulation of glutamate release, and the net effect of their activation on the excitability of the BLA network are not well understood. Here, we show that in amygdala slices from 35- to 50-day-old rats, the GluK1 agonist (RS)-2-amino-3-(3-hydroxy-5-tert-butylisoxazol-4-yl) propanoic acid (ATPA) (300 nM) increased the frequency of spontaneous excitatory postsynaptic currents (sEPSCs) and miniature EPSCs (mEPSCs) recorded from BLA principal neurons, and decreased the rate of failures of evoked EPSCs. The GluK1 antagonist (S)-1-(2-amino-2-carboxyethyl)-3-(2-carboxybenzyl) pyrimidine-2,4-dione (UBP302) (25 or 30 μ M) decreased the frequency of mEPSCs, reduced evoked field potentials, and increased the "paired-pulse ratio" of the field potential amplitudes. Taken together, these results suggest that GluK1Rs in the rat BLA are present on presynaptic terminals of principal neurons, where

they mediate facilitation of glutamate release. In vivo bilateral microinjections of ATPA (250 pmol) into the rat BLA increased anxiety-like behavior in the open field test, while 2 nmol ATPA induced seizures. Similar intra-BLA injections of UBP302 (20 nmol) had anxiolytic effects in the open field and the acoustic startle response tests, without affecting pre-pulse inhibition. These results suggest that although GluK1Rs in the rat BLA facilitate both GABA and glutamate release, the facilitation of glutamate release prevails, and these receptors can have an anxiogenic and seizurogenic net function. Presynaptic facilitation of glutamate release may, in part, underlie the hyperexcitability-promoting effects of GluK1R activation in the rat BLA.

ACETYLCHOLINESTERASE INHIBITION IN THE BASOLATERAL AMYGDALA PLAYS A KEY ROLE IN THE INDUCTION OF STATUS EPILEPTICUS AFTER SOMAN EXPOSURE.

Prager EM, Aroniadou-Anderjaska V, **Almeida-Suhett CP**, Figueiredo TH, Apland JP, Braga MF.

Neurotoxicology. 2013 Sep;38:84-90.

Abstract

Exposure to nerve agents induces intense seizures (status epilepticus, SE), which cause brain damage or death. Identification of the brain regions that are critical for seizure initiation after nerve agent exposure, along with knowledge of the physiology of these regions, can facilitate the development of pretreatments and treatments that will successfully prevent or limit the development of seizures and brain damage. It is well-established that seizure initiation is due to excessive cholinergic activity triggered by the nerve agent-induced irreversible inhibition of acetylcholinesterase (AChE). Therefore, the reason that when animals are exposed to lethal doses of a nerve agent, a small proportion of these animals do not develop seizures, may have to do with failure of the nerve agent to inhibit AChE in brain areas that play a key role in seizure initiation and propagation. In the present study, we compared AChE activity in the basolateral amygdala (BLA), hippocampus, and piriform cortex of rats that developed SE (SE rats) after administration of the nerve agent soman (154µg/kg) to AChE activity in these brain regions of rats that received the same dose of soman but did not develop SE (no-SE rats). The levels of AChE activity were measured at the onset of SE in SE rats, 30min after soman administration in no-SE rats, as well as in controls which received saline in place of soman. In the control group, AChE activity was significantly higher in the BLA compared to the hippocampus and piriform cortex. Compared to controls, AChE activity was dramatically lower in the hippocampus and the piriform cortex of both the SE rats

and the no-SE rats, but AChE activity in the BLA was reduced only in the SE rats. Consistent with the notion that soman-induced neuropathology is due to intense seizures, rather than due to a direct neurotoxic effect of soman, no-SE rats did not present any neuronal loss or degeneration, 7 days after exposure. The results suggest that inhibition of AChE activity in the BLA is necessary for the generation of seizures after nerve agent exposure, and provide strong support to the view that the amygdala is a key brain region for the induction of seizures by nerve agents.

THE RECOVERY OF ACETYLCHOLINESTERASE ACTIVITY AND THE PROGRESSION OF NEUROPATHOLOGICAL AND PATHOPHYSIOLOGICAL ALTERATIONS IN THE RAT BASOLATERAL AMYGDALA AFTER SOMAN-INDUCED STATUS EPILEPTICUS: RELATION TO ANXIETY-LIKE BEHAVIOR.

Prager EM, Aroniadou-Anderjaska V, **Almeida-Suhett CP**, Figueiredo TH, Apland JP, Rossetti F, Olsen CH, Braga MF.

Neuropharmacology. 2014 Jan 31.

Abstract

Organophosphorus nerve agents are powerful neurotoxins that irreversibly inhibit acetylcholinesterase (AChE) activity. One of the consequences of AChE inhibition is the generation of seizures and status epilepticus (SE), which cause brain damage, resulting in long-term neurological and behavioral deficits. Increased anxiety is the most common behavioral abnormality after nerve agent exposure. This is not surprising considering that the amygdala, and the basolateral nucleus of the amygdala (BLA) in particular, plays a central role in anxiety, and this structure suffers severe damage by nerve agent-induced seizures. In the present study, we exposed male rats to lethal doses of the nerve agent soman, and determined the time course of recovery of AChE activity, along with the progression of neuropathological and pathophysiological alterations in the BLA, during a 30-day period after exposure. Measurements were taken at 24 h, 7 days, 14 days, and 30 days after exposure, and at 14 and 30 days, anxiety-like behavior was also evaluated. We found that more than 90% of AChE is inhibited at the onset of SE, and AChE inhibition remains at this level 24 h later, in the BLA, as well as in the hippocampus, piriform cortex, and prelimbic cortex, which we analyzed for comparison. AChE activity recovered by day 7 in the BLA and day 14 in the other three regions. Significant neuronal loss and neurodegeneration were present in the BLA at 24 h and throughout the 30-day period. There was no significant loss of GABAergic interneurons in the BLA at 24 h

post-exposure. However, by day 7, the number of GABAergic interneurons in the BLA was reduced, and at 14 and 30 days after soman, the ratio of GABAergic interneurons to the total number of neurons was lower compared to controls. Anxiety-like behavior in the open-field and the acoustic startle response tests was increased at 14 and 30 days post-exposure. Accompanying pathophysiological alterations in the BLA - studied in in vitro brain slices - included a reduction in the amplitude of field potentials evoked by stimulation of the external capsule, along with prolongation of their time course and an increase in the paired-pulse ratio. Long-term potentiation was impaired at 24 h, 7 days, and 14 days post-exposure. The loss of GABAergic interneurons in the BLA and the decreased interneuron to total number of neurons ratio may be the primary cause of the development of anxiety after nerve agent exposure.

ASIC1a ACTIVATION ENHANCES INHIBITION IN THE BASOLATERAL AMYGDALA AND REDUCES ANXIETY

Volodymyr I. Pidoplichko, Vassiliki Aroniadou-Anderjaska¹, Eric M. Prager, Taiza H. Figueiredo, **Camila P. Almeida-Suhett**, Steven L. Miller, Maria F.M. Braga

Journal of Neuroscience. 2014. In Press

Abstract

The discovery that even small changes in extracellular acidity can alter the excitability of neuronal networks via activation of acid-sensing ion channels (ASICs) could have therapeutic application in a host of neurological and psychiatric illnesses. Antagonists of ASIC1a □ a subtype of ASICs that is widely distributed in the brain □ have been recently proposed as a potential treatment for anxiety. The basolateral amygdala (BLA) plays a central role in the generation of fear, and hyperexcitability of the BLA is a characteristic feature of anxiety disorders. To better understand the role of ASIC1a in anxiety, we have attempted to provide a direct assessment of whether ASIC1a activation increases BLA excitability. In rat BLA slices, activation of ASIC1a by low pH or ammonium elicited inward currents in both interneurons and principal neurons, and increased spontaneous IPSCs recorded from principal cells significantly more than spontaneous EPSCs. Epileptiform activity induced by high potassium and low magnesium was suppressed by ammonium. Antagonism of ASIC1a decreased background, spontaneous IPSCs more than EPSCs, and increased the excitability of the BLA network, as reflected in the pronounced increase of evoked field potentials, suggesting that ASIC1a channels are tonically active. *In vivo* activation or blockade of ASIC1a in the BLA suppressed or increased, respectively, anxiety-like behavior. Thus, in the rat BLA, ASIC1a has an inhibitory and anxiolytic function. The finding that these

channels are tonically active may provide a molecular explanation for the association of hypocapnia and alkalosis with panic attacks.

REFERENCES

1. Abdul-Muneer PM, Schuetz H, Wang F, Skotak M, Jones J, et al. 2013. Induction of oxidative and nitrosative damage leads to cerebrovascular inflammation in an animal model of mild traumatic brain injury induced by primary blast. *Free Radic Biol Med* 60:282-91
2. Adams JH, Doyle D, Graham DI, Lawrence AE, McLellan DR, et al. 1985. The contusion index: a reappraisal in human and experimental non-missile head injury. *Neuropathol Appl Neurobiol* 11:299-308
3. Ahmed S, Bierley R, Sheikh JI, Date ES. 2000. Post-traumatic amnesia after closed head injury: a review of the literature and some suggestions for further research. *Brain injury : [BI]* 14:765-80
4. Alkondon M, Pereira EF, Almeida LE, Randall WR, Albuquerque EX. 2000. Nicotine at concentrations found in cigarette smokers activates and desensitizes nicotinic acetylcholine receptors in CA1 interneurons of rat hippocampus. *Neuropharmacology* 39:2726-39
5. Almeida CP, Pidoplichko V, Marini AM, Li Z, Eiden LE, Braga MFM. 2011. Pathophysiological alterations in temporal lobe structures after TBI and their role in the development of epilepsy. In *Society for Neuroscience. Neuroscience Meeting Planner* Washington, DC
6. Almeida-Suhett CP, Li Z, Marini AM, Braga MF, Eiden LE. 2013. Temporal course of changes in gene expression suggests a cytokine-related mechanism for long-term hippocampal alteration after controlled cortical impact. *Journal of neurotrauma* In Press
7. Angelotti TP, Macdonald RL. 1993. Assembly of GABAA receptor subunits: alpha 1 beta 1 and alpha 1 beta 1 gamma 2S subunits produce unique ion channels with dissimilar single-channel properties. *The Journal of neuroscience : the official journal of the Society for Neuroscience* 13:1429-40
8. Antonucci F, Alpar A, Kacza J, Caleo M, Verderio C, et al. 2012. Cracking down on inhibition: selective removal of GABAergic interneurons from hippocampal networks. *The Journal of neuroscience : the official journal of the Society for Neuroscience* 32:1989-2001
9. Arnaiz-Cot JJ, Gonzalez JC, Sobrado M, Baldelli P, Carbone E, et al. 2008. Allosteric modulation of alpha 7 nicotinic receptors selectively depolarizes hippocampal interneurons, enhancing spontaneous GABAergic transmission. *Eur J Neurosci* 27:1097-110

10. Aroniadou-Anderjaska V, Pidoplichko VI, Figueiredo TH, Almeida-Suhett CP, Prager EM, Braga MF. 2012. Presynaptic facilitation of glutamate release in the basolateral amygdala: a mechanism for the anxiogenic and seizurogenic function of GluK1 receptors. *Neuroscience* 221:157-69
11. Aroniadou-Anderjaska V, Qashu F, Braga MF. 2007. Mechanisms regulating GABAergic inhibitory transmission in the basolateral amygdala: implications for epilepsy and anxiety disorders. *Amino Acids* 32:305-15
12. Ascoli GA, Alonso-Nanclares L, Anderson SA, Barrionuevo G, Benavides-Piccione R, et al. 2008. Petilla terminology: nomenclature of features of GABAergic interneurons of the cerebral cortex. *Nature reviews. Neuroscience* 9:557-68
13. Baddeley A. 1992. Working memory. *Science* 255:556-9
14. Baddeley A. 1992. Working Memory: The Interface between Memory and Cognition. *J Cogn Neurosci* 4:281-8
15. Baratz R, Tweedie D, Rubovitch V, Luo W, Yoon JS, et al. 2011. Tumor necrosis factor- α synthesis inhibitor, 3,6'-dithiothalidomide, reverses behavioral impairments induced by minimal traumatic brain injury in mice. *Journal of neurochemistry* 118:1032-42
16. Barazangi N, Role LW. 2001. Nicotine-induced enhancement of glutamatergic and GABAergic synaptic transmission in the mouse amygdala. *Journal of neurophysiology* 86:463-74
17. Barde YA. 1989. Trophic factors and neuronal survival. *Neuron* 2:1525-34
18. Bartsch T, Dohring J, Rohr A, Jansen O, Deuschl G. 2011. CA1 neurons in the human hippocampus are critical for autobiographical memory, mental time travel, and autonoetic consciousness. *Proceedings of the National Academy of Sciences of the United States of America* 108:17562-7
19. Bartsch T, Schonfeld R, Muller FJ, Alfke K, Leplow B, et al. 2010. Focal lesions of human hippocampal CA1 neurons in transient global amnesia impair place memory. *Science* 328:1412-5
20. Bay EH, Liberzon I. 2009. Early stress response: a vulnerability framework for functional impairment following mild traumatic brain injury. *Res Theory Nurs Pract* 23:42-61
21. Belanger HG, Vanderploeg RD, Curtiss G, Warden DL. 2007. Recent neuroimaging techniques in mild traumatic brain injury. *The Journal of neuropsychiatry and clinical neurosciences* 19:5-20

22. Benzinger TL, Brody D, Cardin S, Curley KC, Mintun MA, et al. 2009. Blast-related brain injury: imaging for clinical and research applications: report of the 2008 st. Louis workshop. *Journal of neurotrauma* 26:2127-44
23. Bigler ED, Maxwell WL. 2012. Neuropathology of mild traumatic brain injury: relationship to neuroimaging findings. *Brain imaging and behavior* 6:108-36
24. Binder LM, Rohling ML, Larrabee GJ. 1997. A review of mild head trauma. Part I: Meta-analytic review of neuropsychological studies. *Journal of clinical and experimental neuropsychology* 19:421-31
25. Bissiere S, Humeau Y, Luthi A. 2003. Dopamine gates LTP induction in lateral amygdala by suppressing feedforward inhibition. *Nature neuroscience* 6:587-92
26. Blennow K, Hardy J, Zetterberg H. 2012. The neuropathology and neurobiology of traumatic brain injury. *Neuron* 76:886-99
27. Block ML, Hong JS. 2005. Microglia and inflammation-mediated neurodegeneration: multiple triggers with a common mechanism. *Prog Neurobiol* 76:77-98
28. Bohnen N, Van Zutphen W, Twijnstra A, Wijnen G, Bongers J, Jolles J. 1994. Late outcome of mild head injury: results from a controlled postal survey. *Brain injury : [BI]* 8:701-8
29. Booth-Kewley S, Highfill-McRoy RM, Larson GE, Garland CF, Gaskin TA. 2012. Anxiety and depression in Marines sent to war in Iraq and Afghanistan. *The Journal of nervous and mental disease* 200:749-57
30. Borg J, Holm L, Cassidy JD, Peloso PM, Carroll LJ, et al. 2004. Diagnostic procedures in mild traumatic brain injury: results of the WHO Collaborating Centre Task Force on Mild Traumatic Brain Injury. *Journal of rehabilitation medicine : official journal of the UEMS European Board of Physical and Rehabilitation Medicine*:61-75
31. Borg J, Holm L, Peloso PM, Cassidy JD, Carroll LJ, et al. 2004. Non-surgical intervention and cost for mild traumatic brain injury: results of the WHO Collaborating Centre Task Force on Mild Traumatic Brain Injury. *Journal of rehabilitation medicine : official journal of the UEMS European Board of Physical and Rehabilitation Medicine*:76-83
32. Bramlett HM, Dietrich WD. 2007. Progressive damage after brain and spinal cord injury: pathomechanisms and treatment strategies. *Prog Brain Res* 161:125-41
33. Bramlett HM, Dietrich WD, Green EJ, Busto R. 1997. Chronic histopathological consequences of fluid-percussion brain injury in rats: effects of post-traumatic hypothermia. *Acta Neuropathol* 93:190-9

34. Brooks WM, Stidley CA, Petropoulos H, Jung RE, Weers DC, et al. 2000. Metabolic and cognitive response to human traumatic brain injury: a quantitative proton magnetic resonance study. *Journal of neurotrauma* 17:629-40
35. Bruns J, Hauser WA. 2003. The epidemiology of traumatic brain injury: a review. *Epilepsia* 44 Suppl 1:2-10
36. Bryant RA. 2008. Disentangling mild traumatic brain injury and stress reactions. *The New England journal of medicine* 358:525-7
37. Bryant RA, Harvey AG. 1999. The influence of traumatic brain injury on acute stress disorder and post-traumatic stress disorder following motor vehicle accidents. *Brain injury : [BI]* 13:15-22
38. Bugno M, Witek B, Bereta J, Bereta M, Edwards DR, Kordula T. 1999. Reprogramming of TIMP-1 and TIMP-3 expression profiles in brain microvascular endothelial cells and astrocytes in response to proinflammatory cytokines. *FEBS letters* 448:9-14
39. Bull RJ, Cummins JT. 1973. Influence of potassium on the steady-state redox potential of the electron transport chain in slices of rat cerebral cortex and the effect of ouabain. *Journal of neurochemistry* 21:923-37
40. Bush TG, Puvanachandra N, Horner CH, Polito A, Ostensfeld T, et al. 1999. Leukocyte infiltration, neuronal degeneration, and neurite outgrowth after ablation of scar-forming, reactive astrocytes in adult transgenic mice. *Neuron* 23:297-308
41. Cafferty WB, Yang SH, Duffy PJ, Li S, Strittmatter SM. 2007. Functional axonal regeneration through astrocytic scar genetically modified to digest chondroitin sulfate proteoglycans. *The Journal of neuroscience : the official journal of the Society for Neuroscience* 27:2176-85
42. Camacho A, Massieu L. 2006. Role of glutamate transporters in the clearance and release of glutamate during ischemia and its relation to neuronal death. *Archives of medical research* 37:11-8
43. Canto CB, Wouterlood FG, Witter MP. 2008. What does the anatomical organization of the entorhinal cortex tell us? *Neural Plast* 2008:381243
44. Carlsen J, Zaborszky L, Heimer L. 1985. Cholinergic projections from the basal forebrain to the basolateral amygdaloid complex: a combined retrograde fluorescent and immunohistochemical study. *The Journal of comparative neurology* 234:155-67
45. Carroll LJ, Cassidy JD, Peloso PM, Borg J, von Holst H, et al. 2004. Prognosis for mild traumatic brain injury: results of the WHO Collaborating Centre Task Force on Mild Traumatic Brain Injury. *Journal of rehabilitation medicine :*

46. Cassidy JD, Carroll LJ, Peloso PM, Borg J, von Holst H, et al. 2004. Incidence, risk factors and prevention of mild traumatic brain injury: results of the WHO Collaborating Centre Task Force on Mild Traumatic Brain Injury. *Journal of rehabilitation medicine : official journal of the UEMS European Board of Physical and Rehabilitation Medicine*:28-60
47. Cederberg D, Siesjo P. 2010. What has inflammation to do with traumatic brain injury? *Child's nervous system : ChNS : official journal of the International Society for Pediatric Neurosurgery* 26:221-6
48. Chavko M, Watanabe T, Adeeb S, Lankasky J, Ahlers ST, McCarron RM. 2011. Relationship between orientation to a blast and pressure wave propagation inside the rat brain. *Journal of neuroscience methods* 195:61-6
49. Chen J, Song Y, Yang J, Zhang Y, Zhao P, et al. 2013. The contribution of TNF- α in the amygdala to anxiety in mice with persistent inflammatory pain. *Neuroscience letters* 541:275-80
50. Chen Y, Constantini S, Trembovler V, Weinstock M, Shohami E. 1996. An experimental model of closed head injury in mice: pathophysiology, histopathology, and cognitive deficits. *Journal of neurotrauma* 13:557-68
51. Cheng J, Gu J, Ma Y, Yang T, Kuang Y, et al. 2010. Development of a rat model for studying blast-induced traumatic brain injury. *Journal of the neurological sciences* 294:23-8
52. Choi JM, Lebowitz B, Wang J, Lee SK, Murray JA, et al. 2011. Increased prevalence of celiac disease in patients with unexplained infertility in the United States. *J Reprod Med* 56:199-203
53. Clausen F, Hillered L. 2005. Intracranial pressure changes during fluid percussion, controlled cortical impact and weight drop injury in rats. *Acta Neurochir (Wien)* 147:775-80; discussion 80
54. Cobb SR, Davies CH. 2005. Cholinergic modulation of hippocampal cells and circuits. *The Journal of physiology* 562:81-8
55. Cohen AS, Pfister BJ, Schwarzbach E, Grady MS, Goforth PB, Satin LS. 2007. Injury-induced alterations in CNS electrophysiology. *Prog Brain Res* 161:143-69
56. Cole JT, Yarnell A, Kean WS, Gold E, Lewis B, et al. 2011. Craniotomy: true sham for traumatic brain injury, or a sham of a sham? *Journal of neurotrauma* 28:359-69

57. Colicos MA, Dixon CE, Dash PK. 1996. Delayed, selective neuronal death following experimental cortical impact injury in rats: possible role in memory deficits. *Brain research* 739:111-9
58. Collinson N, Kuenzi FM, Jarolimek W, Maubach KA, Cothliff R, et al. 2002. Enhanced learning and memory and altered GABAergic synaptic transmission in mice lacking the alpha 5 subunit of the GABAA receptor. *The Journal of neuroscience : the official journal of the Society for Neuroscience* 22:5572-80
59. Conductier G, Blondeau N, Guyon A, Nahon JL, Rovere C. 2010. The role of monocyte chemoattractant protein MCP1/CCL2 in neuroinflammatory diseases. *Journal of neuroimmunology* 224:93-100
60. Coronado VG, Xu L, Basavaraju SV, McGuire LC, Wald MM, et al. 2011. Surveillance for traumatic brain injury-related deaths--United States, 1997-2007. *Morbidity and mortality weekly report. Surveillance summaries* 60:1-32
61. Cozzarelli TA. 2010. Evaluation and treatment of persistent cognitive dysfunction following mild traumatic brain injury. *J Spec Oper Med* 10:39-42
62. Crestani F, Lorez M, Baer K, Essrich C, Benke D, et al. 1999. Decreased GABAA-receptor clustering results in enhanced anxiety and a bias for threat cues. *Nature neuroscience* 2:833-9
63. Dash PK, Orsi SA, Zhang M, Grill RJ, Pati S, et al. 2010. Valproate administered after traumatic brain injury provides neuroprotection and improves cognitive function in rats. *PloS one* 5:e11383
64. Davalos D, Grutzendler J, Yang G, Kim JV, Zuo Y, et al. 2005. ATP mediates rapid microglial response to local brain injury in vivo. *Nature neuroscience* 8:752-8
65. Davies AM. 1994. The role of neurotrophins in the developing nervous system. *Journal of neurobiology* 25:1334-48
66. Davis M, Rainnie D, Cassell M. 1994. Neurotransmission in the rat amygdala related to fear and anxiety. *Trends in neurosciences* 17:208-14
67. Dean PJ, Sterr A. 2013. Long-term effects of mild traumatic brain injury on cognitive performance. *Front Hum Neurosci* 7:30
68. Dibaj P, Nadrigny F, Steffens H, Scheller A, Hirrlinger J, et al. 2010. NO mediates microglial response to acute spinal cord injury under ATP control in vivo. *Glia* 58:1133-44
69. Dietrich WD, Alonso O, Halley M. 1994. Early microvascular and neuronal consequences of traumatic brain injury: a light and electron microscopic study in rats. *Journal of neurotrauma* 11:289-301

70. Dikmen S, Temkin N, McLean A, Wyler A, Machamer J. 1987. Memory and head injury severity. *J Neurol Neurosurg Psychiatry* 50:1613-8
71. Dixon CE, Clifton GL, Lighthall JW, Yaghmai AA, Hayes RL. 1991. A controlled cortical impact model of traumatic brain injury in the rat. *Journal of neuroscience methods* 39:253-62
72. Dixon CE, Kochanek PM, Yan HQ, Schiding JK, Griffith RG, et al. 1999. One-year study of spatial memory performance, brain morphology, and cholinergic markers after moderate controlled cortical impact in rats. *Journal of neurotrauma* 16:109-22
73. Dixon CE, Kraus MF, Kline AE, Ma X, Yan HQ, et al. 1999. Amantadine improves water maze performance without affecting motor behavior following traumatic brain injury in rats. *Restorative neurology and neuroscience* 14:285-94
74. Dixon CE, Lyeth BG, Povlishock JT, Findling RL, Hamm RJ, et al. 1987. A fluid percussion model of experimental brain injury in the rat. *Journal of neurosurgery* 67:110-9
75. Dutar P, Bassant MH, Senut MC, Lamour Y. 1995. The septohippocampal pathway: structure and function of a central cholinergic system. *Physiological reviews* 75:393-427
76. Eakin K, Miller JP. 2012. Mild traumatic brain injury is associated with impaired hippocampal spatiotemporal representation in the absence of histological changes. *Journal of neurotrauma* 29:1180-7
77. Echemendia RJ, Julian LJ. 2001. Mild traumatic brain injury in sports: neuropsychology's contribution to a developing field. *Neuropsychol Rev* 11:69-88
78. Ekstrom AD, Kahana MJ, Caplan JB, Fields TA, Isham EA, et al. 2003. Cellular networks underlying human spatial navigation. *Nature* 425:184-8
79. Elder GA, Dorr NP, De Gasperi R, Gama Sosa MA, Shaughness MC, et al. 2012. Blast exposure induces post-traumatic stress disorder-related traits in a rat model of mild traumatic brain injury. *Journal of neurotrauma* 29:2564-75
80. Ernst M, Brauchart D, Boresch S, Sieghart W. 2003. Comparative modeling of GABA(A) receptors: limits, insights, future developments. *Neuroscience* 119:933-43
81. Etkin A, Wager TD. 2007. Functional neuroimaging of anxiety: a meta-analysis of emotional processing in PTSD, social anxiety disorder, and specific phobia. *The American journal of psychiatry* 164:1476-88

82. Fabian-Fine R, Skehel P, Errington ML, Davies HA, Sher E, et al. 2001. Ultrastructural distribution of the $\alpha 7$ nicotinic acetylcholine receptor subunit in rat hippocampus. *The Journal of neuroscience : the official journal of the Society for Neuroscience* 21:7993-8003
83. Fabricius M, Fuhr S, Bhatia R, Boutelle M, Hashemi P, et al. 2006. Cortical spreading depression and peri-infarct depolarization in acutely injured human cerebral cortex. *Brain* 129:778-90
84. Faraday MM, Elliott BM, Grunberg NE. 2001. Adult vs. adolescent rats differ in biobehavioral responses to chronic nicotine administration. *Pharmacol Biochem Behav* 70:475-89
85. Farovik A, Dupont LM, Eichenbaum H. 2010. Distinct roles for dorsal CA3 and CA1 in memory for sequential nonspatial events. *Learning & memory* 17:12-7
86. Faul M, Xu L, Wald M, Coronado V. 2010. Traumatic Brain Injury in the United States: Emergency Department Visits, Hospitalizations and Deaths 2002–2006. *Atlanta (GA): Centers for Disease Control and Prevention, National Center for Injury Prevention and Control*
87. Feeney DM, Boyeson MG, Linn RT, Murray HM, Dail WG. 1981. Responses to cortical injury: I. Methodology and local effects of contusions in the rat. *Brain research* 211:67-77
88. Fenster CP, Rains MF, Noerager B, Quick MW, Lester RA. 1997. Influence of subunit composition on desensitization of neuronal acetylcholine receptors at low concentrations of nicotine. *The Journal of neuroscience : the official journal of the Society for Neuroscience* 17:5747-59
89. Figueiredo TH, Aroniadou-Anderjaska V, Qashu F, Aplan JP, Pidoplichko V, et al. 2011. Neuroprotective efficacy of caramiphen against soman and mechanisms of its action. *British journal of pharmacology* 164:1495-505
90. Figueiredo TH, Qashu F, Aplan JP, Aroniadou-Anderjaska V, Souza AP, Braga MF. 2011. The GluK1 (GluR5) Kainate/ α -amino-3-hydroxy-5-methyl-4-isoxazolepropionic acid receptor antagonist LY293558 reduces soman-induced seizures and neuropathology. *J Pharmacol Exp Ther* 336:303-12
91. Fineman I, Hovda DA, Smith M, Yoshino A, Becker DP. 1993. Concussive brain injury is associated with a prolonged accumulation of calcium: a ^{45}Ca autoradiographic study. *Brain research* 624:94-102
92. Fleminger S. 2008. Long-term psychiatric disorders after traumatic brain injury. *European journal of anaesthesiology. Supplement* 42:123-30

93. Flierl MA, Stahel PF, Beauchamp KM, Morgan SJ, Smith WR, Shohami E. 2009. Mouse closed head injury model induced by a weight-drop device. *Nature protocols* 4:1328-37
94. Flynn FG. 2010. Memory impairment after mild traumatic brain injury. *Continuum (Minneapolis, Minn.)* 16:79-109
95. Foda MA, Marmarou A. 1994. A new model of diffuse brain injury in rats. Part II: Morphological characterization. *Journal of neurosurgery* 80:301-13
96. Fouquet M, Desgranges B, La Joie R, Riviere D, Mangin JF, et al. 2012. Role of hippocampal CA1 atrophy in memory encoding deficits in amnesic Mild Cognitive Impairment. *Neuroimage* 59:3309-15
97. Fox GB, Fan L, Levasseur RA, Faden AI. 1998. Sustained sensory/motor and cognitive deficits with neuronal apoptosis following controlled cortical impact brain injury in the mouse. *Journal of neurotrauma* 15:599-614
98. Freund TF, Buzsaki G. 1996. Interneurons of the hippocampus. *Hippocampus* 6:347-470
99. Gao HM, Hong JS. 2008. Why neurodegenerative diseases are progressive: uncontrolled inflammation drives disease progression. *Trends in immunology* 29:357-65
100. Gao X, Chen J. 2011. Mild traumatic brain injury results in extensive neuronal degeneration in the cerebral cortex. *J Neuropathol Exp Neurol* 70:183-91
101. Gardner J, Ghorpade A. 2003. Tissue inhibitor of metalloproteinase (TIMP)-1: the TIMPed balance of matrix metalloproteinases in the central nervous system. *Journal of neuroscience research* 74:801-6
102. Gasquoine PG. 1997. Postconcussion symptoms. *Neuropsychol Rev* 7:77-85
103. Gennarelli TA. 1994. Animate models of human head injury. *Journal of neurotrauma* 11:357-68
104. Gingrich KJ, Roberts WA, Kass RS. 1995. Dependence of the GABAA receptor gating kinetics on the alpha-subunit isoform: implications for structure-function relations and synaptic transmission. *The Journal of physiology* 489 (Pt 2):529-43
105. Giza CC, Hovda DA. 2001. The Neurometabolic Cascade of Concussion. *J Athl Train* 36:228-35
106. Goodman JC, Cherian L, Bryan RM, Jr., Robertson CS. 1994. Lateral cortical impact injury in rats: pathologic effects of varying cortical compression and impact velocity. *Journal of neurotrauma* 11:587-97

107. Greer JE, Povlishock JT, Jacobs KM. 2012. Electrophysiological abnormalities in both axotomized and nonaxotomized pyramidal neurons following mild traumatic brain injury. *The Journal of neuroscience : the official journal of the Society for Neuroscience* 32:6682-7
108. Griesbach GS, Hovda DA, Molteni R, Gomez-Pinilla F. 2002. Alterations in BDNF and synapsin I within the occipital cortex and hippocampus after mild traumatic brain injury in the developing rat: reflections of injury-induced neuroplasticity. *Journal of neurotrauma* 19:803-14
109. Griesemer D, Mautes AM. 2007. Closed head injury causes hyperexcitability in rat hippocampal CA1 but not in CA3 pyramidal cells. *Journal of neurotrauma* 24:1823-32
110. Griffin WS. 2013. Neuroinflammatory cytokine signaling and Alzheimer's disease. *The New England journal of medicine* 368:770-1
111. Griffin WS, Sheng JG, Royston MC, Gentleman SM, McKenzie JE, et al. 1998. Glial-neuronal interactions in Alzheimer's disease: the potential role of a 'cytokine cycle' in disease progression. *Brain Pathol* 8:65-72
112. Griguoli M, Cherubini E. 2012. Regulation of hippocampal inhibitory circuits by nicotinic acetylcholine receptors. *The Journal of physiology* 590:655-66
113. Gundersen HJ, Jensen EB, Kieu K, Nielsen J. 1999. The efficiency of systematic sampling in stereology--reconsidered. *J Microsc* 193:199-211
114. Gupta A, Elgammal FS, Proddutur A, Shah S, Santhakumar V. 2012. Decrease in tonic inhibition contributes to increase in dentate semilunar granule cell excitability after brain injury. *The Journal of neuroscience : the official journal of the Society for Neuroscience* 32:2523-37
115. Hall ED, Bryant YD, Cho W, Sullivan PG. 2008. Evolution of post-traumatic neurodegeneration after controlled cortical impact traumatic brain injury in mice and rats as assessed by the de Olmos silver and fluorojade staining methods. *Journal of neurotrauma* 25:235-47
116. Hall ED, Sullivan PG, Gibson TR, Pavel KM, Thompson BM, Scheff SW. 2005. Spatial and temporal characteristics of neurodegeneration after controlled cortical impact in mice: more than a focal brain injury. *Journal of neurotrauma* 22:252-65
117. Hamlin GP, Cernak I, Wixey JA, Vink R. 2001. Increased expression of neuronal glucose transporter 3 but not glial glucose transporter 1 following severe diffuse traumatic brain injury in rats. *Journal of neurotrauma* 18:1011-8
118. Harting MT, Jimenez F, Adams SD, Mercer DW, Cox CS, Jr. 2008. Acute, regional inflammatory response after traumatic brain injury: Implications for cellular therapy. *Surgery* 144:803-13

119. Hartings JA, Watanabe T, Bullock MR, Okonkwo DO, Fabricius M, et al. 2011. Spreading depolarizations have prolonged direct current shifts and are associated with poor outcome in brain trauma. *Brain* 134:1529-40
120. Harvey AG, Bryant RA. 1998. Predictors of acute stress following mild traumatic brain injury. *Brain injury : [BI]* 12:147-54
121. Harvey AG, Bryant RA. 2000. Two-year prospective evaluation of the relationship between acute stress disorder and posttraumatic stress disorder following mild traumatic brain injury. *The American journal of psychiatry* 157:626-8
122. Harvey CD, Svoboda K. 2007. Locally dynamic synaptic learning rules in pyramidal neuron dendrites. *Nature* 450:1195-200
123. Hasselmo ME. 1999. Neuromodulation: acetylcholine and memory consolidation. *Trends Cogn Sci* 3:351-9
124. Hausser M, Spruston N, Stuart GJ. 2000. Diversity and dynamics of dendritic signaling. *Science* 290:739-44
125. Hayashi M, Luo Y, Laning J, Strieter RM, Dorf ME. 1995. Production and function of monocyte chemoattractant protein-1 and other beta-chemokines in murine glial cells. *Journal of neuroimmunology* 60:143-50
126. Henry LC, Tremblay S, Boulanger Y, Ellemberg D, Lassonde M. 2010. Neurometabolic changes in the acute phase after sports concussions correlate with symptom severity. *Journal of neurotrauma* 27:65-76
127. Hicks R, Soares H, Smith D, McIntosh T. 1996. Temporal and spatial characterization of neuronal injury following lateral fluid-percussion brain injury in the rat. *Acta Neuropathol* 91:236-46
128. Hicks RR, Li C, Zhang L, Dhillon HS, Prasad MR, Seroogy KB. 1999. Alterations in BDNF and trkB mRNA levels in the cerebral cortex following experimental brain trauma in rats. *Journal of neurotrauma* 16:501-10
129. Hicks RR, Martin VB, Zhang L, Seroogy KB. 1999. Mild experimental brain injury differentially alters the expression of neurotrophin and neurotrophin receptor mRNAs in the hippocampus. *Experimental neurology* 160:469-78
130. Hicks RR, Numan S, Dhillon HS, Prasad MR, Seroogy KB. 1997. Alterations in BDNF and NT-3 mRNAs in rat hippocampus after experimental brain trauma. *Brain research. Molecular brain research* 48:401-6
131. Hicks RR, Smith DH, Lowenstein DH, Saint Marie R, McIntosh TK. 1993. Mild experimental brain injury in the rat induces cognitive deficits associated with regional neuronal loss in the hippocampus. *Journal of neurotrauma* 10:405-14

132. Hill LE, Droste SK, Nutt DJ, Linthorst AC, Reul JM. 2010. Voluntary exercise alters GABA(A) receptor subunit and glutamic acid decarboxylase-67 gene expression in the rat forebrain. *Journal of psychopharmacology* 24:745-56
133. Hoffmeister PG, Donat CK, Schuhmann MU, Voigt C, Walter B, et al. 2011. Traumatic brain injury elicits similar alterations in alpha7 nicotinic receptor density in two different experimental models. *Neuromolecular Med* 13:44-53
134. Hoge CW, McGurk D, Thomas JL, Cox AL, Engel CC, Castro CA. 2008. Mild traumatic brain injury in U.S. Soldiers returning from Iraq. *The New England journal of medicine* 358:453-63
135. Holzsneider K, Mulert C. 2011. Neuroimaging in anxiety disorders. *Dialogues Clin Neurosci* 13:453-61
136. Humayun MS, Presty SK, Lafrance ND, Holcomb HH, Loats H, et al. 1989. Local cerebral glucose abnormalities in mild closed head injured patients with cognitive impairments. *Nucl Med Commun* 10:335-44
137. Hunkin NM, Parkin AJ, Bradley VA, Burrows EH, Aldrich FK, et al. 1995. Focal retrograde amnesia following closed head injury: a case study and theoretical account. *Neuropsychologia* 33:509-23
138. Iverson GL, Lovell MR, Smith S, Franzen MD. 2000. Prevalence of abnormal CT-scans following mild head injury. *Brain injury : [BI]* 14:1057-61
139. Izquierdo I, Medina JH. 1991. GABAA receptor modulation of memory: the role of endogenous benzodiazepines. *Trends in pharmacological sciences* 12:260-5
140. Jacobson RR. 1995. The post-concussional syndrome: physiogenesis, psychogenesis and malingering. An integrative model. *J Psychosom Res* 39:675-93
141. Ji D, Lape R, Dani JA. 2001. Timing and location of nicotinic activity enhances or depresses hippocampal synaptic plasticity. *Neuron* 31:131-41
142. Jiang L, Role LW. 2008. Facilitation of cortico-amygdala synapses by nicotine: activity-dependent modulation of glutamatergic transmission. *Journal of neurophysiology* 99:1988-99
143. Jordan BD. 2013. The clinical spectrum of sport-related traumatic brain injury. *Nat Rev Neurol* 9:222-30
144. Kanno T, Yaguchi T, Yamamoto S, Nagata T, Yamamoto H, et al. 2005. Bidirectional regulations for glutamate and GABA release in the hippocampus by alpha7 and non-alpha7 ACh receptors. *Biochemical and biophysical research communications* 338:742-7

145. Katayama Y, Becker DP, Tamura T, Hovda DA. 1990. Massive increases in extracellular potassium and the indiscriminate release of glutamate following concussive brain injury. *Journal of neurosurgery* 73:889-900
146. Kay T, Harrington DE, Adams R, Anderson T, Berrol S, et al. 1993. Definition of Mild Traumatic Brain Injury. *Journal of Head Trauma Rehabilitation* 8(3):86-7
147. Kelly JP, Rosenberg JH. 1997. Diagnosis and management of concussion in sports. *Neurology* 48:575-80
148. Kelso ML, Oestreich JH. 2012. Traumatic brain injury: central and peripheral role of alpha7 nicotinic acetylcholine receptors. *Curr Drug Targets* 13:631-6
149. Kennedy JE, Jaffee MS, Leskin GA, Stokes JW, Leal FO, Fitzpatrick PJ. 2007. Posttraumatic stress disorder and posttraumatic stress disorder-like symptoms and mild traumatic brain injury. *J Rehabil Res Dev* 44:895-920
150. Kenney JW, Gould TJ. 2008. Modulation of hippocampus-dependent learning and synaptic plasticity by nicotine. *Molecular neurobiology* 38:101-21
151. Khandaker GM, Jones PB. 2011. Cognitive and functional impairment after severe sepsis. *JAMA : the journal of the American Medical Association* 305:673-4; author reply 4
152. Klausberger T. 2009. GABAergic interneurons targeting dendrites of pyramidal cells in the CA1 area of the hippocampus. *Eur J Neurosci* 30:947-57
153. Klein RC, Yakel JL. 2006. Functional somato-dendritic alpha7-containing nicotinic acetylcholine receptors in the rat basolateral amygdala complex. *The Journal of physiology* 576:865-72
154. Knapska E, Radwanska K, Werka T, Kaczmarek L. 2007. Functional internal complexity of amygdala: focus on gene activity mapping after behavioral training and drugs of abuse. *Physiological reviews* 87:1113-73
155. Kobori N, Dash PK. 2006. Reversal of brain injury-induced prefrontal glutamic acid decarboxylase expression and working memory deficits by D1 receptor antagonism. *The Journal of neuroscience : the official journal of the Society for Neuroscience* 26:4236-46
156. Koen N, Stein DJ. 2011. Pharmacotherapy of anxiety disorders: a critical review. *Dialogues Clin Neurosci* 13:423-37
157. Koenigs M, Huey ED, Raymond V, Cheon B, Solomon J, et al. 2008. Focal brain damage protects against post-traumatic stress disorder in combat veterans. *Nature neuroscience* 11:232-7

158. Kotapka MJ, Gennarelli TA, Graham DI, Adams JH, Thibault LE, et al. 1991. Selective vulnerability of hippocampal neurons in acceleration-induced experimental head injury. *Journal of neurotrauma* 8:247-58
159. Kotapka MJ, Graham DI, Adams JH, Gennarelli TA. 1992. Hippocampal pathology in fatal non-missile human head injury. *Acta Neuropathol* 83:530-4
160. Krettek JE, Price JL. 1978. A description of the amygdaloid complex in the rat and cat with observations on intra-amygdaloid axonal connections. *The Journal of comparative neurology* 178:255-80
161. Kullmann DM. 2011. Interneuron networks in the hippocampus. *Curr Opin Neurobiol* 21:709-16
162. Kumar A, Loane DJ. 2012. Neuroinflammation after traumatic brain injury: opportunities for therapeutic intervention. *Brain, behavior, and immunity* 26:1191-201
163. Lang EJ, Pare D. 1997. Similar inhibitory processes dominate the responses of cat lateral amygdaloid projection neurons to their various afferents. *Journal of neurophysiology* 77:341-52
164. Langlois JA, Rutland-Brown W, Wald MM. 2006. The epidemiology and impact of traumatic brain injury: a brief overview. *The Journal of head trauma rehabilitation* 21:375-8
165. Lenzlinger PM, Morganti-Kossmann MC, Laurer HL, McIntosh TK. 2001. The duality of the inflammatory response to traumatic brain injury. *Molecular neurobiology* 24:169-81
166. Levin ED, Bradley A, Addy N, Sigurani N. 2002. Hippocampal alpha 7 and alpha 4 beta 2 nicotinic receptors and working memory. *Neuroscience* 109:757-65
167. Levin ED, Simon BB. 1998. Nicotinic acetylcholine involvement in cognitive function in animals. *Psychopharmacology (Berl)* 138:217-30
168. Levin H, Smith D. 2013. Traumatic brain injury: networks and neuropathology. *Lancet Neurol* 12:15-6
169. Levin HS, Brown SA, Song JX, McCauley SR, Boake C, et al. 2001. Depression and posttraumatic stress disorder at three months after mild to moderate traumatic brain injury. *Journal of clinical and experimental neuropsychology* 23:754-69
170. Lewine JD, Davis JT, Bigler ED, Thoma R, Hill D, et al. 2007. Objective documentation of traumatic brain injury subsequent to mild head trauma: multimodal brain imaging with MEG, SPECT, and MRI. *The Journal of head trauma rehabilitation* 22:141-55

171. Lighthall JW. 1988. Controlled cortical impact: a new experimental brain injury model. *Journal of neurotrauma* 5:1-15
172. Lighthall JW, Goshgarian HG, Pinderski CR. 1990. Characterization of axonal injury produced by controlled cortical impact. *Journal of neurotrauma* 7:65-76
173. Liu GJ, Nagarajah R, Banati RB, Bennett MR. 2009. Glutamate induces directed chemotaxis of microglia. *Eur J Neurosci* 29:1108-18
174. Liu Q, Nilsen-Hamilton M. 1995. Identification of a new acute phase protein. *The Journal of biological chemistry* 270:22565-70
175. Liu ZW, Yang S, Zhang YX, Liu CH. 2003. Presynaptic alpha-7 nicotinic acetylcholine receptors modulate excitatory synaptic transmission in hippocampal neurons. *Sheng Li Xue Bao* 55:731-5
176. Livak KJ, Schmittgen TD. 2001. Analysis of relative gene expression data using real-time quantitative PCR and the 2(-Delta Delta C(T)) Method. *Methods* 25:402-8
177. Lohr JM, Lilienfeld SO, Rosen GM. 2012. Anxiety and its treatment: promoting science-based practice. *J Anxiety Disord* 26:719-27
178. Long JB, Bentley TL, Wessner KA, Cerone C, Sweeney S, Bauman RA. 2009. Blast overpressure in rats: recreating a battlefield injury in the laboratory. *Journal of neurotrauma* 26:827-40
179. Lu B, Figurov A. 1997. Role of neurotrophins in synapse development and plasticity. *Reviews in the neurosciences* 8:1-12
180. Lykissas MG, Batistatou AK, Charalabopoulos KA, Beris AE. 2007. The role of neurotrophins in axonal growth, guidance, and regeneration. *Current neurovascular research* 4:143-51
181. Malarkey EB, Parpura V. 2008. Mechanisms of glutamate release from astrocytes. *Neurochem Int* 52:142-54
182. Marmarou A, Foda MA, van den Brink W, Campbell J, Kita H, Demetriadou K. 1994. A new model of diffuse brain injury in rats. Part I: Pathophysiology and biomechanics. *Journal of neurosurgery* 80:291-300
183. Matsumura N, Nishijo H, Tamura R, Eifuku S, Endo S, Ono T. 1999. Spatial- and task-dependent neuronal responses during real and virtual translocation in the monkey hippocampal formation. *The Journal of neuroscience : the official journal of the Society for Neuroscience* 19:2381-93
184. Matthews SC, Strigo IA, Simmons AN, O'Connell RM, Reinhardt LE, Moseley SA. 2011. A multimodal imaging study in U.S. veterans of

Operations Iraqi and Enduring Freedom with and without major depression after blast-related concussion. *Neuroimage* 54 Suppl 1:S69-75

185. Matzilevich DA, Rall JM, Moore AN, Grill RJ, Dash PK. 2002. High-density microarray analysis of hippocampal gene expression following experimental brain injury. *Journal of neuroscience research* 67:646-63
186. Mayevsky A, Chance B. 1974. Repetitive patterns of metabolic changes during cortical spreading depression of the awake rat. *Brain research* 65:529-33
187. McAllister TW, Flashman LA, McDonald BC, Saykin AJ. 2006. Mechanisms of working memory dysfunction after mild and moderate TBI: evidence from functional MRI and neurogenetics. *Journal of neurotrauma* 23:1450-67
188. McAllister TW, Flashman LA, Sparling MB, Saykin AJ. 2004. Working memory deficits after traumatic brain injury: catecholaminergic mechanisms and prospects for treatment -- a review. *Brain injury : [BI]* 18:331-50
189. McDonald AJ. 1984. Neuronal organization of the lateral and basolateral amygdaloid nuclei in the rat. *The Journal of comparative neurology* 222:589-606
190. McDonald BC, Saykin AJ, McAllister TW. 2012. Functional MRI of mild traumatic brain injury (mTBI): progress and perspectives from the first decade of studies. *Brain imaging and behavior* 6:193-207
191. McHugh T, Laforce R, Jr., Gallagher P, Quinn S, Diggle P, Buchanan L. 2006. Natural history of the long-term cognitive, affective, and physical sequelae of mild traumatic brain injury. *Brain Cogn* 60:209-11
192. McIntosh TK, Noble L, Andrews B, Faden AI. 1987. Traumatic brain injury in the rat: characterization of a midline fluid-percussion model. *Central nervous system trauma : journal of the American Paralysis Association* 4:119-34
193. McKay BE, Placzek AN, Dani JA. 2007. Regulation of synaptic transmission and plasticity by neuronal nicotinic acetylcholine receptors. *Biochemical pharmacology* 74:1120-33
194. McManus C, Berman JW, Brett FM, Staunton H, Farrell M, Brosnan CF. 1998. MCP-1, MCP-2 and MCP-3 expression in multiple sclerosis lesions: an immunohistochemical and in situ hybridization study. *Journal of neuroimmunology* 86:20-9
195. Meyer DL, Davies DR, Barr JL, Manzerra P, Forster GL. 2012. Mild traumatic brain injury in the rat alters neuronal number in the limbic system and increases conditioned fear and anxiety-like behaviors. *Experimental neurology* 235:574-87

196. Miotto EC, Cinalli FZ, Serrao VT, Benute GG, Lucia MC, Scaff M. 2010. Cognitive deficits in patients with mild to moderate traumatic brain injury. *Arq Neuropsiquiatr* 68:862-8
197. Möhler H. 2006. GABA(A) receptor diversity and pharmacology. *Cell and tissue research* 326:505-16
198. Molosh AI, Sajdyk TJ, Truitt WA, Zhu W, Oxford GS, Shekhar A. 2013. NPY Y1 receptors differentially modulate GABAA and NMDA receptors via divergent signal-transduction pathways to reduce excitability of amygdala neurons. *Neuropsychopharmacology* 38:1352-64
199. Mooney G, Speed J. 2001. The association between mild traumatic brain injury and psychiatric conditions. *Brain injury : [BI]* 15:865-77
200. Moore EL, Terryberry-Spohr L, Hope DA. 2006. Mild traumatic brain injury and anxiety sequelae: a review of the literature. *Brain injury : [BI]* 20:117-32
201. Morales DM, Marklund N, Lebold D, Thompson HJ, Pitkanen A, et al. 2005. Experimental models of traumatic brain injury: do we really need to build a better mousetrap? *Neuroscience* 136:971-89
202. Morganti-Kossmann MC, Rancan M, Stahel PF, Kossmann T. 2002. Inflammatory response in acute traumatic brain injury: a double-edged sword. *Current opinion in critical care* 8:101-5
203. Morganti-Kossmann MC, Satgunaseelan L, Bye N, Kossmann T. 2007. Modulation of immune response by head injury. *Injury* 38:1392-400
204. Moser EI. 2011. The multi-laned hippocampus. *Nature neuroscience* 14:407-8
205. Mchedlishvili Z, Lepsveridze E, Xu H, Kharlamov EA, Lu B, Kelly KM. 2010. Increase of GABAA receptor-mediated tonic inhibition in dentate granule cells after traumatic brain injury. *Neurobiology of disease* 38:464-75
206. Muller JF, Mascagni F, McDonald AJ. 2011. Cholinergic innervation of pyramidal cells and parvalbumin-immunoreactive interneurons in the rat basolateral amygdala. *The Journal of comparative neurology* 519:790-805
207. Murray AJ, Sauer JF, Riedel G, McClure C, Ansel L, et al. 2011. Parvalbumin-positive CA1 interneurons are required for spatial working but not for reference memory. *Nature neuroscience* 14:297-9
208. Nagai T, Kimura H, Maeda T, McGeer PL, Peng F, McGeer EG. 1982. Cholinergic projections from the basal forebrain of rat to the amygdala. *The Journal of neuroscience : the official journal of the Society for Neuroscience* 2:513-20

209. Nai Q, McIntosh JM, Margiotta JF. 2003. Relating neuronal nicotinic acetylcholine receptor subtypes defined by subunit composition and channel function. *Molecular pharmacology* 63:311-24
210. Naude PJ, Nyakas C, Eiden LE, Ait-Ali D, van der Heide R, et al. 2012. Lipocalin 2: novel component of proinflammatory signaling in Alzheimer's disease. *FASEB journal : official publication of the Federation of American Societies for Experimental Biology* 26:2811-23
211. Newhouse PA, Potter A, Levin ED. 1997. Nicotinic system involvement in Alzheimer's and Parkinson's diseases. Implications for therapeutics. *Drugs Aging* 11:206-28
212. Nicholl J, LaFrance W. 2009. Neuropsychiatric Sequelae of Traumatic Brain Injury. *Seminars in Neurology* 29:247-55
213. Nitecka L, Frotscher M. 1989. Organization and synaptic interconnections of GABAergic and cholinergic elements in the rat amygdaloid nuclei: single- and double-immunolabeling studies. *The Journal of comparative neurology* 279:470-88
214. O'Dell DM, Gibson CJ, Wilson MS, DeFord SM, Hamm RJ. 2000. Positive and negative modulation of the GABA(A) receptor and outcome after traumatic brain injury in rats. *Brain research* 861:325-32
215. Ohry A, Rattok J, Solomon Z. 1996. Post-traumatic stress disorder in brain injury patients. *Brain injury : [BI]* 10:687-95
216. Osteen CL, Moore AH, Prins ML, Hovda DA. 2001. Age-dependency of 45calcium accumulation following lateral fluid percussion: acute and delayed patterns. *Journal of neurotrauma* 18:141-62
217. Oyesiku NM, Evans CO, Houston S, Darrell RS, Smith JS, et al. 1999. Regional changes in the expression of neurotrophic factors and their receptors following acute traumatic brain injury in the adult rat brain. *Brain research* 833:161-72
218. Pandya AA, Yakel JL. 2013. Activation of the alpha7 nicotinic ACh receptor induces anxiogenic effects in rats which is blocked by a 5-HT(1)a receptor antagonist. *Neuropharmacology* 70:35-42
219. Pandya AA, Yakel JL. 2013. Effects of neuronal nicotinic acetylcholine receptor allosteric modulators in animal behavior studies. *Biochemical pharmacology*
220. Pare D, Gaudreau H. 1996. Projection cells and interneurons of the lateral and basolateral amygdala: distinct firing patterns and differential relation to theta and delta rhythms in conscious cats. *The Journal of neuroscience : the official journal of the Society for Neuroscience* 16:3334-50

221. Pavlov I, Huusko N, Drexel M, Kirchmair E, Sperk G, et al. 2011. Progressive loss of phasic, but not tonic, GABAA receptor-mediated inhibition in dentate granule cells in a model of post-traumatic epilepsy in rats. *Neuroscience* 194:208-19
222. Paxinos G, Watson C. 2005. *The rat brain in stereotaxic coordinates*. Academic Press
223. Peloso PM, Carroll LJ, Cassidy JD, Borg J, von Holst H, et al. 2004. Critical evaluation of the existing guidelines on mild traumatic brain injury. *Journal of rehabilitation medicine : official journal of the UEMS European Board of Physical and Rehabilitation Medicine*:106-12
224. Perreault ML, Fan T, Alijaniam M, O'Dowd BF, George SR. 2012. Dopamine D1-D2 receptor heteromer in dual phenotype GABA/glutamate-coexpressing striatal medium spiny neurons: regulation of BDNF, GAD67 and VGLUT1/2. *PloS one* 7:e33348
225. Pettus EH, Povlishock JT. 1996. Characterization of a distinct set of intra-axonal ultrastructural changes associated with traumatically induced alteration in axolemmal permeability. *Brain research* 722:1-11
226. Pidoplichko VI, Dani JA. 2005. Applying small quantities of multiple compounds to defined locations of in vitro brain slices. *Journal of neuroscience methods* 142:55-66
227. Pidoplichko VI, Prager EM, Aroniadou-Anderjaska V, Braga MF. 2013. alpha7-Containing nicotinic acetylcholine receptors on interneurons of the basolateral amygdala and their role in the regulation of the network excitability. *Journal of neurophysiology* 110:2358-69
228. Pidoplichko VI, Prager EM, Aroniadou-Anderjaska V, Braga MF. 2013. alpha7-Containing Nicotinic Acetylcholine Receptors on Interneurons of the Basolateral Amygdala and their Role in the Regulation of the Network Excitability. *Journal of neurophysiology*
229. Povlishock JT, Christman CW. 1995. The pathobiology of traumatically induced axonal injury in animals and humans: a review of current thoughts. *Journal of neurotrauma* 12:555-64
230. Povlishock JT, Pettus EH. 1996. Traumatically induced axonal damage: evidence for enduring changes in axolemmal permeability with associated cytoskeletal change. *Acta Neurochir Suppl* 66:81-6
231. Prager EM, Bergstrom HC, Grunberg NE, Johnson LR. 2011. The importance of reporting housing and husbandry in rat research. *Front Behav Neurosci* 5:38

232. Raghupathi R. 2004. Cell death mechanisms following traumatic brain injury. *Brain pathology (Zurich, Switzerland)* 14:215-22
233. Raible DJ, Frey LC, Cruz Del Angel Y, Russek SJ, Brooks-Kayal AR. 2012. GABA(A) receptor regulation after experimental traumatic brain injury. *Journal of neurotrauma* 29:2548-54
234. Rao V, Lyketsos C. 2000. Neuropsychiatric sequelae of traumatic brain injury. *Psychosomatics* 41:95-103
235. Rao V, Lyketsos CG. 2002. Psychiatric aspects of traumatic brain injury. *Psychiatr Clin North Am* 25:43-69
236. Rauch SL, Shin LM, Phelps EA. 2006. Neurocircuitry models of posttraumatic stress disorder and extinction: human neuroimaging research--past, present, and future. *Biological psychiatry* 60:376-82
237. Rauch SL, Whalen PJ, Shin LM, McInerney SC, Macklin ML, et al. 2000. Exaggerated amygdala response to masked facial stimuli in posttraumatic stress disorder: a functional MRI study. *Biological psychiatry* 47:769-76
238. Reeves TM, Kao CQ, Phillips LL, Bullock MR, Povlishock JT. 2000. Presynaptic excitability changes following traumatic brain injury in the rat. *Journal of neuroscience research* 60:370-9
239. Reeves TM, Lyeth BG, Povlishock JT. 1995. Long-term potentiation deficits and excitability changes following traumatic brain injury. *Experimental brain research. Experimentelle Hirnforschung. Experimentation cerebrale* 106:248-56
240. Reger ML, Poulos AM, Buen F, Giza CC, Hovda DA, Fanselow MS. 2012. Concussive brain injury enhances fear learning and excitatory processes in the amygdala. *Biological psychiatry* 71:335-43
241. Reis HJ, Guatimosim C, Paquet M, Santos M, Ribeiro FM, et al. 2009. Neurotransmitters in the central nervous system & their implication in learning and memory processes. *Curr Med Chem* 16:796-840
242. Renner NA, Ivey NS, Redmann RK, Lackner AA, MacLean AG. 2011. MCP-3/CCL7 production by astrocytes: implications for SIV neuroinvasion and AIDS encephalitis. *Journal of neurovirology* 17:146-52
243. Rhodes JK, Sharkey J, Andrews PJ. 2009. The temporal expression, cellular localization, and inhibition of the chemokines MIP-2 and MCP-1 after traumatic brain injury in the rat. *Journal of neurotrauma* 26:507-25
244. Rimel RW, Giordani B, Barth JT, Boll TJ, Jane JA. 1981. Disability caused by minor head injury. *Neurosurgery* 9:221-8

245. Rimel RW, Giordani B, Barth JT, Boll TJ, Jane Ja. 1981. Disability caused by minor head injury. In *Neurosurgery*, pp. 221-8
246. Risling M, Davidsson J. 2012. Experimental animal models for studies on the mechanisms of blast-induced neurotrauma. *Frontiers in neurology* 3:30
247. Rodgers KM, Bercum FM, McCallum DL, Rudy JW, Frey LC, et al. 2012. Acute neuroimmune modulation attenuates the development of anxiety-like freezing behavior in an animal model of traumatic brain injury. *Journal of neurotrauma* 29:1886-97
248. Rolls A, Shechter R, Schwartz M. 2009. The bright side of the glial scar in CNS repair. *Nat Rev Neurosci* 10:235-41
249. Rolls ET, Xiang JZ. 2006. Spatial view cells in the primate hippocampus and memory recall. *Reviews in the neurosciences* 17:175-200
250. Ross DT, Graham DI, Adams JH. 1993. Selective loss of neurons from the thalamic reticular nucleus following severe human head injury. *Journal of neurotrauma* 10:151-65
251. Rossi S, Muzio L, De Chiara V, Grasselli G, Musella A, et al. 2011. Impaired striatal GABA transmission in experimental autoimmune encephalomyelitis. *Brain, behavior, and immunity* 25:947-56
252. Rossi S, Studer V, Motta C, De Chiara V, Barbieri F, et al. 2012. Inflammation inhibits GABA transmission in multiple sclerosis. *Multiple sclerosis* 18:1633-5
253. Roy-Byrne PP. 2005. The GABA-benzodiazepine receptor complex: structure, function, and role in anxiety. *The Journal of clinical psychiatry* 66 Suppl 2:14-20
254. Rubovitch V, Ten-Bosch M, Zohar O, Harrison CR, Tempel-Brami C, et al. 2011. A mouse model of blast-induced mild traumatic brain injury. *Experimental neurology* 232:280-9
255. Rudolph U, Möhler H. 2006. GABA-based therapeutic approaches: GABAA receptor subtype functions. *Current opinion in pharmacology* 6:18-23
256. Ruff RM, Camenzuli L, Mueller J. 1996. Miserable minority: emotional risk factors that influence the outcome of a mild traumatic brain injury. *Brain injury : [BI]* 10:551-65
257. Rusted JM, Newhouse PA, Levin ED. 2000. Nicotinic treatment for degenerative neuropsychiatric disorders such as Alzheimer's disease and Parkinson's disease. *Behav Brain Res* 113:121-9

258. Saatman KE, Feeko KJ, Pape RL, Raghupathi R. 2006. Differential behavioral and histopathological responses to graded cortical impact injury in mice. *Journal of neurotrauma* 23:1241-53
259. Sah P, Faber ES, Lopez De Armentia M, Power J. 2003. The amygdaloid complex: anatomy and physiology. *Physiological reviews* 83:803-34
260. Sah P, Lopez De Armentia M. 2003. Excitatory synaptic transmission in the lateral and central amygdala. *Annals of the New York Academy of Sciences* 985:67-77
261. Samii A, Badie H, Fu K, Luther RR, Hovda DA. 1999. Effects of an N-type calcium channel antagonist (SNX 111; Ziconotide) on calcium-45 accumulation following fluid-percussion injury. *Journal of neurotrauma* 16:879-92
262. Sangha S, Ilenseer J, Sosulina L, Lesting J, Pape HC. 2012. Differential regulation of glutamic acid decarboxylase gene expression after extinction of a recent memory vs. intermediate memory. *Learning & memory* 19:194-200
263. Sbordone R, Liter J. 1995. Mild traumatic brain injury does not produce post-traumatic stress disorder. *Brain Injury* 9:405-12
264. Sbordone RJ, Seyranian GD, Ruff RM. 1998. Are the subjective complaints of traumatically brain injured patients reliable? *Brain injury : [BI]* 12:505-15
265. Schmidt OI, Heyde CE, Ertel W, Stahel PF. 2005. Closed head injury--an inflammatory disease? *Brain research. Brain research reviews* 48:388-99
266. Schmitz C, Hof PR. 2000. Recommendations for straightforward and rigorous methods of counting neurons based on a computer simulation approach. *J Chem Neuroanat* 20:93-114
267. Schousboe A, Waagepetersen HS. 2005. Role of astrocytes in glutamate homeostasis: implications for excitotoxicity. *Neurotox Res* 8:221-5
268. Shah KR, West M. 1983. The effect of concussion on cerebral uptake of 2-deoxy-D-glucose in rat. *Neuroscience letters* 40:287-91
269. Shapira Y, Shohami E, Sidi A, Soffer D, Freeman S, Cotev S. 1988. Experimental closed head injury in rats: mechanical, pathophysiologic, and neurologic properties. *Critical care medicine* 16:258-65
270. Sharma AC, Kulkarni SK. 1990. Evidence for GABA-BZ receptor modulation in short-term memory passive avoidance task paradigm in mice. *Methods and findings in experimental and clinical pharmacology* 12:175-80
271. Shelton CI. 2004. Diagnosis and management of anxiety disorders. *J Am Osteopath Assoc* 104:S2-5

272. Shin LM, Orr SP, Carson MA, Rauch SL, Macklin ML, et al. 2004. Regional cerebral blood flow in the amygdala and medial prefrontal cortex during traumatic imagery in male and female Vietnam veterans with PTSD. *Archives of general psychiatry* 61:168-76
273. Shohami E, Shapira Y, Cotev S. 1988. Experimental closed head injury in rats: prostaglandin production in a noninjured zone. *Neurosurgery* 22:859-63
274. Signoretti S, Vagnozzi R, Tavazzi B, Lazzarino G. 2010. Biochemical and neurochemical sequelae following mild traumatic brain injury: summary of experimental data and clinical implications. *Neurosurgical focus* 29:E1
275. Skoglosa Y, Lewen A, Takei N, Hillered L, Lindholm D. 1999. Regulation of pituitary adenylate cyclase activating polypeptide and its receptor type 1 after traumatic brain injury: comparison with brain-derived neurotrophic factor and the induction of neuronal cell death. *Neuroscience* 90:235-47
276. Smith DH, Soares HD, Pierce JS, Perlman KG, Saatman KE, et al. 1995. A model of parasagittal controlled cortical impact in the mouse: cognitive and histopathologic effects. *Journal of neurotrauma* 12:169-78
277. Smits M, Hunink MG, van Rijssel DA, Dekker HM, Vos PE, et al. 2008. Outcome after complicated minor head injury. *AJNR. American journal of neuroradiology* 29:506-13
278. Sosin DM, Sniezek JE, Thurman DJ. 1996. Incidence of mild and moderate brain injury in the United States, 1991. *Brain injury : [BI]* 10:47-54
279. Squire LR. 1992. Memory and the hippocampus: a synthesis from findings with rats, monkeys, and humans. *Psychol Rev* 99:195-231
280. Stellwagen D, Beattie EC, Seo JY, Malenka RC. 2005. Differential regulation of AMPA receptor and GABA receptor trafficking by tumor necrosis factor- α . *The Journal of neuroscience : the official journal of the Society for Neuroscience* 25:3219-28
281. Stoica BA, Faden AI. 2010. Cell death mechanisms and modulation in traumatic brain injury. *Neurotherapeutics : the journal of the American Society for Experimental NeuroTherapeutics* 7:3-12
282. Strong AJ, Dardis R. 2005. Depolarisation phenomena in traumatic and ischaemic brain injury. *Adv Tech Stand Neurosurg* 30:3-49
283. Stulemeijer M, Vos PE, van der Werf S, van Dijk G, Rijpkema M, Fernandez G. 2010. How mild traumatic brain injury may affect declarative memory performance in the post-acute stage. *Journal of neurotrauma* 27:1585-95

284. Stuss DT, Ely P, Hugenholtz H, Richard MT, LaRoche S, et al. 1985. Subtle neuropsychological deficits in patients with good recovery after closed head injury. In *Neurosurgery*, pp. 41-7
285. Sudweeks SN, Yakel JL. 2000. Functional and molecular characterization of neuronal nicotinic ACh receptors in rat CA1 hippocampal neurons. *The Journal of physiology* 527 Pt 3:515-28
286. Sugaya E, Takato M, Noda Y. 1975. Neuronal and glial activity during spreading depression in cerebral cortex of cat. *Journal of neurophysiology* 38:822-41
287. Sunami K, Nakamura T, Ozawa Y, Kubota M, Namba H, Yamaura A. 1989. Hypermetabolic state following experimental head injury. *Neurosurg Rev* 12 Suppl 1:400-11
288. Swanson LW, Simmons DM, Whiting PJ, Lindstrom J. 1987. Immunohistochemical localization of neuronal nicotinic receptors in the rodent central nervous system. *The Journal of neuroscience : the official journal of the Society for Neuroscience* 7:3334-42
289. Takahashi H, Manaka S, Sano K. 1981. Changes in extracellular potassium concentration in cortex and brain stem during the acute phase of experimental closed head injury. *Journal of neurosurgery* 55:708-17
290. Takizawa S, Matsushima K, Fujita H, Nanri K, Ogawa S, Shinohara Y. 1995. A selective N-type calcium channel antagonist reduces extracellular glutamate release and infarct volume in focal cerebral ischemia. *Journal of cerebral blood flow and metabolism : official journal of the International Society of Cerebral Blood Flow and Metabolism* 15:611-8
291. Tay SY, Ang BT, Lau XY, Meyyappan A, Collinson SL. 2010. Chronic impairment of prospective memory after mild traumatic brain injury. *Journal of neurotrauma* 27:77-83
292. Thompson HJ, Lifshitz J, Marklund N, Grady MS, Graham DI, et al. 2005. Lateral fluid percussion brain injury: a 15-year review and evaluation. *Journal of neurotrauma* 22:42-75
293. Thompson WL, Van Eldik LJ. 2009. Inflammatory cytokines stimulate the chemokines CCL2/MCP-1 and CCL7/MCP-3 through NFkB and MAPK dependent pathways in rat astrocytes [corrected]. *Brain research* 1287:47-57
294. Tosevski J, Malikovic A, Mojsilovic-Petrovic J, Lackovic V, Peulic M, et al. 2002. Types of neurons and some dendritic patterns of basolateral amygdala in humans--a golgi study. *Ann Anat* 184:93-103

295. Truitt WA, Johnson PL, Dietrich AD, Fitz SD, Shekhar A. 2009. Anxiety-like behavior is modulated by a discrete subpopulation of interneurons in the basolateral amygdala. *Neuroscience* 160:284-94
296. Turtzo LC, Budde MD, Gold EM, Lewis BK, Janes L, et al. 2012. The evolution of traumatic brain injury in a rat focal contusion model. *NMR Biomed*
297. Umile EM, Sandel ME, Alavi A, Terry CM, Plotkin RC. 2002. Dynamic imaging in mild traumatic brain injury: support for the theory of medial temporal vulnerability. *Arch Phys Med Rehabil* 83:1506-13
298. van der Naalt J. 2001. Prediction of outcome in mild to moderate head injury: a review. *Journal of clinical and experimental neuropsychology* 23:837-51
299. van der Naalt J, van Zomeren AH, Sluiter WJ, Minderhoud JM. 1999. One year outcome in mild to moderate head injury: the predictive value of acute injury characteristics related to complaints and return to work. *J Neurol Neurosurg Psychiatry* 66:207-13
300. van der Zee EA, Luiten PG. 1999. Muscarinic acetylcholine receptors in the hippocampus, neocortex and amygdala: a review of immunocytochemical localization in relation to learning and memory. *Prog Neurobiol* 58:409-71
301. Vanderploeg RD, Curtiss G, Belanger HG. 2005. Long-term neuropsychological outcomes following mild traumatic brain injury. *J Int Neuropsychol Soc* 11:228-36
302. VanElzakker M, Fevurly RD, Breindel T, Spencer RL. 2008. Environmental novelty is associated with a selective increase in Fos expression in the output elements of the hippocampal formation and the perirhinal cortex. *Learning & memory* 15:899-908
303. VanGuilder HD, Bixler GV, Brucklacher RM, Farley JA, Yan H, et al. 2011. Concurrent hippocampal induction of MHC II pathway components and glial activation with advanced aging is not correlated with cognitive impairment. *Journal of neuroinflammation* 8:138
304. Verbois SL, Hopkins DM, Scheff SW, Pauly JR. 2003. Chronic intermittent nicotine administration attenuates traumatic brain injury-induced cognitive dysfunction. *Neuroscience* 119:1199-208
305. Verbois SL, Scheff SW, Pauly JR. 2002. Time-dependent changes in rat brain cholinergic receptor expression after experimental brain injury. *Journal of neurotrauma* 19:1569-85
306. Verbois SL, Scheff SW, Pauly JR. 2003. Chronic nicotine treatment attenuates alpha 7 nicotinic receptor deficits following traumatic brain injury. *Neuropharmacology* 44:224-33

307. Verbois SL, Sullivan PG, Scheff SW, Pauly JR. 2000. Traumatic brain injury reduces hippocampal alpha7 nicotinic cholinergic receptor binding. *Journal of neurotrauma* 17:1001-11
308. Verweij BH, Muizelaar JP, Vinas FC, Peterson PL, Xiong Y, Lee CP. 1997. Mitochondrial dysfunction after experimental and human brain injury and its possible reversal with a selective N-type calcium channel antagonist (SNX-111). *Neurol Res* 19:334-9
309. Villarreal G, King CY. 2001. Brain imaging in posttraumatic stress disorder. *Semin Clin Neuropsychiatry* 6:131-45
310. Vos PE, Alekseenko Y, Battistin L, Ehler E, Gerstenbrand F, et al. 2012. Mild traumatic brain injury. *European journal of neurology : the official journal of the European Federation of Neurological Societies* 19:191-8
311. Vos PE, Battistin L, Birbamer G, Gerstenbrand F, Potapov A, et al. 2002. EFNS guideline on mild traumatic brain injury: report of an EFNS task force. *European journal of neurology : the official journal of the European Federation of Neurological Societies* 9:207-19
312. Wagner AK, Postal BA, Darrah SD, Chen X, Khan AS. 2007. Deficits in novelty exploration after controlled cortical impact. *Journal of neurotrauma* 24:1308-20
313. Wajant H, Scheurich P. 2011. TNFR1-induced activation of the classical NF-kappaB pathway. *The FEBS journal* 278:862-76
314. Wanaverbecq N, Semyanov A, Pavlov I, Walker MC, Kullmann DM. 2007. Cholinergic axons modulate GABAergic signaling among hippocampal interneurons via postsynaptic alpha 7 nicotinic receptors. *The Journal of neuroscience : the official journal of the Society for Neuroscience* 27:5683-93
315. Wang X, Li X, Yaish-Ohad S, Sarau HM, Barone FC, Feuerstein GZ. 1999. Molecular cloning and expression of the rat monocyte chemotactic protein-3 gene: a possible role in stroke. *Brain research. Molecular brain research* 71:304-12
316. Wang Y, Wei Y, Oguntayo S, Wilkins W, Arun P, et al. 2011. Tightly coupled repetitive blast-induced traumatic brain injury: development and characterization in mice. *Journal of neurotrauma* 28:2171-83
317. Warden D. 2006. Military TBI during the Iraq and Afghanistan wars. *The Journal of head trauma rehabilitation* 21:398-402
318. Washburn MS, Moises HC. 1992. Electrophysiological and morphological properties of rat basolateral amygdaloid neurons in vitro. *The Journal of neuroscience : the official journal of the Society for Neuroscience* 12:4066-79

319. Washburn MS, Moises HC. 1992. Inhibitory responses of rat basolateral amygdaloid neurons recorded in vitro. *Neuroscience* 50:811-30
320. Washington PM, Forcelli PA, Wilkins T, Zapple DN, Parsadanian M, Burns MP. 2012. The effect of injury severity on behavior: a phenotypic study of cognitive and emotional deficits after mild, moderate, and severe controlled cortical impact injury in mice. *Journal of neurotrauma* 29:2283-96
321. Willer B, Leddy JJ. 2006. Management of concussion and post-concussion syndrome. *Current treatment options in neurology* 8:415-26
322. Witgen BM, Lifshitz J, Smith ML, Schwarzbach E, Liang SL, et al. 2005. Regional hippocampal alteration associated with cognitive deficit following experimental brain injury: a systems, network and cellular evaluation. *Neuroscience* 133:1-15
323. Womble MD, Moises HC. 1993. Hyperpolarization-activated currents in neurons of the rat basolateral amygdala. *Journal of neurophysiology* 70:2056-65
324. Wood ER, Dudchenko PA, Eichenbaum H. 1999. The global record of memory in hippocampal neuronal activity. *Nature* 397:613-6
325. Wood RL, O'Hagan G, Williams C, McCabe M, Chadwick N. 2013. Anxiety Sensitivity and Alexithymia as Mediators of Postconcussion Syndrome Following Mild Traumatic Brain Injury. *The Journal of head trauma rehabilitation*
326. Woodruff AR, Sah P. 2007. Inhibition and synchronization of basal amygdala principal neuron spiking by parvalbumin-positive interneurons. *Journal of neurophysiology* 98:2956-61
327. Xiong Y, Mahmood A, Chopp M. 2013. Animal models of traumatic brain injury. *Nat Rev Neurosci* 14:128-42
328. Xiong Y, Peterson PL, Verweij BH, Vinas FC, Muizelaar JP, Lee CP. 1998. Mitochondrial dysfunction after experimental traumatic brain injury: combined efficacy of SNX-111 and U-101033E. *Journal of neurotrauma* 15:531-44
329. Xu B, Gottschalk W, Chow A, Wilson RI, Schnell E, et al. 2000. The role of brain-derived neurotrophic factor receptors in the mature hippocampus: modulation of long-term potentiation through a presynaptic mechanism involving TrkB. *The Journal of neuroscience : the official journal of the Society for Neuroscience* 20:6888-97
330. Yakel JL. 2012. Nicotinic ACh receptors in the hippocampus: role in excitability and plasticity. *Nicotine Tob Res* 14:1249-57

331. Yonkov DI, Georgiev VP. 1985. Memory effects of GABA-ergic antagonists in rats trained with two-way active avoidance tasks. *Acta physiologica et pharmacologica Bulgarica* 11:44-9
332. Yu F, Wang Z, Tchantchou F, Chiu CT, Zhang Y, Chuang DM. 2012. Lithium ameliorates neurodegeneration, suppresses neuroinflammation, and improves behavioral performance in a mouse model of traumatic brain injury. *Journal of neurotrauma* 29:362-74
333. Zappala G, Thiebaut de Schotten M, Eslinger PJ. 2012. Traumatic brain injury and the frontal lobes: what can we gain with diffusion tensor imaging? *Cortex* 48:156-65
334. Zarrindast MR, Bakhsha A, Rostami P, Shafaghi B. 2002. Effects of intrahippocampal injection of GABAergic drugs on memory retention of passive avoidance learning in rats. *Journal of psychopharmacology* 16:313-9
335. Zeilhofer HU. 2008. Loss of glycinergic and GABAergic inhibition in chronic pain--contributions of inflammation and microglia. *International immunopharmacology* 8:182-7
336. Zhang BL, Chen X, Tan T, Yang Z, Carlos D, et al. 2011. Traumatic brain injury impairs synaptic plasticity in hippocampus in rats. *Chin Med J (Engl)* 124:740-5
337. Zhang D, Hu X, Qian L, O'Callaghan JP, Hong JS. 2010. Astrogliosis in CNS pathologies: is there a role for microglia? *Molecular neurobiology* 41:232-41
338. Zhang N, Oppenheim JJ. 2005. Crosstalk between chemokines and neuronal receptors bridges immune and nervous systems. *Journal of leukocyte biology* 78:1210-4
339. Ziebell JM, Morganti-Kossmann MC. 2010. Involvement of pro- and anti-inflammatory cytokines and chemokines in the pathophysiology of traumatic brain injury. *The Journal of the American Society for Experimental NeuroTherapeutics* 7:22-30
340. Ziebell JM, Morganti-Kossmann MC. 2010. Involvement of pro- and anti-inflammatory cytokines and chemokines in the pathophysiology of traumatic brain injury. *Neurotherapeutics : the journal of the American Society for Experimental NeuroTherapeutics* 7:22-30
341. Zoli M, Lena C, Picciotto MR, Changeux JP. 1998. Identification of four classes of brain nicotinic receptors using beta2 mutant mice. *The Journal of neuroscience : the official journal of the Society for Neuroscience* 18:4461-72